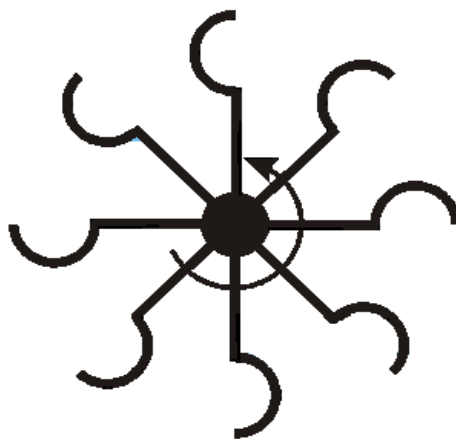


W.D. Bauer

About Energy Conservation, Second Law
and Overunity

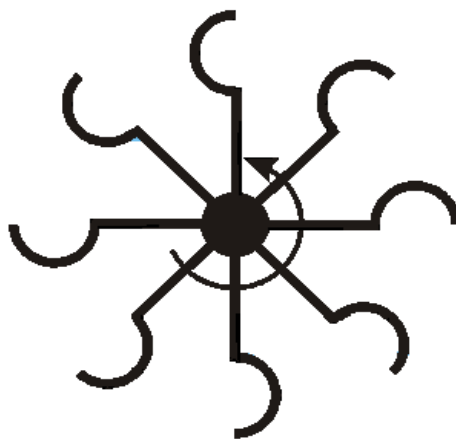
(corrected of found serious errors)



WDB-Verlag

W.D. Bauer

About Energy Conservation, Second Law
and Overunity



WDB-Verlag

Title: About Energy Conservation, Second Law and Overunity

Author: Wolf-Dietrich Bauer

Graphics: W.D. Bauer, if not noted otherwise

Layout: W.D. Bauer, Latex PhD-template

Printing: A8Medienservice GmbH, 10589 Berlin

Binding: A8Medienservice GmbH, 10589 Berlin

1. edition WDB-Verlag Berlin 2015

ISBN: 978-3-9801452-4-4

© Copyright: WDB-Verlag Berlin 2015

corrected version
on the net 6/7 .8. 2019
02. 12.2021

All rights reserved

including any medium copying, translation, storage and transfer

We applied the highest possible care. For any errors and its consequences we decline any liability. We point out that any legally protected names or brands used in this book are not free but subjected to the laws of the local relevant nation.

Preface

It is well known generally since the 1970ties [1, 2] that our natural resources are finite. In order to avoid the end of our comfortable era there exist two possibilities:

Either we spare up and recycle the available resources or change the selection of the "laws" we apply to build our machines consuming the resources.

So about 25 years ago the author decided naively to "crack the Second Law" because this physical law mainly is responsible for the energy crisis. The strategy was to check the many claimed systems discussed by the "underground science" scene because official science was biased and avoided to discuss the theme. So the author was enforced to master autodidactically the basics of classical physics mainly. In the beginning he fell at least into every trap because he was blockheaded and not very competent and also did not found competent willing able partners for discussion. However, after years of learning by flops he got the insight that it does not make sense to crack the Second Law. It was better to comprehend it as a special case embedded in a wider general mathematical framework. This approach allows to recognize other systems hidden and published in the official science literature which are better candidates to produce the wanted effects. These systems are beyond the Second Law because the basic conditions of the application of equilibrium thermodynamics are missing.

The work was difficult especially from the emotional point of view. Suffering under "perpetuum mobilitis" is a taboo of science which drives all honest workers into isolation and errors, both oftenly unconscious mechanisms to reduce stress. Another hindering problem of "perpetuum mobile science" is and ever was [3] that especially fraudulent motivated persons oftenly are involved in the theme. Perpetual motion is a big dream of course. So any open serious effort clarifying the theme attracts immedi-

ately the interests of influential people. However, fearing the consequences they do not really want to participate in the hard painstaking and oftenly frustrating work itself. They prefer to propose the big perpetual money and power machine projects, try to obtain the control and and so they tend to pervert and/or destroy even sincere intentions. In order to protect the project and also myself of being misused, I blocked any interest of my environment in the second half time of this work. So this book is written almost completely alone with no helping field. Although I applied maximum care in the presentation it is clear that under these conditions non-perfectness, mistakes and wishful thinking may be possible in the book despite of all efforts. So I decline any liability for wrong informations and its consequences. I transfer the responsibility back to the reader. Nevermind I am sure that some good ideas will remain. I am glad if I obtain any critics if it is sincere, helpful and constructive.

I have to add the following disclaimer:

This book is grown as an individual and private non-profit initiative. If it is not noted otherwise the author speaks only for himself and not for any institution or company.

Berlin, in summer 2014

email: w.d.bauer@t-online.de

Contents

1	Introduction	1
2	General System Theory	3
2.1	Mathematics, System Theory and Physics	3
2.2	the Helmholtz Decomposition	4
2.2.1	Potential Field Systems	4
2.2.2	Vortex Systems	5
2.3	System Theory Concepts	6
2.4	System Theory applied to Economy	7
2.5	Conservativeness or Stability abstracted	9
3	About Energy Conservation	11
3.1	the Philosophy behind Energy Conservation	11
3.2	the Energy Flux Network	14
3.3	How to handle Overunity Systems	15
4	Thermodynamics at the Limit	17
4.1	Introduction	17

4.2	Continuum Thermodynamics	18
4.3	Thermostatistics	21
4.4	the Concept of Temperature	28
4.5	Thermodynamics vs. Second Law ?	29
4.5.1	Second Law Violations in Conservative Fields ?	29
4.5.2	Second Law Violations at Low Pressures ?	33
4.5.3	Nonconservative Systems beyond the Second Law	34
4.5.4	Further Candidate Systems	36
4.6	Conclusions	36
4.7	Appendix-Calculating the Fluid Stratification	37
4.7.1	the Equation of State	37
4.7.2	the Phase Equilibrium	38
4.7.3	Inverting the Equation of State	39
4.7.4	Spatial Distribution of Pressure and Chemical Potential	40
4.7.5	the Mass Conservation	41
4.7.6	Synthesizing the whole Compartment Solver	42
4.7.7	Results	43
5	No Second Law in Thermodynamics ?	47
5.1	Historical Introduction	47
5.2	The Work of Irinyi, Doczekal and Schaeffer	49
5.2.1	Irinyi	49
5.2.2	Doczekal	53
5.2.3	Schaeffer	58

5.3	The Thermodynamic Theory of Water-Benzene	60
5.3.1	stable case	60
5.3.2	labile case	72
5.4	How to replace the Second Law	91
5.5	Summary	96
5.6	Appendix	97
6	Beyond the Second Law	101
6.1	Systems driven by Fluctuations	101
6.1.1	Introduction	101
6.1.2	Noise Driven Systems	102
6.1.3	van der Waals Force and Zero Point Energy	103
6.2	Inverted Hysteresis Systems	104
6.2.1	Introduction	104
6.2.2	Basics for Hysteresis Measurements	106
6.2.3	Magnetic Systems	109
6.2.4	Electric Systems	113
6.3	Permanent Magnet Motors	128
6.3.1	Historical Permanent Magnet Motors	128
6.3.2	a Basic Mechanism of a Permanent Magnet Motor	128
6.3.3	the Simulation of a Permanent Magnet Motor	130
6.3.4	Discussion and Outlook	132
6.4	Appendix	133
6.4.1	the Derivative of the Electromagnetic Flux	133

6.4.2	Moment and Energy Conservation of Charges	136
6.4.3	the Derivation of the ODE of the Parametric Oscillation	138
6.4.4	List of Electromagnetic Symbols	141
7	Summary	143
8	Bibliography	145
9	Index	177

Chapter 1

Introduction

A functioning perpetuum mobile is an old dream of mankind containing much philosophic projections we have about the world. The oldest ideas are from India going back to the 5th century AC. The two volumes of Dircks [4, 5] refer the "state of the art" until 1870 and the book of Ord-Hume [3] until ≈ 1970 . Today many websites of the internet discuss the theme and its systems mostly on a popular level.

The scientific discussion began with the age of Enlightenment and was positive in the beginning. Bernoulli und Boyle discussed Perpetui Mobilia, Leibnitz wrote a letter of recommendation for Bessler [6] (the constructor of the Bessler wheel). But due to many failures and frauds the climate changed. Hamilton's mechanics destroyed the belief in a mechanical Perpetuum Mobile. The First Law (energy conservation) suggested, that energy can not be gained, the Second Law braked down any research with the claim to change heat to work without losses. So the mainstream thermodynamic scientist of today prescribes dogmatically that every material description has to implement the Second Law a priori. In deed the highly busy scientific colleagues from the other departments do not note this theoretical stuff normally. Oftenly they do not realize or consciously ignore the consequences of their results they are publishing. This allowed me to find systems beyond the old conventional scope hidden in the scientific literature. These I present here as non-volunteering candidates for an evaluation.

I will banalize the idea of the perpetuum mobile: I define a Perpetuum mobile as

- 1) a machine which comes back to the initial state after a cyclic process - and
- 2) a machine which gains mechanical, electrical or chemical energy by a cycle exchanging with a regenerative environment. It does not change the materials in the environment at the interesting space and timescale.

In order to avoid gambling and to reduce the number of flops I apply diagnostic criteria in order to recognize these systems with the aim to pick out the more promising cases.

So this book is organized as follows:

In chapter 2 I consider the tools of system theory and discuss which type of candidate systems are allowed by mathematics. In chapter 3 it is discussed what the term energy conservation really means seen by the different philosophical points of view. In chapter 4 I derive the equilibrium thermodynamics in the field formulation. This is done in order to check it against Second Law violating claims in fields. I show that the thermodynamic framework is not complete and that the concept of temperature and entropy can loose its original sense in the general case. In chapter 5 I discuss a unpublished historical system of a mixed steam engine including spontaneous condensation processes. I evaluate the system and develop a new theory of the nonlinear dynamics of the phase transition gas to liquid. From this example I conclude that changing to the terminology of nonlinear dynamics makes the Second Law obsolete. In chapter 6 I show that the phenomenon of inverted hysteresis is outside of equilibrium thermodynamics and so beyond the Second Law. As an example it is shown that the conventional energy balance of a storage FET capacity is violated because this system consist of a cycle patched together inconsistently by classical and quantum mechanical elements. According to my analysis this system gives off net energy after an electric capacitive cycle. ~~Furthermore I show that permanent running magnet motors are possible. They can be understood easily and are engineered by standard methods.~~

Chapter 2

General System Theory

2.1 Mathematics, System Theory and Physics

Mathematics imagines what can be thought logically. Physics investigates what can be realized. System theory translates the terms of mathematics into physical language in order to bring both disciplines together as far as possible in order to allow physics to realize what can be imagined. Table 2.1 shows the idea of "inter concept mapping".

Table 2.1: Translation Tabel between Mathematical and Physical Concepts

mathematics	system theory
variable	observable
function	system answer
operator	measurement process
theory	experimental setup

2.2 the Helmholtz Decomposition

The Helmholtz decomposition [7][8] splits up any field $F := F_V + F_P$ (or more generally any tensor) into two components : an antisymmetric vortex field F_V and a symmetric potential field F_P . The vortex field F_V is derived from a vector potential describing a state field, the potential field F_P is derived from a unique potential state function U . Consequently we can separate any classical physical system into two pure components, one is the potential field system, the other is the vortex system. Generally any classical physical system can be composed again by adding the pure components. The pure classes are discussed in the next two subsections.

2.2.1 Potential Field Systems

We make here the restriction to potential field systems whose physical state $F_i(X_i)$ is derived from a potential function $U(X_i)$. X_i is a vector of experimental values characterizing the empirical state of the system. Then the differential

$$dU = \sum_i \frac{\partial U}{\partial X_i} dX_i = \sum_i F_i(X_i) dX_i \quad (2.1)$$

describes the part of a cyclic reproducible process, cf. also 2.3. After a cycle it holds

$$\oint_C dU = \oint_C \sum_i \frac{\partial U}{\partial X_i} dX_i = 0. \quad (2.2)$$

This yields $rot \vec{F} = 0$ [8]. If all terms $F_i dX_i$ coincide with work definitions it follows "energy conservation" as the logical consequence of the reproducibility of the system, cf. the definition of reproducibility in sec. 2.3.

These consideration here fit exactly to known physical systems like the Hamilton function $H(p, x)$ of classical mechanics or the internal energy $U(S, V)$ of thermodynamics. In mechanics there exists energy conservation from point to point, i.e. $dH(p, x) = 0$, in thermodynamics this is energy conservation after a cycle, i.e. $\oint dU \equiv \oint dH(V, S) = 0$.

2.2.2 Vortex Systems

We make here the restriction to vortex systems whose states are derived from a vector field $\vec{W}(\vec{X})$ by $\text{rot } \vec{W}(\vec{X}) = \vec{F}(\vec{X})$. This yields $\text{div } \vec{F} = 0$. \vec{X} is a vector of independent experimental values being the empirical state of the system. $\vec{F}(\vec{X}) := F_i(X_i)$ is the field function whose choice allows the description of all dependent experimental parameters which depend from X_i . For a vortex field it holds after a reproducible cycle:

$$\oint_C \sum_i F_i(X_i) dX_i \neq 0. \quad (2.3)$$

If all terms $F_i(X) dX_i$ coincide with work definitions we have "energy non-conservation". So we can select out classes of "perpetuum mobile candidates" as [9]

a) systems $F_i(X_i; \lambda)$ driven by fluctuations and b) full non-conservative systems $F_i(X_i)$. Under a) we find- sorted from big to small scale - tide power plants, clocks driven by the fluctuations of air pressure [3] or arm movement, energy harvesting and ratchet systems [10], Maxwell demons and zero-point-energy systems [11]. As a limit case we obtain the classical perpetuum mobile of 2nd kind if the driving fluctuating ambient medium is purely thermal. This classical type of perpetuum mobile changes heat energy to mechanical energy with 100% efficiency and cools down the environment. Under b) we find systems applying a non-conservative coupling, cf.fig. 2.1 to a conservative or non conservative driving field. This are generalized wind wheels i.e. electro-magnetic inverted hysteresis systems, see 6.2. or permanent magnet motors, see 6.3.1.

System	Parameter	Field
windmill	angle	wind
magnet	angle	magnetic
electret	angle	electric
capacity	time	electric
inductivity	time	magnetic

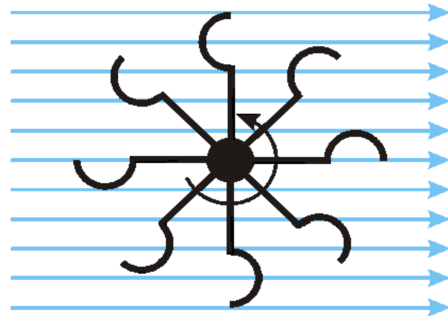


Figure 2.1: generalized system with non-conservative coupling to a field

2.3 System Theory Concepts

System theory concepts are the building blocks of a meta-language of the different disciplines of science. We illustrate this idea by reintroducing here some well known simple terms and definitions. Some are applied in section 2.2.1 .

reproducibility:

A system is called reproducible if it is possible to perform a cyclic process starting at any state $X(t_0)$ at t_0 coming back again at t_1 to the initial point $X(t_1) = X(t_0)$ and $F_i(X(t_0)) = F_i(X(t_1))$ on any path. Therefrom one concludes:

If the system is completely defined by a potential state function $U(X_i(t))$, then the reproducibility of the system holds also for the potential definition because

$$\oint dU = \sum_i \oint \frac{\partial U}{\partial X_i} dX_i = \sum_i \oint F_i(X_i) dX_i = 0. \quad (2.4)$$

For vortex field systems, however, the situation is different. They are reproducible but the cycle integral in the field is non-zero for the most general case, i.e.

$$\sum_i \oint F_i(X_i) dX_i \neq 0. \quad (2.5)$$

However, here an interesting special case exists for spatially system where any cycle around the singularity yields the same integral sum on any cyclic path. This may be the cause of the quantization of systems.

symmetry:

A system is said to have a symmetry if its properties are reproducible after a transformation of the coordinates X_i . This may be a mirroring, a translation or a rotation.

isotropy:

A system property is called isotropic if its definition does not depend from the position or the direction in space.

2.4 System Theory applied to Economy

Between physics and economy there exists a system theory analogy between money and energy which I will complete here. Therefore I present the following examples:

We take 4 points from a arbitrary force field in space. We assume a test object moving in the field with forces acting on the object . The energy differences of the object between these points are shown in tab.2.2. We calculate now the energy necessary to move the object over the points in the field on different closed pathways. According to tab.2.2 this difference between $P_1 \rightarrow P_3$ is 3. If one returns directly $P_3 \rightarrow P_1$ the difference is -3 and the sum of both pathes is 0. But, if one returns over P_2 , i.e. $P_3 \rightarrow P_2 \rightarrow P_1$ then the differences are summed up to $-4+2=-2$! This yields :

$$P_1 \rightarrow P_3 \rightarrow P_2 \rightarrow P_1 \hat{=} 3 - 2 = 1 .$$

Because a closed cycle with a non-zero result is found for this system the generating field is called non-conservative. In physics, chemistry and material science, however, the most well known systems fullfil energy conservation. I remember here to the electrochemical row of potentials, to the energies of the spectral states in quantum mechanics, to the Hess heat theorem in thermodynamics and the table of the thermovoltages of the different materials (Seebeck-effect). If the potential differences of these systems are represented in a matrix as done above, a zero has to be the result for any closed (loss free) cycle.

Table 2.2: energy differences in an arbitrary force field

from	point1	point2	point3	point4
point1	0	2	-3	-5
point2	-2	0	-4	-11
point3	3	4	0	-8
point4	5	11	8	0

Table 2.3: Exchange Rates of Different Stock Markets on 12.6.03

place currency	London (Pfund)	Frankfurt (Euro)	New York (Dollar)	Tokyo (Yen)
Pfund	1	0.70	0.5932202	0.0503597122
Euro	1.428571	1	0.8474576	0.00719424461
Dollar	1.68571378	1.18	1	0.0084892086
Yen	198.571369	139	117.7966	1

The idea can be generalized principally also for the other conserved quantities like momentum and angular momentum. And it can be transferred as well to economics: In tab. 2.3 exchange rates of currencies are shown valid at the different stock markets. If one tries to run money on any paths over the different stock markets at the exchange rates from tab. 2.3 a gain is not possible (overlook the errors in the last digits !) on any path. Because any gain (or loss) is impossible for any cycle here we call the matrix "conservative". In other words the market is stable due to an equilibrium between offer and sales.

Of course this is a situation which is not desirable for any merchant. He will look for a non-conservative situation on the market in order to make money by a gain cycle of his investment.

So I can summarize the comparison between physical and economic cycles by the following tabel of analogies tab.2.4:

Table 2.4: Tabel of Analogies between Physical and Economic Concepts

physics	economy
energy	money
field	market
cycle	economic money cycle
gain	return of investment
stable state	equilibrium between sales and offers
non-conservative cycle	economic cycle with gain or loss

2.5 Conservativeness or Stability abstracted

From the examples of the last section the following question arises:

What are the general mathematical properties of conservative matrices which characterize the "borderline" where any cycle can be proceeded without gain or loss ?

There, applying the addition as operation, -see the example with the energy field - the "energy" sum or the gain is zero after any cycle. If this is fulfilled, the cycle is called conservative, otherwise the cycle is non-conservative.

If we apply the multiplication as operation the overall factor has to be 1 after the conservative cycle is closed. Otherwise - see the economic example - the market is not in equilibrium and the matrix is non-conservative. So, generally I ask:

Is it possible to find a test operation to check whether the matrix is conservative ?

To answer this question we regard the elements a_{1i} und a_{3i} from the first and third line of table 2.3. We multiply the element a_{31} with every element of line 1. If all elements of the new calculated row 1 coincide with line 3, then the matrix may be conservative - i.e. in formulas

$$a_{3i} = a_{1i} \cdot a_{31} .$$

This fact has to be generalized for all rows of the matrix. Then, we can define the rows to be "multiplicatively" dependent which is also an equivalent conservative property. The analogue is done for addition with the values of tab.2.2 . Row n is compared with row m. Due to the additivity the worked performed on a path over three points is

$$a_{ni} = a_{mi} + a_{nm}$$

if the field is conservative. If a_{ni} can be transformed according to this operation then the lines are "additively dependent". If this operation is done with any rows of the matrix no gain or loss can be obtained in any closed cycle. Under this conditions the set in matrix is defined to be conservative.

If the lines are multiplicatively dependent the last definition of conservativeness can be applied as well if one writes.

$$\log(a_{ni}) = \log(a_{mi}) + \log(a_{nm})$$

I summarize my considerations in terms of group theory [12] by the following definition:

We have a matrix \mathbf{M} containing a set of elements a_{ik} . We denote the generalized operation as \circ . We write down a generalized definition of the conservative property of the set of a matrix as follows:

A matrix \mathbf{M} is called conservative, if all elements indexed by i of any row a_{mi} can be transformed into another present row a_{ni} according to the general transformation

$$a_{ni} = a_{nm} \circ a_{mi}$$

This proposal may be the most generalized definition of a conservative systems.

An alternative weaker diagnostic definition is:

For a conservative matrix holds:

$$a_{mn} = a_{nm}^{-1} \quad \text{and} \quad (\quad a_{mn} = e \quad \text{if} \quad m = n \quad)$$

This holds because $a_{mn} \circ a_{nm} = a_{nm}^{-1} \circ a_{nm} = e$ ($e \equiv \text{identity element}$) .

This means: any action to a state and back again has to yield no gain or loss.

Any conservative system fulfills this necessary condition. However, not every system is conservative which fulfills the condition, cf. the example from sec. 2.4 and tabel 2.2.

Chapter 3

About Energy Conservation

3.1 the Philosophy behind Energy Conservation

Discussing basic ideas like the first law inside or outside of the scientific mainstream is sometimes difficult. This is caused oftenly by the fact that the people do not realize that they discuss unconsciously with different philosophical projections in which they are believing. This hinders an effective communication and understanding. To explain I give here an example illustrating the typical discussion about the first law :

A thermodynamic textbook [13],p.7, denotes the total differential of internal energy U

$$dU = T * dS - p * dV \quad (3.1)$$

as the first law i.e. the law of energy conservation. De facto the term dU is not empirically founded and can not be determined independently by one instrument in one measurement. It is calculated normally from the terms of the right side of the equation, which are all empirically accessible. So equation 3.1 is a defining equation for dU only and not an empirically proved valid law of nature as suggested in textbooks.

In order to clarify the present different points of view I characterize here three different typical philosophical positions called natural philosophic, mathematical and operative.

1) The natural philosophic standpoint is the oldest in history. It is very near to the most common general belief of the people. It regards energy like a fluidum which cannot be created or destroyed. The typical "scientific" protagonist of this way of thinking is Rudolf Mayer. He was very lucky that he found the first working example of energy conservation law beyond mechanics. Mayer derived the energy equivalent between heat and work [14] for the very strong special case of the ideal gas which in deed obeys an observable energy conservation from point to point due to the thermodynamic condition $dU = 0$ valid for this case. Of course Mayer overgeneralized his findings and proclaimed a general valid new law of nature. If he chosed liquid water between 0° and 4° Celsius as working substance instead of an ideal gas, his considerations would have failed due to $dU \neq 0$. Since Clausius [15] and Gibbs [16] the description of these real systems is achieved by using potential functions. Energy conservation can be proved only after a closed cycle due to $\oint dU = - \oint p dV + \oint T dS = 0$.

Later, Mayer's philosophy obtained support by Einstein's discovery of the equivalence formula between energy and mass $E = m * c^2$ which enforced as well the materialistic point of view of the common popular natural philosophy.

2) The mathematical way of speaking about energy conservation is exactly the way how a variable is handled in mathematics. These statements are purely formal and contain no physical contents. So this point of view can be opposite to any natural philosophy. The mathematical statement is strongly depending from the way how we have chosen the description of the system by the arbitrary choice of the system border. For example we assume a simple mechanical system consisting of a spring and a mass coupled together. If both parts together (friction is neglected) are regarded to be the system then the energy is conserved. If the mass only is regarded to be the system which is driven from outside by the spring represented by a non-holonomic forcing term then the mass system alone does not conserve energy [17]. So, the flexible mathematical rhetorics can be made helpful in order to see the "scientific" physical law what we want to see. It is clear that these arguments are oftenly misused by the natural philosophic propaganda. We note that the resulting "energy conservation by selective perception" cannot be an argument in favour of any "law of nature".

3) If one follows the work of a physicist one observes that he wants to establish quantitative balances of measureable entities. In other words: the belief in energy conservation is an useful driving hypothesis of his scientific work. If an energy balance can be established one has "energy conservation", sometimes even stronger "energy conservation per definition" finally. Writing down an equation of the energy balance enables the description of the investigated system finally. I call this strategy the operative standpoint. It was the line of H. v.Helmholtz [18] and it is rationalized also by the philosophy of Kant, Wittgenstein and by the school of neopositivism [19].

Today the last point of view is the most actual, pragmatic and honest one in my eyes. So "religious" symbol oriented physical concepts are avoided. In the end it is irrelevant whether the first law is proven empirically or not. "The principle of energy conservation" [18] is applied as an instrument for explanation always if it is appropriate. ~~this projection~~ If the application is not so obvious or impossible the discussion of the energetic aspect is avoided. It is clear that under this condition any discussion about the scientific correctness of this "law of nature" does not make much sense.

This consideration holds also for other conserved quantities. This is shown in the example of fig.3.1. There the angular momentum J of the masses mounted on the two weighless wheels is "conserved" according to $\dot{J} = \dot{J}_1 + n\dot{J}_2 = 0$ (with $n = \text{gear ratio}$).

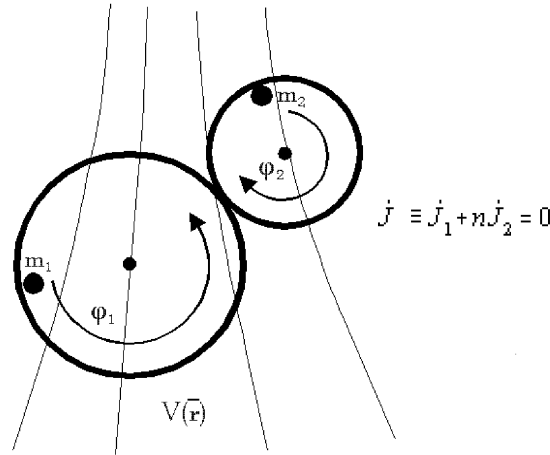


Figure 3.1: two masses mounted on wheels in a field and connected by a gear (constraint)
If constraints are introduced between independent objects conserved entities may change.

3.2 the Energy Flux Network

Due to the axiomatic natural philosophic belief in energy conservation the normal way of physics to handle non-conserving energy systems is to look for a compensation by manipulating the system border and by adding to the energy balance a complement of elements which may represent the outside energy influxes and losses. This procedure makes the energy balance "correct" and describes an energy flux network.

For instance if one regards a pure electrical description of a relaxing RC-low pass network it contains no thermodynamical variables. But the differential equation of the charge Q (with $C :=$ capacitance $R :=$ resistance and $U(t > 0) = 0 :=$ voltage)

$$U(t) = Q/C + R\dot{Q} \quad (3.2)$$

is also an energy balance of W_R and W_C if the voltage $U(t)$ is multiplied by the current I and integrated over the time t

$$W_C + W_R := \int_0^{\Delta t} I(Q/C + R\dot{Q}) dt = 0 \quad (3.3)$$

In the end one obtains the simple energy equation describing that the energy W is given off from the capacitance C and taken up by the resistor R .

Nothing about heat and temperature is said here so far.

In order to include the thermodynamic aspects like temperatures and heat one has to enlarge the describing equation to a system and include here for instance a simple heat transport equation describing the heat loss

$$U(t) = \quad Q/C + R\dot{Q} \quad (3.4)$$

$$C_E \frac{dT}{dt} = K(T_e - T) - T.V(\partial \mathbf{P} / \partial T)_E \partial \mathbf{E} / \partial t \quad (3.5)$$

In the second equation I introduced $T :=$ temperature of the object, $T_e :=$ temperature of the environment, $C_E :=$ heat capacity at constant field \mathbf{E} , $K :=$ heat resistance, $V :=$ volume $\mathbf{P} :=$ polarisation. The first term on the right side of the second equation describes the heat flux from and to the environment, the second term is the adiabatic contribution if the field is changing fast. If we increase the accuracy of the

description by complication one may obtain in the end a spatial "multiphysics" partial differential equation system which represents all nodes of the more complete energy flux network system + environment whose nodes are the "multiphysics" "energy conservation" balances of the different sorts of energy.

3.3 How to handle Overunity Systems

In the case of the pretended "overunity" systems the source of energy is not obvious at first sight. The conventional approach suggests chemical or nuclear processes burning down slowly. "Overunity people", however, oppose this and prefer here theories believing that the energy source may be a sort of "dark energy" from space or from the fluctuating vacuum field of zero point energy [11]. For instance a proposal exists how to connect a "vacuum flux" directly to the Maxwell theory [20]. These theories appear to be strange at the first sight, they seem to be doubtful because their interconnection with experimental reality is weak normally and the ideology behind the math too speculative. So they are far off from being generally accepted by the scientific community[21]. Nevermind, we will profit by this ideas and will show in sec. 6.2 that a similar conventional approach based only on a modified interpretation of the Maxwell equation is sufficient to handle so called "overunity" problems.

In this way we remain open for any experimental explanation with respect to the source of energy. Before we assume an "outside" source of energy we recommend to check first the trivial hypotheses by tests of long durance. If any burn down processes in the material can be excluded then we can test the overunity ideas which include the environment. Again the multiphysics ansatz is appropriate and we need experiments including other disciplines of physics in the environment of the system in order to be able to find the energy flux system at the outer nodes of the energy network.

So I conclude: overunity systems have to be handled as unknown physical systems. Especially vortex systems may have features attributed to overunity systems.

Chapter 4

Thermodynamics at the Limit

4.1 Introduction

In this chapter I discuss systems existing in a regime at the limits of classical equilibrium thermodynamics. First I derive in section 4.2 the classical equilibrium continuum thermodynamics conventionally in a field formulation. The variational method is applied here for the Hamiltonian, the most results derived are well known and near to textbook knowledge. In section 4.3 the same is done for thermostatistics. Again the results are old, but the derivation method may be new: I will derive the equilibrium distribution of the particles from a variational principle of the Hamiltonian energy. The theory is applied to a mixed gas in a centrifuge. In section 4.4 I present a general definition of temperature which is able to describe more classes of phenomena than the conventional definition of temperature. In section 4.5 I discuss known systems which may point for the limits where the application of the equilibrium thermodynamics and the Second Law may be questionable. Section 4.6 shows the conclusions.

4.2 Continuum Thermodynamics

The total Hamilton energy (or internal energy) H^* of a thermodynamic system including an external potential field U is defined as (the definition symbol is \equiv)

$$\begin{aligned} H^* &\equiv H(S(\mathbf{r}), \mathbf{r}, n_i(\mathbf{r})) + U(S(\mathbf{r}), \mathbf{r}, n_i(\mathbf{r})) \\ &= H(S, \mathbf{r}, n_i) + \sum_i \int U_i(S, \mathbf{r}, n_i) dn_i, \end{aligned} \quad (4.1)$$

where H is the internal energy of the fluid without the outer influence of the field. H and H^* are denoted here also as a Hamilton energy. S is the entropy, n_i is the mole number of each particle, $U_i \equiv \partial U / \partial n_i$ is the partial potential energy of a species i and \mathbf{r} is the space coordinate. From (4.1) the total differential follows

$$\begin{aligned} dH^*(S, \mathbf{r}, n_i) &= \left(\frac{\partial H}{\partial S} + \sum_i \int \frac{\partial U_i}{\partial S} dn_i \right) dS \\ &+ \left(\frac{1}{A} \frac{\partial H}{\partial \mathbf{r}} + \frac{1}{A} \sum_i \int \frac{\partial U_i}{\partial \mathbf{r}} dn_i \right) A d\mathbf{r} \\ &+ \sum_i \left(\frac{\partial H}{\partial n_i} + \frac{\partial U}{\partial n_i} \right) dn_i. \end{aligned} \quad (4.2)$$

I restrict the local pressure tensor of the fluid to be isotropic. It holds $\partial H / \partial \mathbf{r} \equiv \hat{\mathbf{P}} \cdot \mathbf{A}$ with $\hat{\mathbf{P}} \equiv$ pressure tensor and $A \equiv |\mathbf{A}| \equiv$ area of the space cell. Then, using the definition $dV \equiv A \cdot dr$ the derivatives of (4.2) can be written as

$$\begin{aligned}
T &\equiv \frac{\partial H}{\partial S} + \sum_i \int \frac{\partial U_i}{\partial S} dn_i \\
-P^* &\equiv \frac{\partial H}{\partial V} + \sum_i \int \frac{\partial U_i}{\partial \mathbf{r}} \rho_i(\mathbf{r}) d\mathbf{r} \\
&\equiv -P + \sum_i \int \frac{\partial U_i}{\partial \mathbf{r}} \rho_i(\mathbf{r}) d\mathbf{r} \\
\mu_i^* &\equiv \frac{\partial H}{\partial n_i} + \frac{\partial U}{\partial n_i} \equiv \mu_i + U_i .
\end{aligned} \tag{4.3}$$

The definitions are: $T \equiv$ temperature, $\mu_i^* \equiv$ the global chemical reference potential of a substance, $P^* \equiv$ global reference pressure, $\mu_i \equiv$ chemical potential of a substance, $P \equiv$ empirical barometric or hydrostatic pressure, $\rho_i \equiv A^{-1} \partial n_i / \partial r \equiv$ density of a species of particles and $A \equiv$ area of the space cell due to fluctuations.

The equilibrium between two adjacent space cells at r_k and r_{k+1} in a potential field can be found if the variation of Hamilton energy H^*

$$\begin{aligned}
dH^* &= T(r_k) dS(r_k) + T(r_{k+1}) dS(r_{k+1}) \\
&\quad - P^*(r_k) dV(r_k) - P^*(r_{k+1}) dV(r_{k+1}) \\
&\quad + \sum_i (\mu_i^*(r_k) dn_i(r_k) + \mu_i^*(r_{k+1}) dn_i(r_{k+1})) \\
&= (T(r_k) - T(r_{k+1})) dS - (P^*(r_k) - P^*(r_{k+1})) dV \\
&\quad + \sum_i (\mu_i^*(r_k) - \mu_i^*(r_{k+1})) dn_i = 0
\end{aligned} \tag{4.4}$$

is minimized to zero in the equilibrium. The last line of the last equation follows due to the constraints $dS = dS(r_k) = -dS(r_{k+1})$, $dV \equiv A dr \equiv dV(r_k) = -dV(r_{k+1})$ and $dn = dn_i(r_k) = -dn_i(r_{k+1})$ which describe the fluctuating exchange of entropy, volume and particles at the border between two adjacent space cells in space. Because the differentials dS , dV and dn are non zero, (4.4) yields the equilibrium conditions

$$\begin{aligned}
T(r_k) &= T(r_{k+1}) \\
P^*(r_k) &= P^*(r_{k+1}) \\
\mu_i^*(r_k) &= \mu_i^*(r_{k+1}) .
\end{aligned} \tag{4.5}$$

These equilibrium conditions above can be rewritten as well in the form

$$\begin{aligned}
\frac{T(r_k) - T(r_{k+1})}{r_k - r_{k+1}} &= \frac{\partial T}{\partial \mathbf{r}} = 0 \\
\frac{P^*(r_k) - P^*(r_{k+1})}{r_k - r_{k+1}} &= \frac{\partial P^*}{\partial \mathbf{r}} = 0 \\
\frac{\mu_i^*(r_k) - \mu_i^*(r_{k+1})}{r_k - r_{k+1}} &= \frac{\partial \mu_i^*}{\partial \mathbf{r}} = 0 .
\end{aligned} \tag{4.6}$$

The equilibrium can be interpreted as well as the trivial case result of an variation where the (physical) total Hamilton energy $H^*(\mathbf{u}(\mathbf{r}))$ is the (mathematical) Lagrange function to be optimized. \mathbf{u} is the ("velocity") variable which is identified here as $\mathbf{u} \equiv (S(\mathbf{r}), V(\mathbf{r}), n_i(\mathbf{r}))$. We have to to optimize the function

$$\frac{1}{\Delta R_j} \int_0^{\Delta R_j} H^*(\mathbf{u}) dr_j \rightarrow \text{extremum} \quad \text{or} \quad \int_0^{\Delta R_j} \delta H^*(\mathbf{u}) dr_j = 0 . \tag{4.7}$$

In the context of non-equilibrium thermodynamics the equations (4.6) are the thermodynamic forces [22] which are zero in the case of equilibrium. The equation system (4.6) is sufficient information in order to solve for the spatial distributions of pressure, density and molar ratio of a mixture in a field under isothermal conditions if the distributions of the particle components do not influence the field itself. This holds for thermodynamic systems in any gravitational or centrifugal potential fields. In the appendix 4.7 the numerical calculation method is demonstrated for a binary system in a centrifugal field near to the critical point.

For systems with electric and magnetic fields other partial differential equations like the Poisson equation or the Laplace equation have to be added to the whole equation system because the spatial distribution of dielectric or magnetostatic liquids [23] in the volume can modify the field itself.

4.3 Thermostatistics

It is well known that the mechanic equations of motion can be found as solutions of a Lagrange variation problem. The solution is obtained, if the Lagrange function L has an extremum, where $x(t_0) = x_0$ and $x(t_1) = x_1$ are start and end point of the path. Then it holds

$$I(x) = \int_{t_0}^{t_1} L(x, \dot{x}; t) dt \rightarrow \text{extremum} . \quad (4.8)$$

The Lagrange variation problem can be regarded as well as a special case of a general problem of control theory [24] [8] where the control variable $u(t)$ coincides with the velocity variable $\dot{x} = f(u, x; t) = u$. The functional of this control theory problem is

$$J(x) = \int_{t_0}^{t_1} L(x, u; t) dt \rightarrow \text{extremum} \quad (4.9)$$

with $\dot{x} = u$, $x(t_0) = x_0$, and $x(t_1) = x_1$ for the special case discussed here.

The Hamiltonian is defined as

$$H = pu - L(x, u; t) . \quad (4.10)$$

The adjunct system is defined by

$$\dot{p} \equiv L_x(x, u; t) . \quad (4.11)$$

According to the Pontryagin theorem of control theory this problem can be solved if the extremum of the Hamiltonian $H(p, x, u; t)$ is found. (For proofs, see [24]). So in order to obtain a determining equation for the extremum, $H(p, x, u; t)$ is derived for u and set to zero

$$H_u = p - L_u(x, u; t) = 0 . \quad (4.12)$$

If this equation is differentiated for t the solution is the Euler-Lagrange equation

$$\frac{d}{dt}L_{\dot{x}} - \frac{dL}{dx} = 0 \quad (4.13)$$

if $\dot{x} = u$ and $\dot{p} = L_x$ as defined above.

The equation $\dot{x} = f(u, x; t) = u$ applied here describes the uncontrolled free running system. It represents the trivial case of control theory which coincides with the Hamiltonian mechanics. In this case (4.10) is also a Legendre transform.

Because a thermodynamic system can be regarded as a mechanic many particle system, the variational features of Hamiltonian mechanics should be present in thermostatics as well. In equilibrium, due to energy conservation, the Hamiltonian of mechanics is constant. We assume the hypothesis of ergodicity to be valid for the system. Then the time mean of total energy is identical to the ensemble average of thermostatics. Or translated into mathematic language (with ΔT as the measuring time interval)

$$\begin{aligned} H_{tot} &\equiv \frac{1}{\Delta T} \int_0^{\Delta T} \sum_i (\varepsilon_i + U_i + \sum_{j,i} U_{ij}) dt \\ &= \int_0^\infty \int_0^\infty W(\varepsilon_K, n_i) \varepsilon_K d\varepsilon_K d\mathbf{n}_i \\ &= \int_0^\infty \int_0^\infty \int_0^\infty \int_{\varepsilon_0}^\infty \hat{W}(\varepsilon, n_i, V) \varepsilon \rho(n_i, V) d\varepsilon_{int} d|U| d\mathbf{n}_i dV \quad . \end{aligned} \quad (4.14)$$

$W(\varepsilon_K, n_i)$ is the canonic probability distribution of the total volume as defined in Mayer's book [25] p. 6+7 with the eigenvalue of the total Hamilton energy ε_K . In the third line $\hat{W}(\varepsilon(\varepsilon_{int}, U), n_i(\mathbf{r}), V(\mathbf{r}))$ is the probability function of each volume element $dV(\mathbf{r})$. The density $\rho(n_i(\mathbf{r}), V(\mathbf{r}))$ represents the space profile of the total particle number density. The energy ε of a particle is defined by

$$\varepsilon \equiv \varepsilon_{kin} + U_{int}(n_i(\mathbf{r}), \mathbf{r}) + U(n_i(\mathbf{r}), \mathbf{r}) \equiv \varepsilon_{int} + U(n_i(\mathbf{r}), \mathbf{r}) \quad (4.15)$$

where ε_{kin} is the kinetic energy of the particle in the field, U_{int} is the mean field potential between the particles due to the real fluid behavior, ε_{int} is defined as $\varepsilon_{int} \equiv \varepsilon_{kin} + U_{int}$ and U is the potential energy due to a field applied from outside. An integration $\int \dots d\mathbf{n}_i$ like in the last line of (4.14) should be read always as $\int \dots dn_1 \dots dn_m$, where m is the number of components in the mixture.

As shown above the mechanic Hamiltonian has an extremum. We will see in the following that this feature can be transferred analogously to thermostatics. Then, at every space cell the Hamilton energy density function

$$\hat{\mathcal{H}} \equiv \hat{W} \varepsilon \rho \quad (4.16)$$

should have an extremum as well.

For the following calculation all symbols are made dimensionless by defining

$$\begin{aligned} \mathcal{H}' &\equiv \pm \hat{\mathcal{H}}(m+3)/(kT) & W' &\equiv -\hat{W} \mu^{*-m} (kT/(m+3))^{m+2} \\ V_0 &\equiv kT/((m+3)P^*) & \rho' &\equiv \rho V_0 \\ \varepsilon' &\equiv (m+3)\varepsilon_{int}/(kT) & U' &\equiv \pm(m+3)U/(kT) \\ n'_i &\equiv -(m+3)\mu^* n_i/(kT) & V' &\equiv V/V_0 . \end{aligned} \quad (4.17)$$

So, the calculation of mechanics (from (4.8) to (4.13)) can also be done similarly in thermodynamics if the mechanical variables are exchanged by thermodynamical terms according to table 4.1 . After having defined the function $X \equiv (\varepsilon' + U')\rho'$ and identifying W' as the adjunct function of control theory we perform the optimization

$$\mathcal{H}'_{tot} \sim \int W' X d\varepsilon' dU' dV' d\mathbf{n}'_i \rightarrow \text{extremum} . \quad (4.18)$$

Due to the present coincidence of the control theory with the Hamiltonian formalism, the Lagrangian \mathcal{L}' can be calculated by a Legendre transformation of $\mathcal{H}'(W', X)$, namely (cf. table 4.1)

$$\mathcal{L}'(\varepsilon', V', U', n'_i) = W' \frac{\partial X}{\partial \varepsilon'} + W' \frac{\partial X}{\partial U'} + W' \frac{\partial X}{\partial V'} + \sum_i W' \frac{\partial X}{\partial n'_i} - W' X . \quad (4.19)$$

Applying the abbreviations $X_{\varepsilon'} \equiv \partial X / \partial \varepsilon'$, $X_{U'} \equiv \partial X / \partial U'$, $X_{V'} \equiv \partial X / \partial V'$ and $X_{n'_i} \equiv \partial X / \partial n'_i$, we calculate the Euler-Lagrange equation (cf. [26] p.191)

$$\left(\frac{\partial}{\partial \varepsilon'} \frac{\partial}{\partial X_{\varepsilon'}} + \frac{\partial}{\partial U'} \frac{\partial}{\partial X_{U'}} + \frac{\partial}{\partial V'} \frac{\partial}{\partial X_{V'}} + \sum_i \frac{\partial}{\partial n'_i} \frac{\partial}{\partial X_{n'_i}} - \frac{\partial}{\partial X} \right) \mathcal{L}' = 0 . \quad (4.20)$$

The result is the differential equation for W'

$$\frac{\partial W'}{\partial \varepsilon'} + \frac{\partial W'}{\partial U'} + \frac{\partial W'}{\partial V'} + \sum_i \frac{\partial W'}{\partial n'_i} + W' = 0 . \quad (4.21)$$

The solution of (4.21) is the distribution function

$$W' = W'_0 \exp[-(\varepsilon' + U' + V' + \sum_i n'_i)/(m+3)] . \quad (4.22)$$

If the definitions (4.15) and (4.17) are reinserted one obtains

$$\hat{W} = \hat{W}_0 \exp[(-\varepsilon - P^*V + \sum_i \mu_i^* n_i)/kT] . \quad (4.23)$$

W'_0 is set to 1 for convenience in (4.22). Then (4.23) is the grand canonic distribution function which is extended here for thermodynamic systems in potential fields.

The norm of W' or \hat{W} are chosen to be

$$\begin{aligned} \int_0^\infty \int_0^\infty \int_0^\infty W'(n'_i, \varepsilon', U') d\mathbf{n}'_i dU' d\varepsilon' &= 1 \\ \int_{\varepsilon_0}^\infty \int_0^\infty \int_0^\infty \hat{W}(n_i, \varepsilon_{int}, U) d\mathbf{n}_i d|U| d\varepsilon_{int} &= 1 . \end{aligned} \quad (4.24)$$

These constraints also fix P^* from (4.23) for given V, T and μ^* and lead to $P^*V/kT = \ln(Z')$ with the grand canonical sum being defined as

$Z' \equiv \int \int \int \exp[-(\varepsilon' + U' + \sum n'_i)] \mathbf{d}\mathbf{n}'_i d|U'| d\varepsilon'$, cf. reference [25].

Now, by using (4.17) the standard representation of thermodynamics can be derived according to the procedure presented in Mayer's book [25] p.8.

The mean number of particles in a volume is

$$\bar{n}_i = \int_{\varepsilon_0}^{\infty} \int_0^{\infty} \int_0^{\infty} n_i \hat{W}(n_i, \varepsilon_{int}, U) \mathbf{d}\mathbf{n}_i d|U| d\varepsilon_{int} . \quad (4.25)$$

The mean of the total Hamilton energy \mathcal{H}^* is

$$\bar{\mathcal{H}}^* = \int_{\varepsilon_0}^{\infty} \int_0^{\infty} \int_0^{\infty} \hat{W}(n_i, \varepsilon_{int}, U) \varepsilon \mathbf{d}\mathbf{n}_i d|U| d\varepsilon_{int} . \quad (4.26)$$

The mean of the total Gibbs's free energy \mathcal{G}^* is

$$\bar{\mathcal{G}}^* = \int_{\varepsilon_0}^{\infty} \int_0^{\infty} \int_0^{\infty} \sum_k \hat{W}(n_i, \varepsilon_{int}, U) n_i \mu_i^* \mathbf{d}\mathbf{n}_i d|U| d\varepsilon_{int} . \quad (4.27)$$

Using the definitions (4.15) and (4.17) it follows from (4.23) by differentiation

$$\begin{aligned} \frac{\partial \hat{W}}{\partial \mu_i^*} &= \frac{\hat{W}}{kT} [n_i - V \frac{\partial P^*}{\partial \mu_i^*}] \\ \frac{\partial \hat{W}}{\partial T} &= \frac{\hat{W}}{kT^2} [P^*V - \sum_i n_i \mu_i^* + \varepsilon - VT \frac{\partial P^*}{\partial T}] . \end{aligned} \quad (4.28)$$

If both equations are integrated over all possibilities each sum of all derivatives is zero because the sum of \hat{W} is 1 according to (4.24). Therefore, the relations between the corresponding mean values (indicated by bars) are

Table 4.1: Analogous solution methods in mechanics and thermodynamics.

	Mechanics	Thermodynamics
functional	$H_{tot} \equiv \frac{1}{\Delta T} \int_0^{\Delta T} \sum_i \left(\frac{p_i^2}{2m_i} + U_i + \sum_{j,i} U_{ij} \right) dt$	$\rightarrow \mathcal{H}'_{tot} \equiv \int_0^\infty \int_0^\infty \int_0^\infty \int_{\varepsilon_0/kT}^\infty W' \times$ $\times (\varepsilon' + U') \rho' d\varepsilon' dU' dn'_i dV'$
Hamilton function	$H \equiv \sum_i \left(\frac{p_i^2}{2m_i} + U_i + \sum_{j,i} U_{ij} \right)$	$\rightarrow \mathcal{H}' \equiv W'(\varepsilon' + U') \rho' \equiv W' X$
independent variable	t	$\rightarrow \mathbf{t} \equiv (\varepsilon', U', n'_i, V')$
dependent variable	x_i	$\rightarrow X \equiv (\varepsilon' + U') \rho'$
Lagrange function	$L \equiv \sum_i p_i(t) \cdot \dot{x}_i - H$	$\rightarrow \mathcal{L}' \equiv \sum_i X \cdot \frac{\partial X}{\partial t_i} - \mathcal{H}'$
solution of Euler-Lagrange	$x_i(t) = \dots$	$\rightarrow W'(\varepsilon', U', n'_i, V') = \dots$

$$\begin{aligned}
\frac{\partial P^*}{\partial \mu_i} &= \bar{n}_i / V \\
\frac{\partial P^*}{\partial T} &= (VT)^{-1} [\bar{\mathcal{H}}^* + P^* V - \bar{\mathcal{G}}^*] = \frac{\bar{\mathcal{S}}}{V} .
\end{aligned} \tag{4.29}$$

From the second equation of (4.29) the entropy $\bar{\mathcal{S}}$ can be calculated to be proportional to Shannon's definition of entropy

$$\bar{\mathcal{S}} = -k \int_0^\infty \int_0^\infty \int_{\varepsilon_0/kT}^\infty W' \ln(W') d\varepsilon' d|U'| d\mathbf{n}'_i , \tag{4.30}$$

cf. as well the definitions (4.22) and (4.23).

Note that the entropy of the field extended formalism of thermodynamics has the same structure as without field. Therefore, it can be concluded that the maximum entropy property holds as well if fields are taken into account.

The calculation procedure from (4.16) to (4.30) works as well for non-extensive thermostatics and allows to calculate the Tsallis distribution.

For Tsallis non-extensive thermodynamics W' is replaced by $f(W') = W'^q/N$ where N is the normalizing factor, cf. [27]). Starting with the Hamiltonian $\mathcal{H}' \equiv W'^q \varepsilon' \rho' / N$ the differential equation of the distribution is

$$\frac{\partial W'}{\partial \varepsilon'} + \frac{\partial W'}{\partial U'} + \frac{\partial W'}{\partial V'} + \sum_i \frac{\partial W'}{\partial n'_i} + W'^q = 0. \quad (4.31)$$

A possible solution has the form $W' = [c + (1 - q)s]^{\frac{1}{1-q}}$ with $s \equiv -(\varepsilon' + U' + V' + \sum_i n'_i)/(m+3)$. Coincidence of the solution with the Boltzmann distribution for $q \rightarrow 1$ demands an initial condition $W'(s = 0) = 1$. This can be resolved for $c = 1$. Hence follows the solution

$$W' \equiv e_q^x = [1 + (1 - q)x]^{\frac{1}{1-q}}. \quad (4.32)$$

This is the Tsallis distribution.

Similarly, if every symbol W' is replaced by $f(W') = W'^q/N$ in the equations (4.24) - (4.30) the Tsallis entropy

$$\bar{\mathcal{S}} = -\frac{k}{N} \int_0^\infty \int_0^\infty \int_{\varepsilon_0/kT}^\infty W'^q \log_q(W') d\varepsilon' dU' d\mathbf{n}'_i. \quad (4.33)$$

follows. Here we applied the definition $\log_q x \equiv \frac{x^{1-q}-1}{1-q}$ as inverse function of e_q^x .

The formalism can be generalized replacing W' or W'^q by a general $f(W'(s))$ to find the adequate entropy. With a generalized logarithm $s \equiv \log_f(W')$ [27] as the inverse function of a generalized exponential function $W'(s) \equiv e_f^s$, a general definition of the entropy for any arbitrary function $f(W'(s))$ follows as

$$\bar{\mathcal{S}} = \frac{k}{N} \sum_i f(W'_i) \log_f(W'_i). \quad (4.34)$$

This general entropy definition is consistent to the thermodynamics in section 4.2.

4.4 the Concept of Temperature

The thermodynamic entropy S is defined by the so-called Gibb's fundamental equation

$$\sum_j dQ_j = \sum_j T_j dS_j = dU + pdV - \sum_i \mu_i dn_i + \dots \quad (4.35)$$

The points in equation (4.35) indicate forgotten possible contributions like field energies for instance. The entropy S or the entropies S_j are necessary functions which have to be introduced in order to be able to close the cycle.

Gibbs and Boltzmann found out that the entropy of equilibrium thermodynamics could be derived as well from a probability distribution function of the particles of the considered system. Because their conclusion is regarded to be generally valid today (it is applied even for non-equilibrium and non-extensive thermodynamics) one may say that today it is not a conclusion furthermore but has changed to be a definition. So one assumes oftenly tentatively as an unproven approach that the thermodynamic and the statistic interpretation are always equivalent despite of many different statistic forms of entropy in non-extensive-thermodynamics and despite of the further complication by time-dependent non-linear thermodynamics. According to this interpretation the temperature is the fit parameter to the distribution and it can loose the link to the classical empirical thermometer definition.

So this definition of temperature can be applied even if the system is beyond or outside of equilibrium thermodynamics maybe if the cycle path is not unique or if no potential exists. For ideal and real equilibrium fluids this alternative approach coincides with the classical definition in the case of equilibrium thermodynamics.

If the particle distribution can be determined experimentally, it follows for a thermodynamic situation that the heat exchange may be defined by $dQ_j \equiv T dS_j$ if a statistic definition of S like Gibbs' definition of entropy or another like Tsallis entropy is applied. Then, the temperature T is the fit parameter to the distribution and - as well in the case of any thermodynamics with caloric measurements - it is the proportional factor between energy and entropy. So a temperature could be defined even for cases if the cycle path is not unique or if it cannot be derived from a potential.

If the potential model description is thermodynamically correct and unique then the cycle can be closed conventionally. In some non-equilibrium cases more entropies and

temperatures have to be introduced for fitting and closing the cycle. Only then the thermodynamic approach can close the cycle and maintain the energy conservation. In the most general case temperatures and entropies lose their original experimental meaning and have only a formal describing character. So the original definitions change their meaning and thermodynamics becomes a theory "for at least everything". It can be applied in order to describe systems like spectral distributions in terms of colour temperatures, macroscopic clusters like star nebulae in terms of a gas of stars.

4.5 Thermodynamics vs. Second Law ?

4.5.1 Second Law Violations in Conservative Fields ?

From the beginning of the development of the theory of thermodynamics there existed doubts whether Gibbs' rules of stability are correct if outer potential forces are applied to a thermodynamic system [28]. The discussion started when Maxwell calculated erroneously that the temperature changes with the height in a gravity field. He corrected soon this error and, by applying the kinetic theory of gases, he derived that the temperature is constant for any equilibrium [29], cf. also equation 4.5.

By this initial error, however, Maxwell woke up Loschmidt who tried to discredit now the Second Law if potential fields are present [30–33]. The primitive idea (neglecting internal forces known only after van der Waals' PhD 1873 [34]) behind the doubts is the following: If any molecule moves up or down in a potential it loses or gains kinetic energy. Because the velocity of a particle represents its temperature in the kinetic theory, temperature has to lower if a particle moves to higher potential energies. So the idea came up that the stratification in atmosphere is not isothermal but isentropic [35]. This idea is applied until today for instance in the popular meteorology to explain climatic situations known as "Foehn", "Mistral" or "Sirocco".

Furthermore, no experimental observations of temperature vs. height so far confirm Maxwell's calculation. Better than Maxwell's barometric pressure equation seems to be a calculation of an isentropic equilibrium stratification applying the assumption $dS(h) = 0$ over the space coordinate h . In dry air v. Dallwitz-Wegner calculates

$\Delta h = 103 \text{ m}$ for $\Delta T = 1K$, the measurement is $\Delta h = 173 \text{ m}$ for $\Delta T = 1K$. [36]

If one checks the isentrope hypothesis of v. Dallwitz-Wegner numerically, one can estimate the difference to the standard view for standard substances for instance by looking into a water steam table. The result is, that the effect can be neglected quantitatively as long as standard thermodynamic problems are regarded. Only near to the critical point of a phase diagram such temperature difference problems are important as shown by high precision thermodynamic measurements. Then, much effort is needed to obtain precise isothermal conditions in a volume [37, 38].

If we regard the stratification of the hydrostatic water pressure we find the opposite gradient dT/dh . The temperature sinks down to 4° Celsius from the surface to the bottom of the sea. This consideration shows that the primitive kinetic idea of temperature (neglecting the real vdW-interactions) is misleading and does not predict generally and correctly the temperature stratification of fluids.

Today the stratification and inversion are explained as non-equilibrium phenomena. Recently Graeff measured a self-organized temperature differences in an strongly isolated dewar volume [39, 40], cf. fig. 4.1. He reports a temperature decrease with height of $7 \times 10^{-2} K/m$ for air and $4 \times 10^{-2} K/m$ for water. Because it is difficult to calibrate the sensors, he applies a difference method. He measures a dewar in a turnable drum filled with material isolating the measurement from the environment. Theoretically he estimates according to the equation ($g \equiv$ gravity, $C_v \equiv$ specific heat)

$$\frac{dT}{dh} = -\nabla_z T = \frac{g}{C_v} \quad (4.36)$$

This equation 4.36 I rewrite the last equation (with $s \equiv$ entropy density)

$$T \frac{ds}{dT} dT = -\rho g dh \quad (4.37)$$

Graeff calculates for air $9 \times 10^{-3} K/m$ and for water $2 \times 10^{-3} K/m$ with height according this method. In his recent book [41] he avoids the significant difference experiment-theory for (ideal) air by taking account for the degrees of freedom n of the gas. He replaces C_v by C_v/n . His maximum value estimation is for Xe $3, 11 \times 10^{-1} K/m$. This estimation explains the values of the ideal gas but it fails for liquid water.

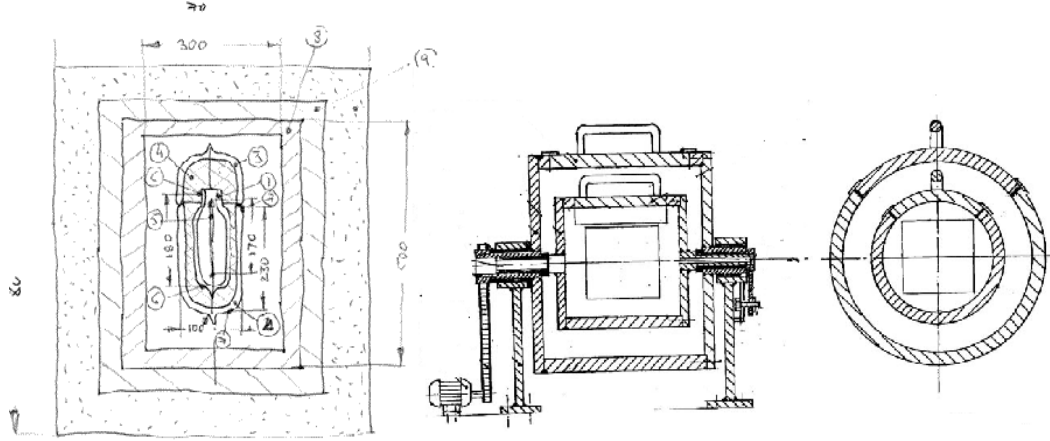


Figure 4.1: the experimental setup of Graeff, cf. [41]

left: dewar with medium and glass wool; middle and right: rotatable drum construction as housing of the dewar cf. text. all free space was filled by thermically isolating material

More accurate values, however, yields his newest kinetic estimation ansatz by applying $mv^2/2 = -m.g.h = k_B T$ in the graviational field. So he obtains (with $v = \sqrt{2.g.h}$)

$$\frac{dT}{dh} \approx -\frac{1}{2}mv^2/(hk) \quad (4.38)$$

This better estimation method yields the correct experimental values for air -0.07 K/m and for water -0.04 K/m .

The formulas remember known effects called entropic forces [42]. Note that the equation 4.37 is contrary to a thermodynamic equilibrium described by eq. 4.6. If Graeff's well documented claims are correct and can be scaled up it would mean that the describing funtion of the material may be not a potential or does has an optimum under additional constraints like eq. 4.36 or 4.37.

I compare now Graeff's result with independent experiments done by P.Fred [43, 44]: Inspired by the experiments of Shaw [45] he performed an "inverse" experiment to Graeff's work and showed that a thermic flow generates an additive mechanical force field of the same direction like the thermal flow in the object. So the thermal gradient can enhance or weaken the gravitational field according to each experimental design, cf. fig.4.2. Similar observations were done by N. Reiter [46, 47] at Peltier elements.

doubtful after own pilot experiments

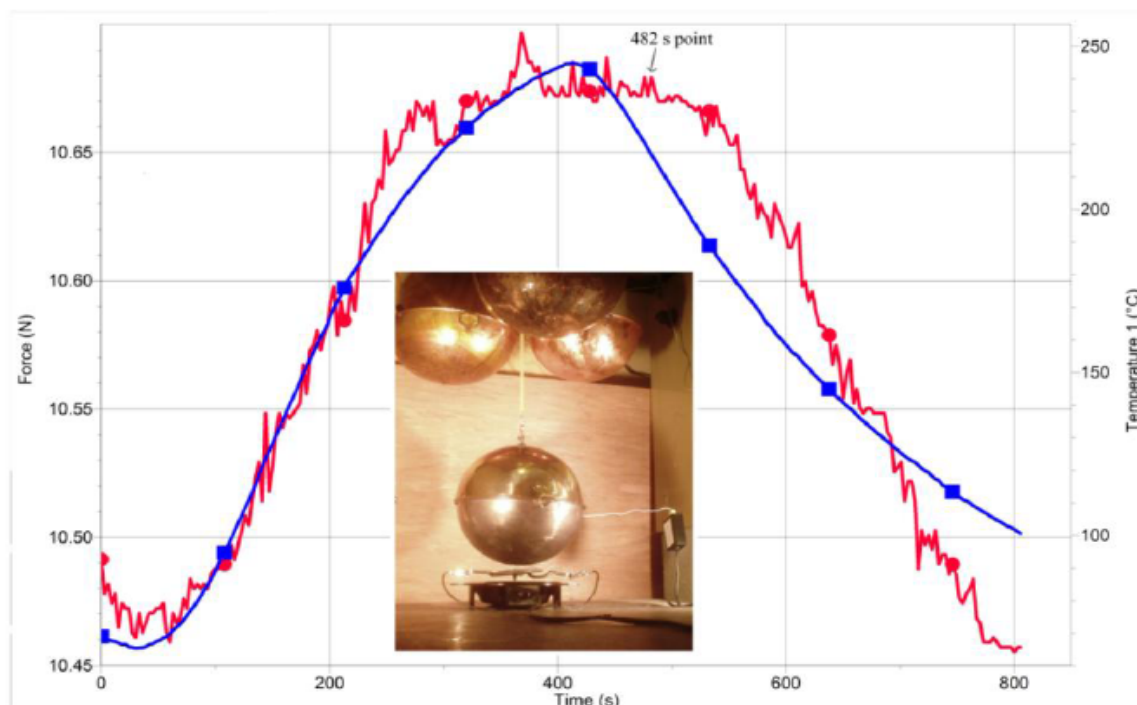


Figure 4.2: "A 1068 gm hollow copper sphere hovers above a 1000 W heat element. The sphere is attached to a wooden dowel, which in turn is attached to force sensor that is located above and is housed in a wooden box (not shown). In order to facilitate the upward flow of heat, three copper hemispheres filled with ice were placed above the sphere. After power was applied to the heat element for 400 s, the means of the first and last 6 force measures indicate that the spheres gravitational mass increased by 1.9 % or 20 gm. At the 400-second point, power was turned off. After 400 s of cooling time, the means of the first and last 6 weight measures indicate that the spheres 'gravitational mass decreased by 2.0 % or 21 gm. The graph with the circles depicts the spheres' weight as a function of time. The graph with squares depicts the temperature as a function time of the lowest point inside the sphere as sensed by a thermocouple wire." from [44]

The "inverse" statement can also be read off qualitatively from equation 4.38 because it holds for the heat flux $\equiv \dot{Q} \propto dT/dh$. Note that the order of magnitude is different. Interesting would be as well experiments in thermoisolated centrifuges where the acceleration g can be set according to $g = r\omega^2$ ($\omega \equiv$ angular velocity, $r \equiv$ radius)[48]. If Graeff's experiments are confirmed they may support the idea of the "perpetuum mobile" centrifuge of von Platen [49] (who invented the adsorption cooling cycle at Electrolux [50]). I simulated the postulated equilibrium cycle and disproved the simplified idea of the machine [50–52]¹, but if modifying effects have to be added these constraints can be implemented in the algorithm for a test.

There exist one reference [48] [41] testing Graeff's claims. This was done also under a centrifugal field. The coincidence between the references [48] and [41] is weak.

4.5.2 Second Law Violations at Low Pressures ?

Interesting claims violating the second law may exist at a sufficient vacuum where the continuum approximation of equilibrium thermodynamics fails, cf. eq.4.5. Then, the mean path length of the particles is higher than the housing vessel dimensions.

Basing on the discussion of his time [36, 53] Holm designed such experiments at low pressures already in the twenties of the last century [53–56]. Because he estimated that a selforganized gravitational temperature gradients is too small due to the equilibrating heat transport in the walls of a metal vessel he built a perpetual (convection ? - W.D.B) motion system at low pressures above 10^{-4} Torr with an turnable drum-like brass housing filled preferentially by a high atomic molecular gas. So he believed to be able to show a "gravitomolecular pressure" detected by a small force on the area of a metal sheet in the volume under isothermal conditions. He supposed that the energy supply of this force was due to the thermal energy equilibrating the internal gradient of the brass housing. He did not discuss the transport balances (for mass, momentum, heat) in space because the relevant theory was developed later [57]. Holm's setup

¹In these cited articles there are some typographic errors:

in [52] equation 5 is $dP/dx_1 = \infty$ $K(P, T, x_1) = 0$. v_c on p.60 is defined as a critical value.

In Table 4.3 the missing definition is $Zwgr2 \equiv Mix1_{ij}.Mix2_{ij}.(x_i.x_j)^{Mix2_{ij}}$

in [51] equation 34 has to be corrected to $K(P, T, x_1) = 0$ $dP/dx_1 = \infty$

and the experiment is described in [54]. The base pressure in his experiment was 10^{-4} Torr. One has to take into account that high vacuum technology and surface science were developed not far at that time. Only with a gas of higher molecular weight (Dimethylacetonylose ($C_{11}H_{18}O_5$)) a "gravimolecular" effect was detectable for him, cf. [55, 56]. Any effect due to adsorption of gases on the surface of the sensor plates he tried to annihilate by his experimental procedures.

Sheehan[58][59] treats a low pressure model theoretically by molecular dynamics. He published about a system consisting of a nonequilibrium steady gas state producing a permanent force field by asymmetric momentum transfer of the rarified gas atmosphere to a bowl body with surfaces of different dissipative properties at the front and at the rear side (similar to a Crooke radiometer wheel). Experimentally the astrophysical assumptions of his model make any experimental testing difficult.

Sheehan discusses as well chemical models basing on surface effects [60][59]. These models also have no thermodynamic equilibrium state according to his opinion. His models show that different reacting surfaces (i.e. spatially distributed different fixed chemical potentials ?) in a volume generate a "dynamic" equilibrium. It generates a pressure gradient near to the reacting surface due to the catalytic dissociation of molecules - or a voltage difference due to different rates of generation or recombination of the plasma charge. He illustrates these claims by experiments with the dissociation of hydrogen plasmas in a black cavity as a single heat bath. This delivers a permanent current due to different electron emission at different metal electrodes according to the Richardson formula. This generates a pressure difference.

Sheehan does not prove non-conservativeness. Pressure gradients can be equilibrium states in fields. Stored chemical potentials of the used materials may explain these effects also as very small (and therefore long lasting) battery effects, cf. also [61] [62].

4.5.3 Nonconservative Systems beyond the Second Law

Quite clear is the situation for systems with time dependent vortex fields. They are beyond the potential formalism of classical equilibrium thermodynamics and can show features of a perpetuum mobile-like behaviour. In terms of non-equilibrium thermodynamics they may be explained also by a permanent stationary influx or a force which

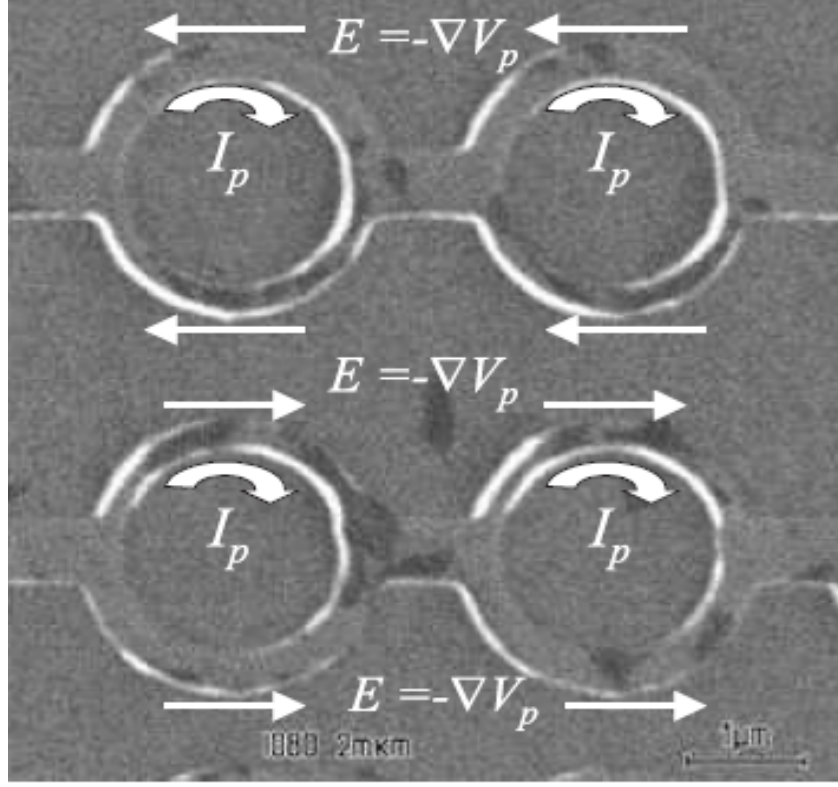


Figure 4.3: "A fragment of the system of 1080 series-connected asymmetric aluminum rings with the same diameter $2r \approx 2 \mu\text{m}$. The sign of the potential difference V_p and the electric field $E = -\nabla V_p$ direction depend on the I_p direction in the narrow half-ring $w_n \approx 0.3 \mu\text{m}$, having higher resistance $R_n > R_w$. In the wide half-ring $w_w \approx 0.4 \mu\text{m}$ the persistent current flows against the electric field $E = -\nabla V_p$ " from [63]

is compensated by a permanent dissipative efflux or a permanent force from outside. Very "modern" systems of this type are published by Gurtovoi, Dubobos et al. [63–73]: They investigate experimentally supraconducting rings in a stationary magnetic field. The magnetic field destroys the uncorrelated noise movement of the electrons and enforces them to move on a cyclic path. The system is set thermally to the phase border of supraconductivity. So the supraconductivity is switched on and off in one half of the rings, cf. also section 6.4.2. This is done by thermal noise. The switching does not cost energy because superconductivity is a phase transition of first order. So the system couples alternately to a quantum and a thermal bath of fluctuations. This generates

a mean voltage difference which can be observed at the resistive non-supraconducting part of the ring. Most articles about the theme are peer-reviewed today, cf [73].

The systems are initiated and explained theoretically by Nikulov [74–78]. Experimentally they are quite complicated to engineer and are not efficient in energy, however they have a theoretical perspective which perhaps can be generalized and transferred.

4.5.4 Further Candidate Systems

The book of Capek and Sheehan[59] and the conference proceedings of the "Quantum Limits of the Second Law", San Diego 2002, cf. [39], summarize the modern theoretical and experimental candidate model systems. The mathematics of these second law violating systems includes typically non-conservativeness, non-continuum thermodynamics, vortex fields, quantum effects and nonlinear dynamics. For these systems Second Law compatibility is not well tested and not sure at all. So far quite all systems are still difficult to realize, at low efficiency and far off from any economic application.

4.6 Conclusions

In this chapter I derived the equilibrium thermodynamics in fields and its statistical distribution by a Hamiltonian variational method which may be new in thermostatics. This was done in order to refer to some critical objections to the Second Law based on equilibrium thermodynamics in fields theoretically and experimentally. It was not possible for me to find second law violating contradictions theoretically if the claimed effects are explained by the standard equilibrium thermodynamics. However, leaving the basic conditions of the equilibrium thermodynamics, there exist systems which violate the second law. So I can conclude:

The classical Second Law stems from classical thermodynamics and implies some implicit not mentioned hidden assumptions. If we drop them by the appropriate choice of preconditions the development of Second Law violating systems may be possible.

4.7 Appendix-Calculating the Fluid Stratification

I solve numerically the stratification of a gaseous mixture near to the critical point. So I describe first the subelements which are used below to build up the algorithm.

4.7.1 the Equation of State

The Bender equation of state [79] is applied for the computation of thermodynamic state of the mixture in the field. The equation has the form

$$\frac{Pv}{RT} = 1 + \delta\Xi(1) + \delta^2\Xi(2) + \delta^3\Xi(3) + \delta^4\Xi(4) + \delta^5\Xi(5) + \delta^2 \exp(-\delta^2)[\Xi(6) + \delta^2\Xi(7)] \quad (4.39)$$

The abbreviations δ and $\Xi(j)$ have the following meaning

$$\begin{aligned} \delta &\equiv v_c/v, \\ \Xi(1) &\equiv e_1 - e_2\tau - e_3\tau^2 - e_4\tau^3 - e_5\tau^4, \\ \Xi(2) &\equiv e_6 + e_7\tau + e_8\tau^2, \\ \Xi(3) &\equiv e_9 + e_{10}\tau, \\ \Xi(4) &\equiv e_{11} + e_{12}\tau, \\ \Xi(5) &\equiv e_{13}\tau, \\ \Xi(6) &\equiv e_{14}\tau^3 + e_{15}\tau^4 + e_{16}\tau^5, \\ \Xi(7) &\equiv e_{17}\tau^3 + e_{18}\tau^4 + e_{19}\tau^5 \end{aligned} \quad (4.40)$$

The subscript c denotes values at the critical point, τ is defined by $\tau \equiv T_c/T$, and the e_j by $e_j \equiv g_{4,j} + g_{1,j}\omega + g_{2,j}\chi + g_{3,j}\omega\chi + g_{5,j}\chi^2$. The g -coefficients are tabulated in [80], ω (the acentric factor) and χ (the Stiel polar factor) are taken from [81].

In the generalized Bender equation of state eq.4.39 and 4.40 the critical values v_c and T_c of the mixture appear which we will mark by an additional index M as v_{cM}, T_{cM} . Also the material constants ω and χ belong to the mixture and will be denoted as ω_M and χ_M . The values of these four quantities are calculated by the pseudo-critical mixture rule of Tsai and Shuy [82] in a version of Platzer [80]: Characterizing the

components of the mixture by indices i, j, \dots we have

$$\begin{aligned} v_{cM} &= \sum_{ij} x_i x_j v_{cij} \quad \text{with} \quad v_{cij} \equiv \frac{1}{8} [v_{ci}^{1/3} + v_{cj}^{1/3}]^3 \zeta_{ij} \\ T_{cM} &= v_{cM}^{-\eta} \sum_{ij} x_i x_j \sqrt{T_{ci} T_{cj} (v_{ci} v_{cj})^\eta k_{ij}} \\ \omega_M &= \sum_i x_i \omega_i, \quad \chi_M = \sum_i x_i \chi_i. \end{aligned} \quad (4.41)$$

Here the constants η , k_{ij} and ζ_{ij} are fitting parameters. The material data of the pure components were taken from [80, 81, 83], where more constitutive data can be found.

4.7.2 the Phase Equilibrium

In order to calculate the phase equilibrium we have to solve Gibbs' equilibrium conditions. The first equation bases on equal pressures in vapour(index $_g$) and liquid($_f$)

$$P(T, v^g, x_1^g) = P(T, v^f, x_1^f). \quad (4.42)$$

The other equations base on equal chemical potentials or fugacities in vapour and liquid valid for each component. In our case we use the definition of fugacity

$$f_i \equiv x_i P \varphi_i = f(T, v, x_1), \quad (i, j = 1, 2; i \neq j). \quad (4.43)$$

Here the fugacity coefficients are calculated according to a formula derived in [84]

$$\begin{aligned} \ln \varphi_i &= Z_M - 1 - \ln Z_M + \frac{1}{RT} \int_v^\infty \left(P - \frac{RT}{v} \right) dv \\ &\quad - \frac{1}{RT} \int_v^\infty \sum_{i \neq j, j=1}^n \left(\frac{\partial P}{\partial x_j} \right)_{T, v, x_l} x_j dv, \end{aligned} \quad (4.44)$$

using the abbreviation $Z_M \equiv \frac{Pv}{RT}$. Because x_1^f and T are fixed variables (therefore they are dropped down) and v^f , v^g , and x_1^g are wanted we get the equation system

$$\begin{pmatrix} \Delta P(v^f, v^g, x_1^g) \\ \Delta f_1(v^f, v^g, x_1^g) \\ \Delta f_2(v^f, v^g, x_1^g) \end{pmatrix} \equiv \begin{pmatrix} P(v^f) - P(v^g, x_1^g) \\ f_1(v^f) - f_1(v^g, x_1^g) \\ f_2(v^f) - f_2(v^g, 1 - x_1^g) \end{pmatrix} = \vec{0} \quad (4.45)$$

which is solved by using a Gauss-Newton or Newton-Raphson algorithm.

After having solved this problem numerically all thermodynamic quantities can be derived. [52] contains more details of the used program routine. The relevant formulas necessary for the iteration and the derivation of all relevant thermodynamic quantities can be found there as well. In our program the calculating subroutine is called *EOS*.

4.7.3 Inverting the Equation of State

The Bender equation of state is formulated analytically in the form $P(v, T, x_i, \dots, x_{n-1})$ with v , T and x_i as independent variables. (n is the number of components). However, for our calculation purposes below the equation of state (EOS) should be dependent from other variables.

So, in some situations we have to know the thermodynamical state dependent from P_0 , T and x_i . This inversion can be done numerically by solving the equation for v

$$P_0 - P(v) = 0 \quad (4.46)$$

by a Newton algorithm. P_0 is the given pressure, $P(v)$ is the Bender EOS in dependence of v which is iterated until the accuracy of 4.46 is sufficient. The variables T and x_i are constant during the iteration. Our corresponding subroutine is called *V_PTX*. In order to calculate the equation of state in the different spatial compartments we have to be able to solve also the set of constitutive equations dependent from P and μ_i . The numerical solution of this problem is done if the system of equations

$$\begin{aligned} P_0 - P(v, T, x_i) &= 0 \\ \mu_1^0 - \mu_1(v, T, x_i) &= 0 \\ \dots\dots\dots &= 0 \quad (i = 1, 2, \dots, n-1) \\ \mu_n^0 - \mu_n(v, T, x_i) &= 0 \end{aligned} \quad (4.47)$$

is solved by a Newton-Raphson iteration procedure. P_0 is the given pressure, μ_i^0 are the given chemical potentials, $P(v, T, x_i)$ and $\mu_i(v, T, x_i)$ are the calculated values from the Bender equation in dependence of the wanted values of v , T and x_i which all are iterated until the accuracy is sufficient. This subroutine is called *VTX_PMu*.

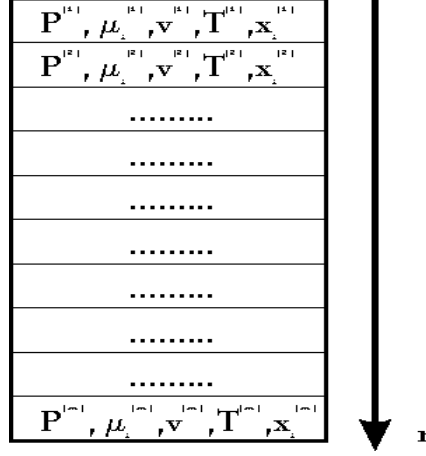


Figure 4.4: Calculating the volume array of the fluid, cf. text of section 4.7.4

4.7.4 Spatial Distribution of Pressure and Chemical Potential

We calculate here the pressures and the chemical potentials in the volume if a known field from outside is applied. Our calculation is only one-dimensional. For calculation the whole volume is divided into a array of m compartment $\Delta V(r_j) = \Delta r_j * A_j$ of specific volume v_i and molar mass M_i at the space coordinate r_j at the field acceleration $g(r_j)$ in the potential $U(r_j)$. Then, if we know the pressure $P(r_{ref})$ and the concentration x_i^{ref} in one compartment at r_{ref} , we can calculate the pressure and the chemical potential of all other compartments subsequently by

$$\begin{aligned}
 P(r_j) &= P(r_{j-1}) + \frac{g(r_{j-1})}{v(r_{j-1})} \sum_{i=1}^n M_i x_i(r_{j-1}) \Delta r \\
 \mu_i(r_j) &= \mu_i(r_{j-1}) + M_i (U(r_{j-1}) - U(r_j))
 \end{aligned}
 \tag{4.48}$$

For programming the formula $\mu_i = \mu_{i0}(p^+, T) + RT \ln(f_i/p^+) + M_i U(r)$ has to be applied, cf. [84]. In our code the corresponding subroutine is called *VOLUME*.

If the thermodynamic state of the reference compartment is given this routine calculates the full state of all other compartments of the total volume (cf. fig.4.4) by applying the subroutines from sec.4.7.3.

4.7.5 the Mass Conservation

The total particle number is conserved, therefore the whole volume array in the field is subjected to the constraints

$$N_i^0 = \sum_{j=1}^n N_i(j) = \text{const}_i. \quad (4.49)$$

As shown above the total particle numbers N_i in the volume can be calculated in each compartment by the subroutine VTX_PMu if no field is applied. If a field is applied mass conservation is achieved by finding the appropriate starting values for $P(r_{ref})$ and x_i^{ref} . Therefore the following system of equations has to be solved by help of the subroutine *VOLUME*

$$N_i^0 - N_i(P_{ref}, x_i^{ref}) = N_i - \sum_{j=1}^{m-1} \frac{x_i(r_j)A(r_j)}{v(r_j)} \Delta r \quad (4.50)$$

Although we do not know the function $N_i^0 - N_i(P_{ref}, x_i^{ref})$ explicitly we can approximate numerically its Jacobi matrix by calculating the difference quotients stepwise from the solving Newton-Raphson iteration procedure. This allows to solve for P_{ref} and x_i^{ref} . The corresponding subroutine is called *N_PX*.

4.7.6 Synthesizing the whole Compartment Solver

The algorithm determining the state of the volume in the field proceeds as follows :

- Define the number M of volume array cells, initialize $N_i = 0$
- Give temperature T_0 and mean concentrations x_i^0
- Sum up the particle number $N_i(0)$ of each species
- Calculate the full thermodynamic state at no field using *EOS*
- Choose the angular velocity and calculate the centrifugal field at each r
- Choose the arbitrary reference volume at r_{ref}
- Estimate P_{ref} and x_i^{ref} at r_{ref}
- **ITERATE** N_PX i.e. $(N_i(0) - N_i) \rightarrow 0$
 - Determine the full state at P_{ref} and x_i^{ref} using *V_PX* and *EOS*
 - Determine full thermodynamic state at each r_j using *VOLUME*
 - Determine the number of particles $\Delta N_i(r_j)$ of each sort i in the subvolume $\Delta V(r_j)$ from *VOLUME*
 - Calculate $N_i := N_i + \Delta N_i(r_j)$ adding up the particle numbers of the whole compartment
- **CONTINUE IF** P_{ref} and x_i^{ref} is not accurate enough for $(N_i(0) - N_i) < \epsilon$
- Give out all calculated values !

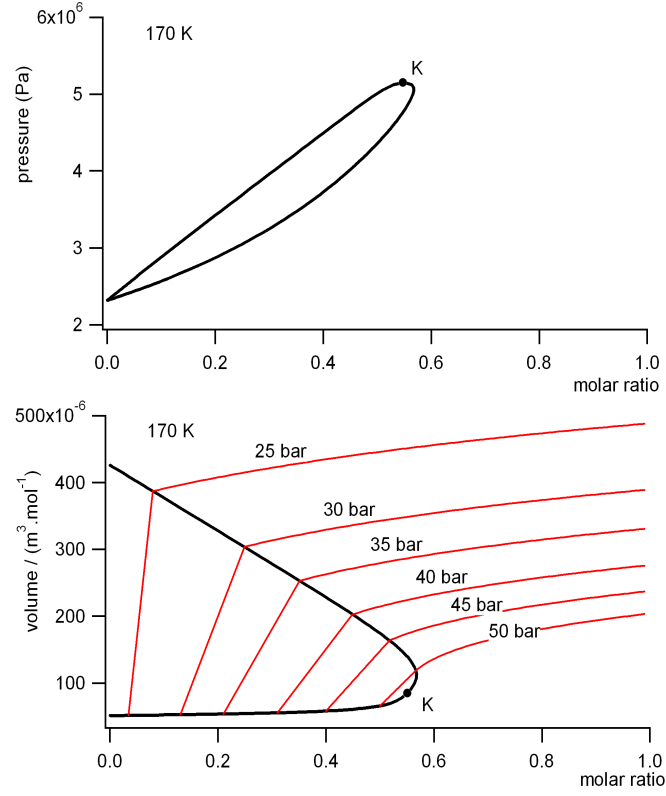


Figure 4.5: Phase diagrams of the mixture $Ar - CH_4$ at $170^\circ K$

Upper diagram : pressure vs. molar ratio of Argon.

Lower diagram: spec. volume vs. molar ratio of Argon

4.7.7 Results

I used the mixture Argon-Methan at $177^\circ C$ as numeric lab rat in order to test the algorithm. First, I calculated the fit constants (result $k_{12} = .9977865068023702$, $\chi_{12} = 1.033181352446963$, $\eta_M = 2.546215505163194$) to the data using the least square routine described in [52] and in [85]. With these model data I calculated the rotator cycle shown in fig.4.6. The starting state was a mixture with a molar ratio of Argon of 56 %, 55 bar and 170 K . This is near to the critical point K in the gaseous area of the phase diagram, cf. fig.4.5. The vessel is assumed to extend from a radius of 20cm to 30cm. The cross section of the vessel is set to be the same at each radius. If the vessel

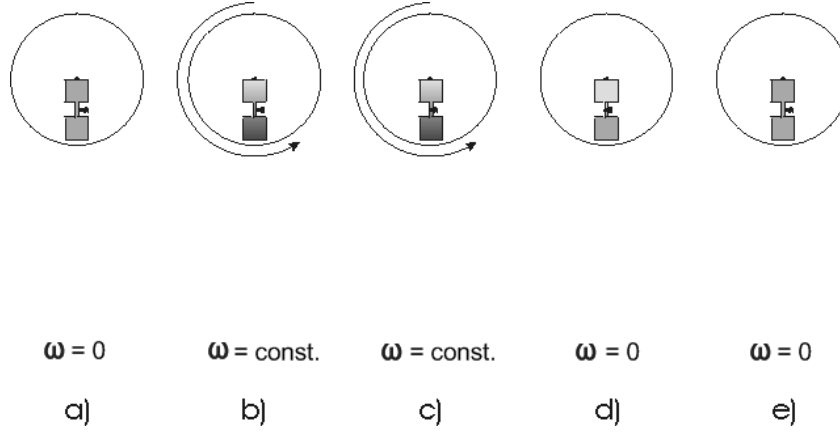


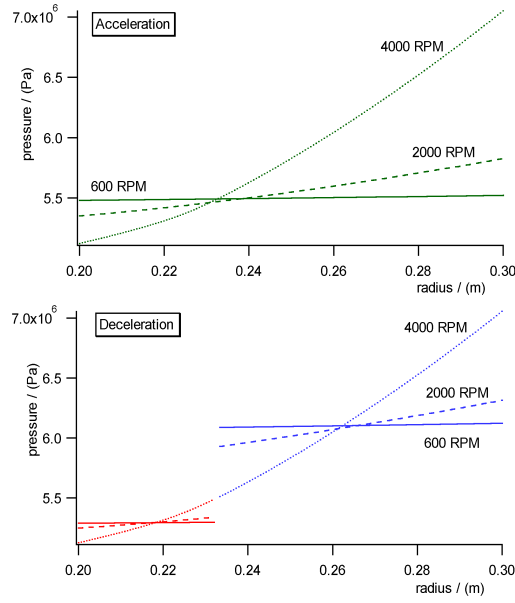
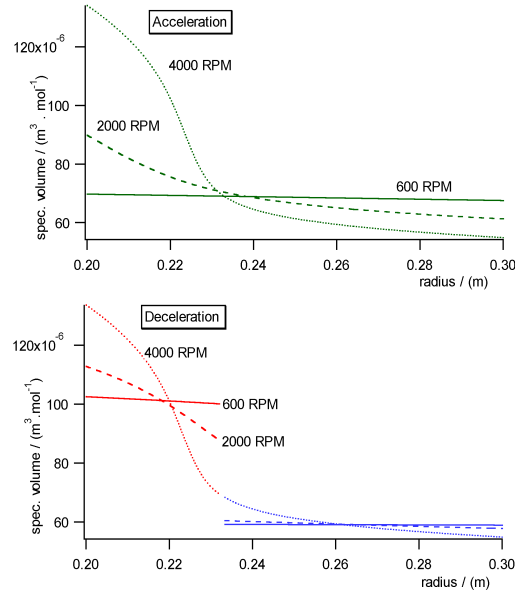
Figure 4.6: the kinetic rotation cycle in a centrifuge ($\omega \equiv$ angular velocity)
a) initial state b) after acceleration c) separation d) after deceleration e) mixing

volume is under rotation at 4000 RPM the total volume is split unsymmetrically into two halves by a tap. The split point is chosen arbitrarily where the specific volume in the field equals about the specific volume without field. Then, both volumes are decelerated again to the field free situation. Fig. 4.7 - Fig. 4.9 shows the pressure, concentration and specific molar volume profiles vs. radius in the centrifugal field of the vessel each during acceleration (upper diagram) and deceleration (lower diagram). Fig. 4.6 shows the integrated work diagram of the cycle acceleration - volume splitting by tap - deceleration calculated from the diagrams 4.7 - Fig. 4.9. A tabel calculation program performs the numeric integration of the mass distributed in the volume array. Note that the profiles depend on the shape of the vessel due to the mass conservation (not shown here explicitly by numeric examples!).

Our calculation of the isothermal cycle indicates a mechanical energy loss and therefore an entropic dissipation. This can be seen if one analyzes the orientation of the rotation work diagram, where W_{rot} is defined as

$$W_{rot} = \int T d\varphi = \int \dot{L} \omega dt = \int \omega dL \quad (4.51)$$

Fig. 4.10 shows the calculated work area with an orientation of an entropic loss.

Figure 4.7: the kinetic rotation cycle of the centrifuge , Pressure P vs. radius r Figure 4.8: the kinetic rotation cycle of the centrifuge, spec. volume v vs. r

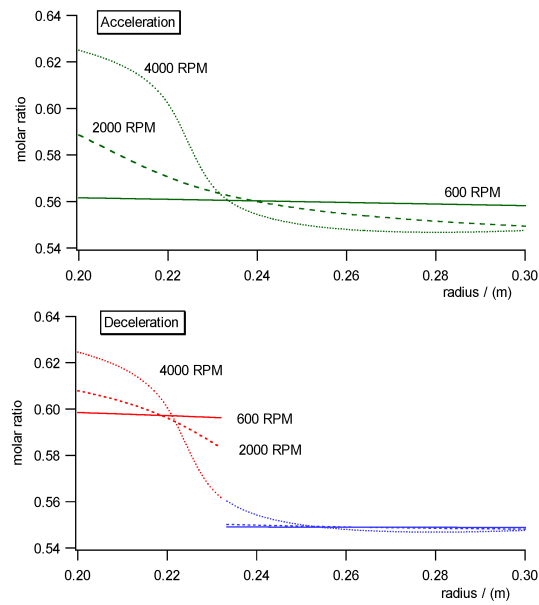


Figure 4.9: the kinetic rotation cycle of the centrifuge, molar ratio x vs. radius r

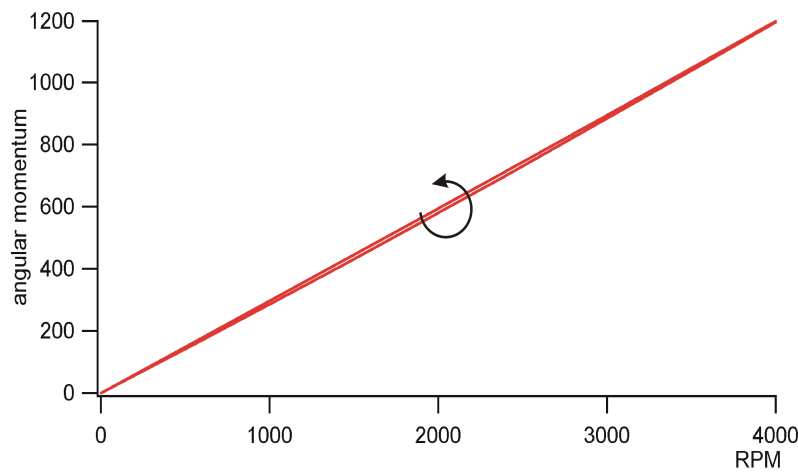


Figure 4.10: the total kinetic rotation work area of the cycle of the centrifuge.

Chapter 5

No Second Law in Thermodynamics ?

5.1 Historical Introduction

The Hungarian engineer Arnold Irinyi had the idea to enhance the efficiencies of steam engines by vapor mixtures. In 1928 he used a mixed vapor of water-benzene as fluid in ordinary steam engines [86]. It was confirmed by independent referies that his machine had an efficieny significantly higher than the conventional water steam engines. Irinyi himself claimed that efficiencies are possible higher than predicted by Carnot. Rudolf Doczekal from Vienna overtook the idea and analysed the thermodynamic processes of the fluid mixture in experiment and in theory as far it was possible to him [87]. He identified a so named "dual effect". This meant that he observed condensation of fluid during expansion and compression. He stated that labile effects are responsible

for these effects. His steam engine is documented in a patent [88]. He claimed to have obtained an efficiency higher than allowed by Carnot. His steam engine could run at reduced power even if the condensor was switched off [89]. With the death of Rudolf Doczekal in 1944 this research finished. However the memory in this machine project was carried over in our time by Alois Urach, a non-expert [90] who was acquainted over his life with the Austrian underground outsider scene of alternative science. He rescued the unpublished scientific papers and drafts after the death of Doczekal and distributed copies of them. One of his "clients", the German journalist Gottfried Hielscher revived the memory in this scientific work in his book "Energie im Überfluss" in 1981 [50]. So many people in the German speaking Europe were informed about this science. And before Urach died around 1990 Bernhard Schaeffer from Berlin succeeded to get copies of Doczekal's scientific bequest from Alois Urach's library. At this time Schaeffer had a professional workshop. Additionally he was the official head of the "Werkstatt für dezentrale Energieforschung", a little association in Berlin interested in green and alternative science. The author himself was a member of this association and so he could get some of the hidden information from Doczekal's bequest reported in this chapter here. Schaeffer succeeded to get money for an evaluating research and -with the help of his studying sons Jörg (hardware) and Kai (software) - he built an test apparatus to observe the thermodynamic effects of this vapor mixture. This was a boiler for water-benzene connected to a cylinder with piston including sensors for fast measurements of pressure and temperature plus computer control and readout. Later an optical observation of the steam was added. The first results were very encouraging. Although they were quite irregular and not very reproducible some of them showed a tremendous gain of this cycle. A patent was filed [91], an article was written [92]. Due to this "success" a big party was organized on a ship where this success was celebrated. Some weeks later the mood changed into the depressive. It seemed that the sensor that was affected by the water-benzene mixture. Some changes at the sensors let disappear the huge effect. From my memory the curves after this changes were as expected from conventional thermodynamics and showed a small loss at the first sight. The matter was regarded like a flop and the spread-out of the article was stopped. Schaeffer's interests changed and he tried to get help from Prof. Albert Serogodsky from Russia who claimed to have measured similar labile effects with high pressure systems either liquid water below 4°C or nitrogen-butane at about 100°C [93]. Therefore, for some

years the water-benzene project slept. In 2005 the author heard that Schaeffer must have followed the theme and claimed now to have rebuilt successfully a little Irinyi labile state steam engine with over Carnot efficiency. Schaeffer claimed now to have measured an efficiency of about 60% driven by a temperature difference from 180°C or 160°C to 80°C. He claimed to have confirmed Doczekal's observations with vapor mixtures. With Gelia Lerche he founded the LESA-GmbH [94], a company in Berlin with the mission, to produce and to sell the electricity and/or the power plants.

Therefore the author decided to evaluate these claims theoretically, first by equilibrium thermodynamics and later by non-equilibrium thermodynamics in order to evaluate the system. The new developed theoretical methods and results are presented here.

5.2 The Work of Irinyi, Doczekal and Schaeffer

5.2.1 Irinyi

Irinyi worked at the Deutsche Institut für Energieforschung in Hamburg. He built a test steam engine which could be driven either by steam of water or by a mixed steam of water-benzene. He held patents in Germany and Austria [95][96]. The principal simple setup and a photo of the machine is shown in fig.5.1 . It was a two cylinder engine constructed for pressures of 10-12 atü typical and 45 PS power at 260 rpm. The heat was feeded into the machine cycle by pressured water (6 atü) as medium over a heat exchanger-boiler S (cf. fig.5.1). Therein the liquid medium (water or water / benzene) was evaporated. The mechanical work was produced in the machine M, the remaining steam was condensed in the condenser C . The condensed liquid was pressed back into the boiler S by a pump Sp. For the calculation the authors define the energy fluxes Q_i of the fluid cyle. The location of the heat fluxes Q_i in the cycle are found in the left diagram of fig.5.1. The following balances can be read off:

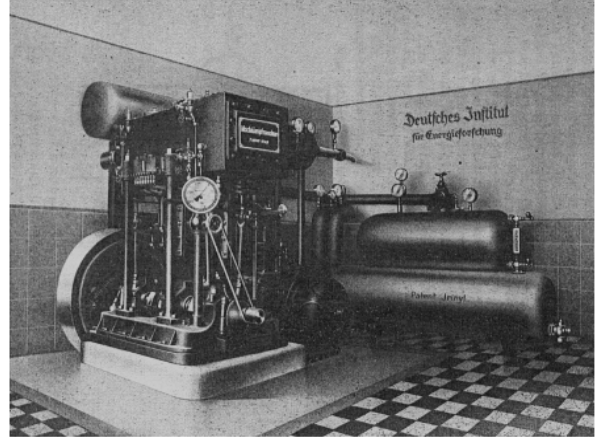
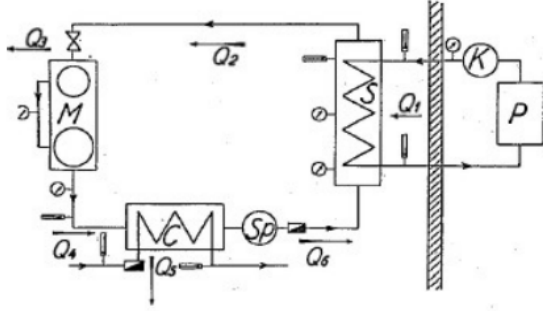


Figure 5.1: Irinyi's steam engine (from[96])

M machine, C condensor, Sp pump for liquid, S heat exchanger boiler, P boiler, K pump for heat transporting pressured water, Q_i -arrows indicate energy fluxes

$$\begin{aligned} Q_1 &= Q_5 - Q_2 \\ Q_3 &= Q_4 - Q_2 \\ Q_5 &= Q_6 - Q_4 \end{aligned} \tag{5.1}$$

The relevant exchanged energy fluxes are:

Q_1 : input heat flux supplied at the heat exchanger measured by temperature difference between water inflow and outflow; the water flux is measured by a flow meter;

Q_3 : mechanical power output measured by a generator;

Q_5 : heat loss flux at the condensor measured similar like Q_1 ;

The performance of the machine was checked by five independent referies [86]. R. Meyer measured the ratio Q_3/Q_1 . He observed that approximately that the half of the heat was needed for the same mechanical work output if the changed the fluid from pure water steam to water/benzene mixed steam. More exact are the experiments by W. Ketterer. His results can be found in tabel 5.1 and confirm R. Meyer's report.

Table 5.1: The measurement of Irinyi's steam engine according to W. Ketterer[86]

	Water	Water-Benzene
work Q_3	5160	17440
heat input Q_1	75090	109940
heat loss Q_5	86350	132700
experimental efficiency Q_3/Q_1	6.86 %	15.85 %
highest temperature T_2	208.8 C	176.2 C
lowest temperature T_1	85.8 C	54.0 C
theoretical Carnot efficiency $(T_2 - T_1)/T_2$	43,3 %	27,2 %

From this data one can read off also that the machine performance was less than the Carnot efficiency for water and for the mixed steam. However, the order of magnitude of the measured efficiency of the mixed steam is similar if compared with predictions for conventional ORC-cycle machines today [97]. Irinyi however claims that over-Carnot efficiency can be achieved. This claim may base on his diagrams shown in fig. 5.2 and fig. 5.3. Because the experimental origin is unclear and its explanation was not found I do not discuss it in detail.

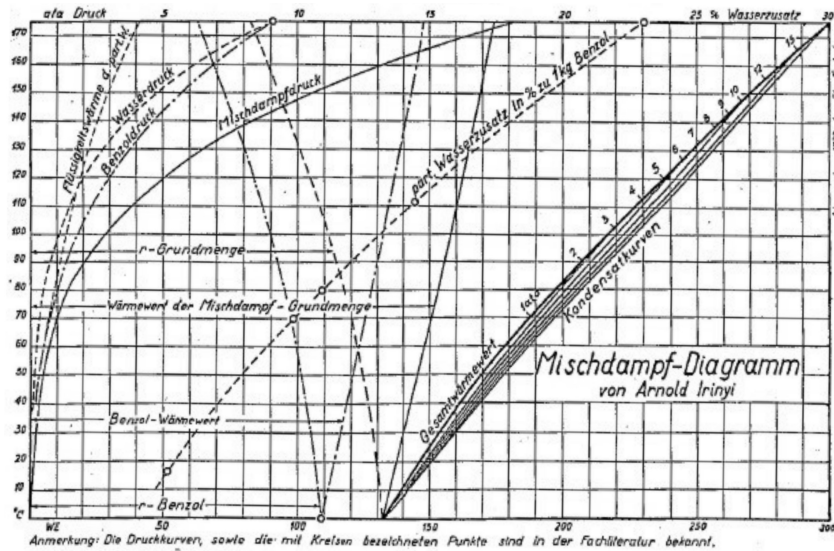


Figure 5.2: Irinyi's diagram of mixed vapour steam (from[96])

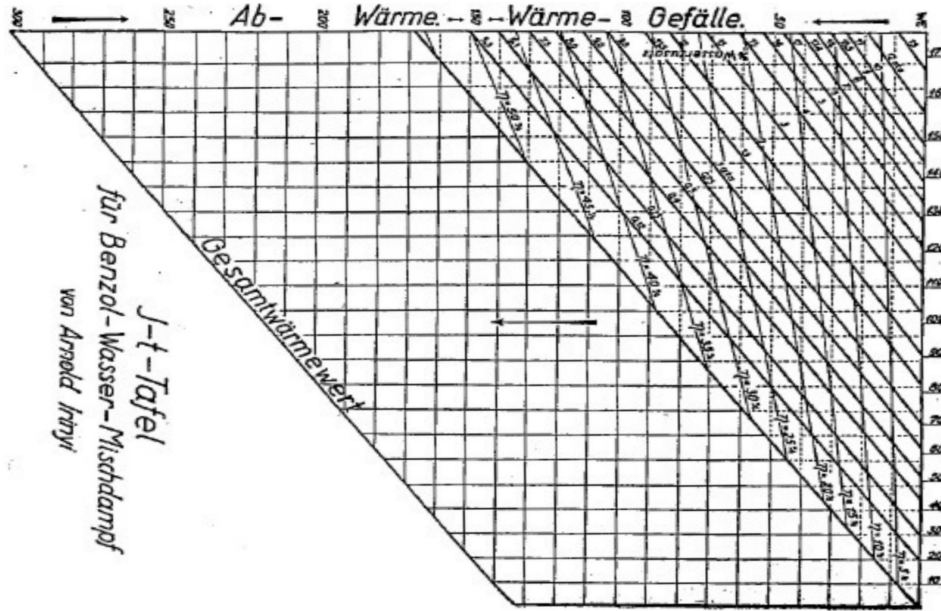


Figure 5.3: Irinyi's enthalpy (J) - temperature(t) diagram (from[96])

In Irinyi's booklet [86] the referee Lothar Grosse calculates a (Rankine) cycle between $T = 170^{\circ}\text{C}$ and $T = 30^{\circ}\text{C}$ with water benzene as fluid.

His result shows in deed an over-Carnot efficiency.

However, it has to be doubted that the underlying assumptions of the calculation are correct. For Grosse does not notice that he assumes implicitly that the mixed steam has to be always in the saturated and azeotropic state. Later this wrong assumption was overtaken by Schaeffer [98]. In both cases the real equilibrium phase diagram water benzene is not accounted for. The phase diagram suggest also unsaturated or partly saturated states of the mixed steam. We will see below that a corrected quasi-equilibrium calculation includes these states. My own rough equilibrium calculation of the cycle confirms the large efficiency as claimed by Irinyi. From Irinyi's booklet it is not clear whether a over-Carnot efficiency was measured in his institute in deed or whether the claims are only predictions based on unfounded assumptions.

5.2.2 Doczekal

Rudolf Doczekal in Vienna overtook the scientific heritage of Irinyi and investigated the theme with the modern methods of his time. He tested out also other water-hydrocarbon mixtures. He discovered that the mixed steam was a non-equilibrium system and investigated this aspect in more detail. So he built up the following test apparatus for the measurement of P-V -diagrams[89]: "You see in fig. 5.4 the experimental setup consisting of a cylinder, an evaporator and a pressure bomb in order to produce the counter pressure. The cylinder walls were heated up electrically in order to reduce heat exchange between the dual-vapor and the walls".

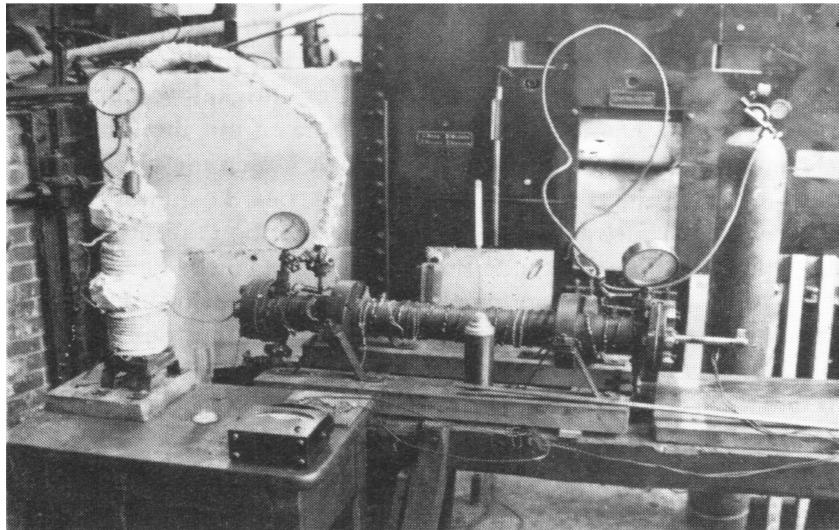


Figure 5.4: Doczekal's working bench for measuring P-V -diagram of mixture vapors [50] left side in the photo: the electro boiler wrapped in isolation material and working as vapor evaporator of the liquid mixture; middle: the horizontal cylinder tube which contains a invisible plunger inside. The cylinder can be pressurized from both sides as plungers in old steam engines. One side of the cylinder is loaded by the vapor mixture produced in the boiler, the other side of the cylinder is loaded by the bomb of pressured air standing in the background at the right side. The cylinder can be heated may be by some heating coils wrapped around its circumference. The volume is measured by the length of the long thin moveable rod pointing out to the right side at the right end of the cylinder.

Doczekal calculated also theoretically these curves with methods available.

The data taken by this setup are shown in fig. 5.5. Doczekal writes: "In fig.5.5 you see the calculated p-v diagram with the calculated adiabatic exponents. The adiabatic coefficient is one for the isotherm. For the dual vapour the exponents change with temperature. The coefficients are below 1 for most values. Furthermore you see two diagrams which coincide with the calculated prediction for most values. The temperature was measured by a thermocouple fixed to the plunger in the cylinder. It was interesting to observe what happened if the plunger went back. Without any

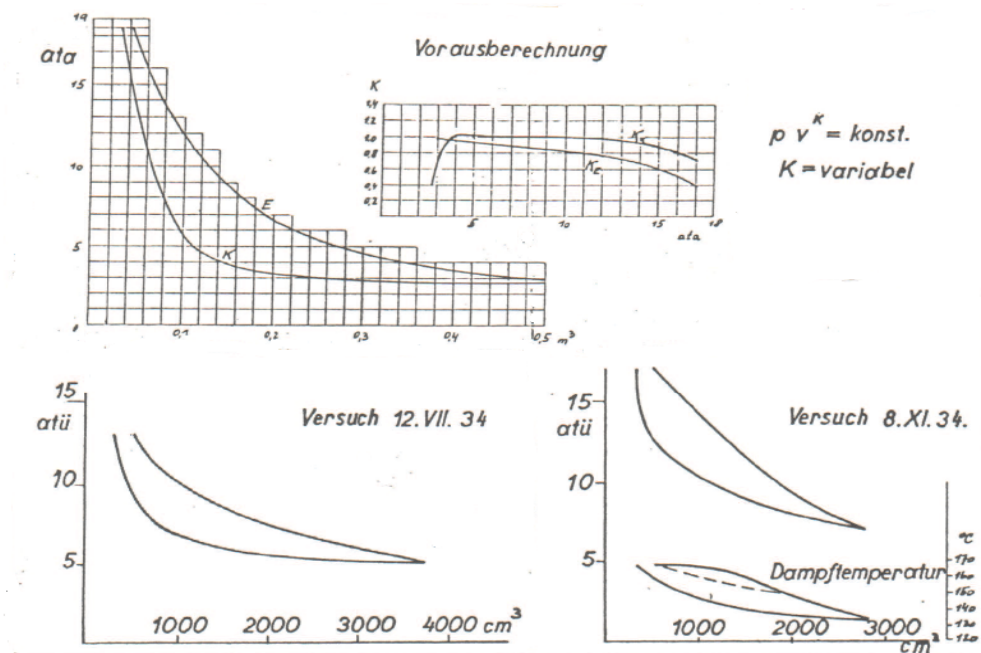


Figure 5.5: Doczekal's results with mixture vapor measured with the previous setup [89]

The upper two diagrams represent theoretical calculated values .

Lower row left diagram: expansion and recompression at a initial expansion factor of $V=7$. The starting temperature is 164°C recalculated by a saturated pressure equation.

Lower row right diagrams: expansion and recompression at a initial expansion factor of $V=5.6$. The starting temperature is $173,6^{\circ}\text{C}$ calculated by a saturated pressure equation. Probably there happened an error in the drawing of the temperature-volume diagram. The theory starting value shows a mismatch in temperature of ≈ 10 degree too low, cf. fig. 5.21.

remarkable change of the pressure the plunger jumped back to half of the full expansion volume - a strong argument that half-labile states were responsible for the effect.” Because these test measurement were promising ”...I decided to build a test machine in order to be able to confirm a high efficiency. The photo and the scheme of the apparatus you see in fig. 5.6. In an electric boiler dual vapor is generated which feeds a reconstructed FIAT four cylinder motor working as a steam motor. The first cylinder worked as a high pressure cylinder, two parallel connected cylinders worked as low pressure cylinders and the last cylinder worked as a compressor. It had to compress the vapor again to the pressure of the boiler. It was shown that this was possible. But in order to avoid water strokes a pump was installed between the compressor and the boiler. In order to start the machine a condensor was implemented. It is clear that the machine could not work if the condensor was switched off. In deed the machine stopped immediately if it was filled only with water as working fluid. The things were different if dual steam was used. If the condensor was switched off and at relatively low pressures ($\approx 1 - 5$ bar estimated WDB) the engine run in deed.

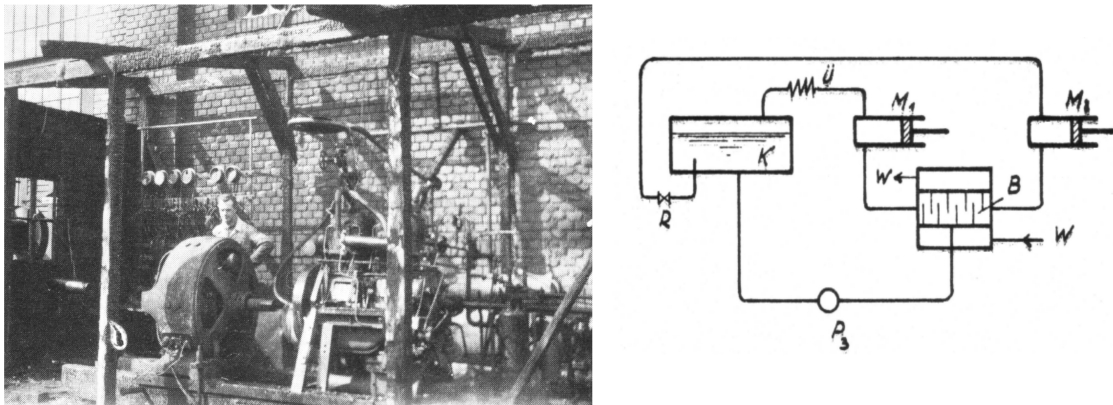


Figure 5.6: Doczekal's steam engine

left side: photo of the setup (from [50]);

right insert: Sceme of Doczekal's patented dual vapor cycle machine (from [88])

M3 expansion cylinder, M1 compression cylinder' B separator and condensor of liquid and gas, R valve, UE overpressure valve, P3 pump

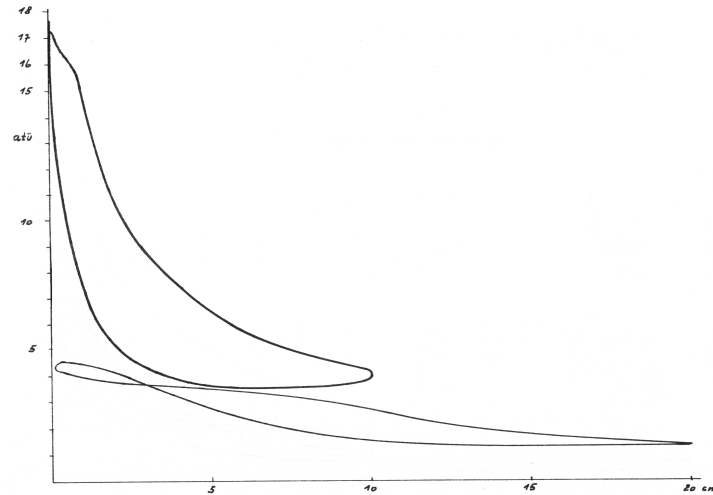


Figure 5.7: typical double working diagram of Doczekal's steam engine (from [89])
 interpretation: the expansion of the first loop may refer to the first expansion, then the steam is pressed into the double expansion cylinder and is recompressed. Note that the first loop has a gain and the second loop a loss orientation

This proved that the predicting calculations were correct.”

A typical pressure diagram of this setup in the normal state is shown in fig. 5.7.

Doczekal built also a demonstration apparatus in order to make visible qualitatively the labile effects standing behind his measurements. He writes [87]: ” In order to make visible what happens in a dual vapor the apparatus in fig. 5.8 was used. If pressured air is applied to the mercury in the vessel the mercury can be pressed into the glass column. In this column the liquid under investigation is filled in above the mercury. After the air is removed the glass is screwed off and the liquid is heated to the wanted temperature by the radiation heaters around the column from outside. In order to avoid any condensation in the tube not only the mercury is heated in the upper part but also the space between the glass and the protecting tube is heated by a copper coil filled with flowing hot water. This is done by a thermostat which sets the temperature also in the vessel with mercury”.

The observed mixture was water-gasoline (Octane number 43). Probably this mixture was chosen in order to protect the glass tube. Gasoline is apolar and has a similar phase diagram like benzene but it exerts less pressure at the same temperature.

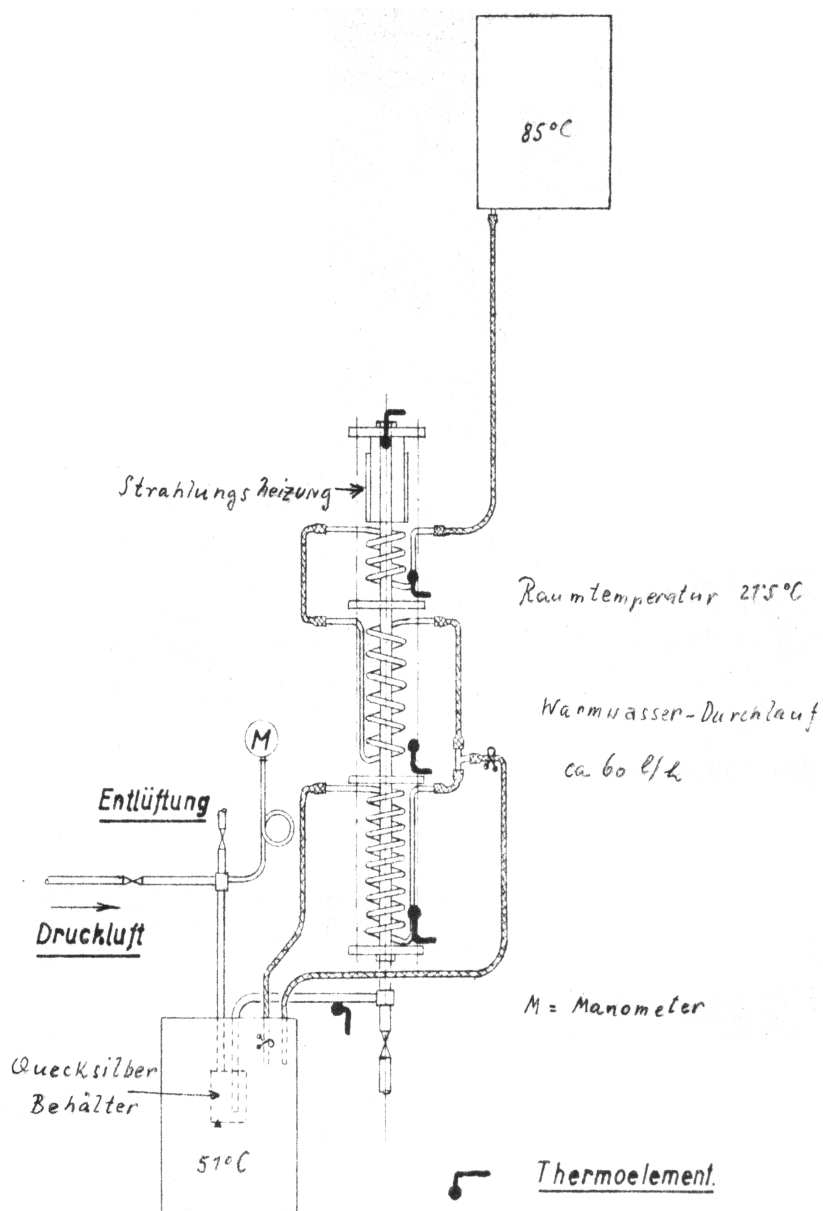


Figure 5.8: Doczekal's demonstration experiment for labile states in mixtures (from [87])
translations: Druckluft=pressured air, Entlüftung= gas outlet, Quecksilberbehälter= mer-
cury reservoir, Raumtemperatur= room temperature, Strahlungsheizung= radiation heater,
Warmwasser-Durchlauf=hot water flow.

Doczekal writes about the experiments, cf. fig.5.9: "By lowering the mercury column the whole liquid can be evaporated in the glass tube. If the pressure is enhanced slightly by rising the mercury column from II to III a significant amount of turpid liquid appears. If the mercury column is lowered again liquid critical phases are generated which change into anisotropic liquid if the pressure is changed only a little bit. If it is expanded from I to II oscillations of mercury appear at constant pressure of the air, see fig IIa. Very strong oscillation appear if the mercury is lifted from position II to I. These oscillations represent the labile state, they have a high pressure at a large volume or a low pressure at a small volume. These meta-stabile or labile phases are the cause for the big difference between the expansion and compression curves." The measurement values are shown in fig.5.10. In today language this means that Doczekal claimed to have observed nonlinear oscillations. Of course the measurements of Doczekal arise many questions regarding his technical abilities which can not be answered due to the loss of information after a delay of more than 70 years.

5.2.3 Schaeffer

Schaeffer at LESA rebuilt Irinyi's and Doczekal's steam engine with the actual modern technology. Some strategies of their improvement of the machine design are obvious:

- 1.) They use pistons with a high compression factor. This is necessary in order to enable a good removal of the condensed liquid after a cycle.
- 2.) They detect electronically the pressure in each piston by fast sensors.
- 3.) They use magnet valves. This enables a fast precise steering of the valves in a feedback loop by a computer and allows to optimize the cycles by charging or discharging the pistons in the right moment.
- 4.) The construction should be strong enough for higher pressures and chemicals in order to allow the testing of mixtures working similarly at environment temperatures.

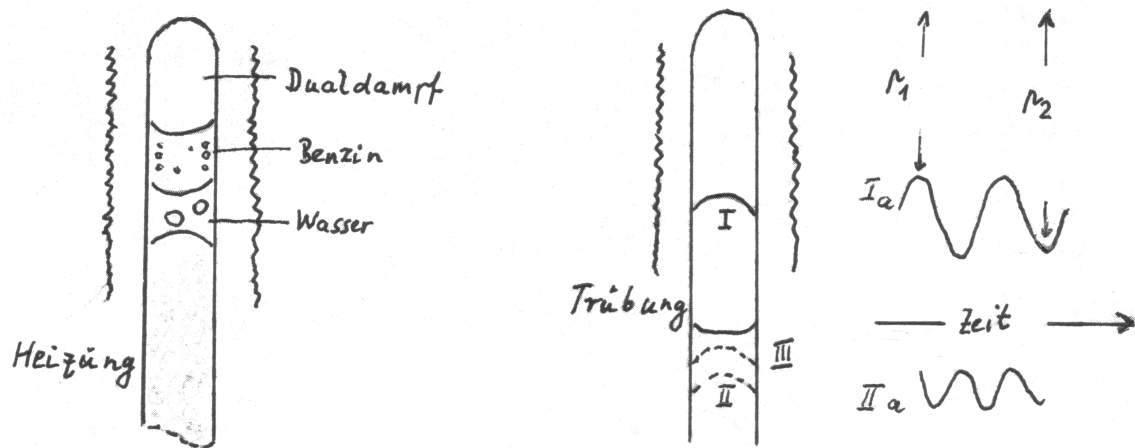


Figure 5.9: Doczekal's demo experiment for labile states (from [87])

left picture: water-gasoline in glass tube before expansion in the stationary state

right picture: same after expansion - observation of pressure oscillations

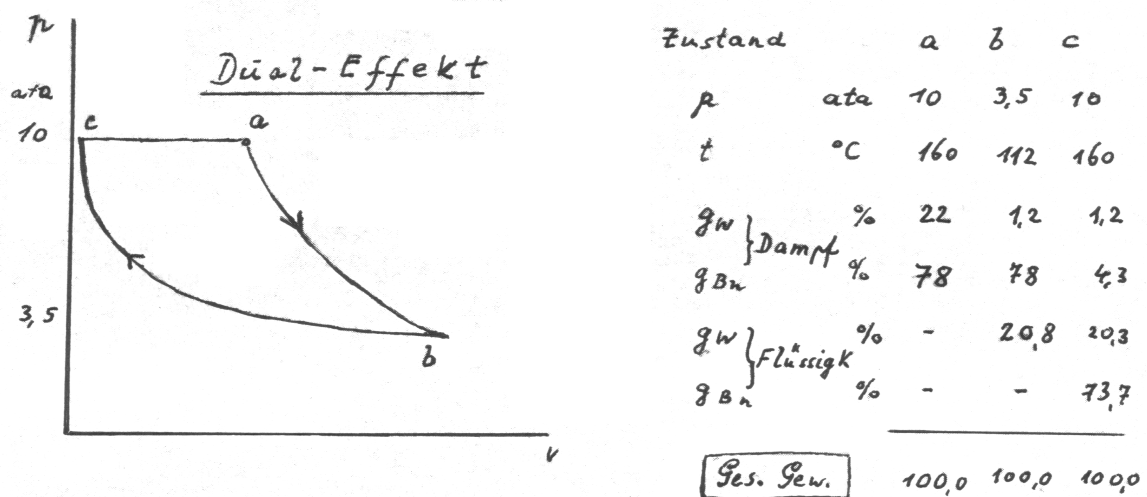
translations: Dualdampf=dual vapor, Benzin= benzene, Heizung=heating, Wasser=water
Zeit=time p = pressure, Trübung = opacity gasoline

Figure 5.10: Doczekal's dual adiabatic cycle experiment with water-gasoline (from [87])

pressure (p)- volume (v) - diagram and tabel of measurements of the cycle

5.3 The Thermodynamic Theory of Water-Benzene

5.3.1 stabile case

The material description

It is known that the mixture water-benzene represents a limit case of an azeotropic mixture[84], cf. also fig 5.11. The gas mixes ideally meaning that the ideal pressures of each gas add up to the total pressure of the mixture. In the liquid state the polar-apolar liquid mixture demixes quite completely into two liquid phases in the region of the state space below 450°K. For a description by a semiquantitative model I use an approach called by me "Mollier approximation" because some of the basic simplifications of the model are overtaken from the theory of wet air by Mollier. *)

It is assumed for simplification that

- 1) both gases of the mixture are ideally
- 2) the liquids demix completely
- 3) the liquid volumes are constant for all temperatures
- 4) the specific heats of the vapor C_p are ideal and dependent from temperature only.
- 5) the enthalpies at the phase border lines can be approximated by an interpolation of second order dependent from temperature, vgl. tab.5.2.
- 6) For the equilibrium calculation holds: on the left side of the phase diagram (relative to the azeotropic line, cf. fig. 5.11) the water corresponds to the liquid, the benzene to the air, on the right side the roles are interchanged.

Applying these approximations the phase border lines of water and benzene vs. temperature in °C are calculated. Differently and more accurately as Mollier's first order calculation we use a polynom of second order as fit for the enthalpy values at the phase boundary. The enthalpy values are from [99] and [100] . By adding a constant they are shifted so that the zero value point for the enthalpy of each liquid is at 273.15°K or 0°C. This is justified because the processes considered here are purely physical processes and contain no chemical reactions. If the heat capacitances of the gaseous state are interesting the ideal heat capacity C_{p0} of the vapors are calculated applying the approximation formulas with the tabulated material coefficients.

*) the terminus "azeotropic" in this book is overtaken from the original literature. This was done erroneously.
 Here we have always a saturated vapour pressure line of a 2-component mixture consisting of 3 phases.
 This contradicts to azeotropic points and lines which are 2-component systems changing from a 2- to a 1-phase system .

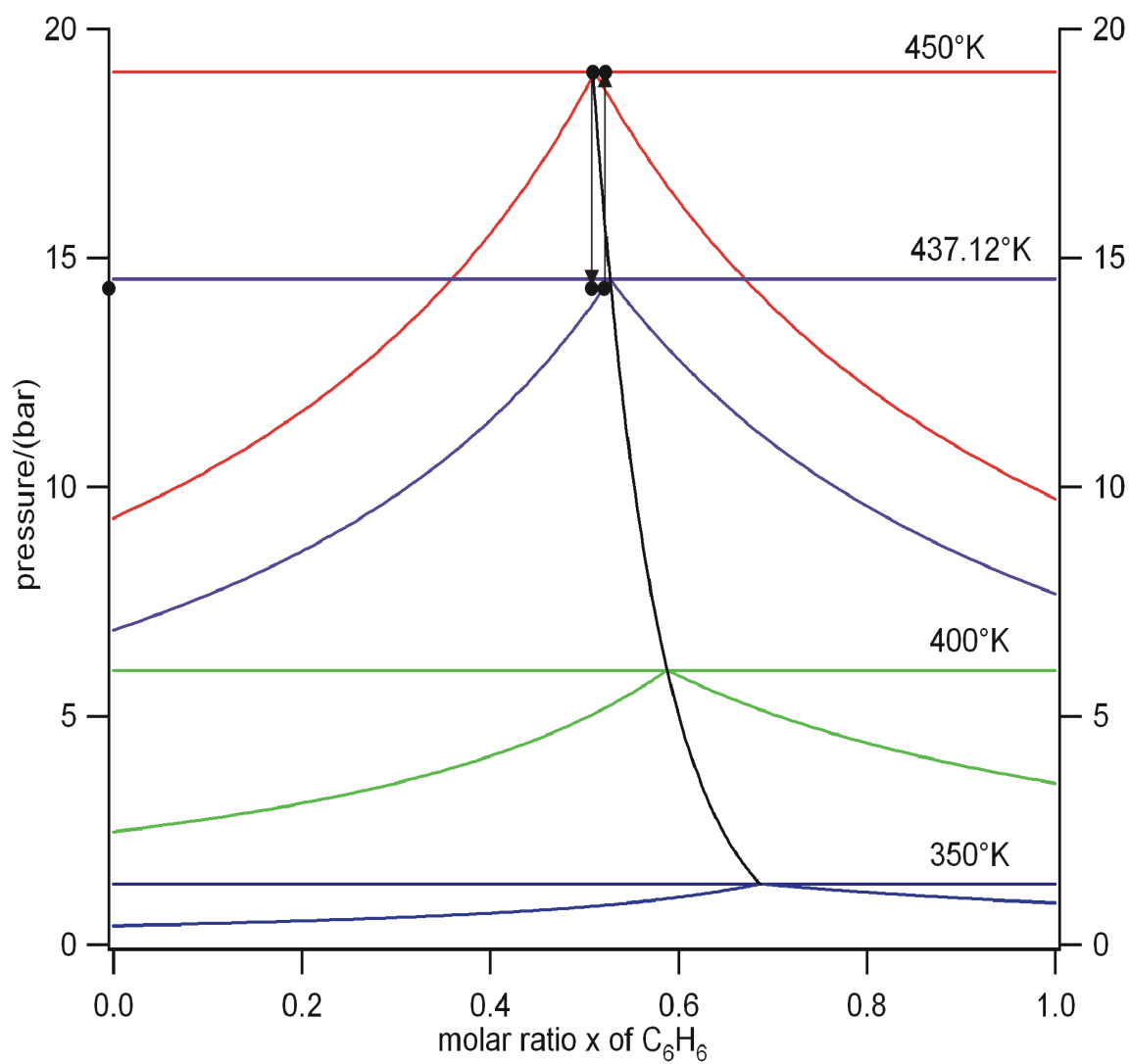


Figure 5.11: the P-x phase diagram of benzene-water
 black line shows the line of the azeotropic points; the liquid state is above horizontal lines,
 two-phase area are between lines of same color, gaseous state below lines of same color.
 Arrows denote the path of an idealized equilibrium Doczekal's cycle, cf. text

Table 5.2: the applied material data and formulas for Water and Benzene

	Water
$Molwt$	18.015
T_c / (K)	647.2
P_c /(Pa)	$221.2 * 10^5$
$r_{(W/B)}/(kJ.kg^{-1})$	2483.75 at 273.15K
P_{sat}	$\log(P_{sat}/P_c) = (1 - T_r)^{-1} \times$ $(Vp_1 * T_r + Vp_2 * T_r^{1.5} + Vp_3 * T_r^3 + Vp_4 * T_r^5)$ with $T_r = 1 - T/T_c$
with	$Vp_1 = -7.76451$; $Vp_2 = 1.45838$ $Vp_3 = -2.7758$; $Vp_4 = -1.23303$
enthalpy $h/(kJ.kg^{-1})$	$h = k_o + k_1T + k_2T^2$ boiling line
with $T/(C)$ and	$k_0 = 0$; $k_1 = 4.0533$; $k_2 = .0008698$
enthalpy $h/(kJ.kg^{-1})$	$h = k_o + k_1T + k_2T^2$ dew line
with $T/(C)$ and	$k_0 = r_W$; $k_1 = 2.2206$; $k_2 = .0034201$
specific ideal heat of gas	
per mass in $(J/(g * K))$	$Cp^o = (((E * T - D) * T + C) * T - B) * T + A$
with	$A = 1.9408$; $B = -9.6766 * 10^{-4}$
and	$C = 3.0885 * 10^{-6}$; $D = -2.6314 * 10^{-9}$
and	$E = 8.6095 * 10^{-13}$
per mol in $(J/(mol * K))$	$Cp^o = A + BT + CT^2 + DT^3$
with	$A = 32.24$; $B = 1.924 * 10^{-3}$;
and	$C = 1.055 * 10^{-5}$; $D = -3.596 * 10^{-9}$
surface tension $\sigma/(Nm^{-1})$	$\sigma = 235.8 * 10^{-3} * T_r^{1.256} * (1 - 0.625 * T_r)$
heat conductivity $/(W/(m*K))$	$\lambda = (A + BT + CT^2 + DT^3)(1 + p_i/(bar) \%)$
with	$A = 7.341 * 10^{-3}$; $B = -1.013 * 10^{-5}$
and	$C = 1.801 * 10^{-7}$; $D = -9.1 * 10^{-11}$

Benzene	References
78.108	[81]
562.2	[81]
$48.9 * 10^5$	[81]
438.7 at 273.15K	[81]
$\log(P_{sat}/P_c) = (1 - T_r)^{-1} \times$ $(Vp_1 * T_r + Vp_2 * T_r^{1.5} + Vp_3 * T_r^3 + Vp_4 * T_r^5)$ with $T_r = 1 - T/T_c$ $Vp_1 = -6.98273$; $Vp_2 = 1.33213$ $Vp_3 = -2.62863$; $Vp_4 = -3.33399$	[81]
$h = k_o + k_1T + k_2T^2$ boiling line $k_0 = 0$; $k_1 = 1.3966$; $k_2 = 0.002681$ [99]	fitted from data of [100]
$h = k_o + k_1T + k_2T^2$ dew line $k_0 = r_B$; $k_1 = 1.0141$; $k_2 = 0.0010733$	fitted from data of [99][100]
$Cp^o = (((E * T - D) * T + C) * T - B) * T + A$ $A = -0.4781755$; $B = 6.186488 * 10^{-3}$ $C = -3.803634 * 10^{-6}$; $D = 6.996479 * 10^{-10}$ $E = 4.266088 * 10^{-14}$ $Cp^o = A + BT + CT^2 + DT^3$ $A = -33.92$; $B = 0.4739$; $C = -3.017 * 10^{-4}$; $D = 7.13 * 10^{-8}$	[83] [81]
$\sigma = 70.969 * 10^{-3} * T_r^{(11/9)}$	[100][101]
$\lambda = (A + BT + CT^2 + DT^3)(1 + p_i/(bar) \%)$ $A = -8.455 * 10^{-3}$; $B = 3.618 * 10^{-5}$ $C = 9.799 * 10^{-8}$; $D = -4.058 * 10^{-11}$	[81]

If the heat capacitances of the gaseous state are needed the ideal heat capacity Cp^0 of each vapor are calculated from approximation formulas[81].

For the surface tension γ (in N/m) of water the following formula is taken from [100]

$$\gamma = 235.8 * 10^{-3} * T_r^{1.256} * (1 - 0.625 * T_r) \quad (5.2)$$

with T temperature, T_c critical temperature and the reduced temperature T_r defined as $T_r \equiv 1 - T/T_c$. For the calculation of surface tension γ (in N/m) of benzene the following approximation [101] is applied

$$\gamma = 70.969 * 10^{-3} * T_r^{(11/9)} \quad (5.3)$$

The proportional fit constant $70.969 * 10^{-3}$ has been obtained from a fit to 3 experimental values taken from a tabel of [81] p.634. The temperature dependent heat conductivity value λ (in Watt/(meter*.Kelvin)) of each liquid substance at 1 bar is calculated according to a polynomial approach [81] p.515

$$\lambda = A + BT + CT^2 + DT^3 \quad (5.4)$$

The material constants A, B, C , and D are from [81] p.548 . In the program calculations the heat conductivities are corrected for pressure by multiplying a factor $(1 + P/bar\%)$ in order to take into account for the approximative pressure dependence of these substances, see [81] p.514. The heat conductivity of the binary gas mixture are obtained from the estimation methods of Wassilewa, Mason and Saxena, Ray and Thodos described all explicitly in [81], p. 498 to p.531.

So the approximative value of the heat conductivity λ of a gas binary mixture (with

$x \equiv$ molar ratio) is obtained by the following program code lines:

$$\begin{aligned}
\Gamma_W &= 210 * (T_{cW} * M_W^3 / P_{cW}^4)^{(1/6)}; \quad \% \text{ index W } \equiv \text{ water} \\
\Gamma_B &= 210 * (T_{cB} * M_B^3 / P_{cB}^4)^{(1/6)}; \quad \% \text{ index B } \equiv \text{ benzene} \\
\lambda_{WB} &= \frac{\Gamma_B(\exp(.0464 * T_{rW}) - \exp(-.2412 * T_{rW}))}{\Gamma_W(\exp(.0464 * T_{rB}) - \exp(-.2412 * T_{rB}))}; \\
\lambda_{BW} &= 1/\lambda_{WB}; \\
A_{12} &= (1 + \lambda_{WB}^{(1/2)} * (M_W/M_B)^{(1/4)})^2 / (8 * (1 + M_W/M_B)^{(1/2)}); \\
A_{21} &= (1 + \lambda_{BW}^{(1/2)} * (M_B/M_W)^{(1/4)})^2 / (8 * (1 + M_B/M_W)^{(1/2)}); \\
W1 &= x * A_{12} + (1 - x); \\
W2 &= x + (1 - x) * A_{21}; \\
\lambda &= (x * \lambda_W)/W1 + ((1 - x) * \lambda_B)/W2;
\end{aligned}$$

the equilibrium calculation

Due to the basic ideal assumptions in the description of the mixture (see sec 2.1) it is recommended to write down the free energy as a Taylor expansion. Then, for water-benzene only the terms of first order are sufficient in order to describe the molar free energy F of the system [9], i.e.

$$F(v, T, x_1) = x_1 F_1(\rho_1) + (1 - x_1) F_2(\rho_2) = x_1 F_1(v/x_1) + (1 - x_1) F_2(v/(1 - x_1)) \quad (5.5)$$

where $v \equiv$ spec. volume, $T \equiv$ temperature, $x \equiv$ molar ratio, $\rho \equiv$ molar density. The indices 1 and 2 stand here for benzene and for water. Therefrom follows the additivity of the partial pressures p_i to the total pressure P

$$P = -\partial F / \partial v = p_1 + p_2 \equiv p_{C_6H_6} + p_{H_2O} . \quad (5.6)$$

Now, using the ideal properties of the mixture, the phase diagram, cf. fig. 5.11, can be constructed for not too high temperatures ($< 200^\circ\text{C}$):

The pressure follows from eq. 5.6. The maximum pressure of the mixture is the sum of the saturated pressure of water and benzene (3-phase state or azeotropic point).

The dew lines in the p-x diagram from the azeotropic point are horizontal. Only in the very close neighbourhood of a pure substance ($x = 0$ or $x = 1$, omitted in fig. 5.11) the saturated pressure of the mixture deviates from the azeotropic pressure and approaches the saturated pressure of each substance.

The boiling line between the 2-phase area and the gas is determined by the equations

$$\begin{aligned} \text{total pressure : } P &= p_{H_2O} + p_{C_6H_6} \\ \text{right to the azeotropic point : } x_{C_6H_6} &= p_{C_6H_6, sat} / P \\ \text{left to the azeotropic point : } x_{H_2O} &= p_{H_2O, sat} / P = 1 - x_{C_6H_6} \end{aligned} \quad (5.7)$$

where the index $_{sat}$ denotes the saturated state of the vapor.

Generally, the vapor pressure of the saturated vapor species (called "steam") depends from T and is determined by a Wagner equation [81], the unsaturated species (called "air") is calculated by the ideal gas law. Then, the molar ratio x_{sat} of saturated "steam" on the azeotropic line can be calculated

$$x_{sat} = p_{steam} / (p_{steam} + p_{air}) \quad (5.8)$$

This allows to calculate the saturated molar enthalpy of the "steam-air" mixture

$$h_{sat} = (1 - x_{sat})h_{air}^g + x_{sat}h_{steam}^g \quad (5.9)$$

Here h are the molar enthalpies here taken at the dew line for air and steam at the temperature T .

We calculate also the total molar enthalpy h of the partly saturated liquid-gas mixture

$$h = (1 - x_0)h_{air}^{gas} + x_g x_{sat} h_{steam}^{gas} + (1 - x_g)h_{steam}^{liquid} \quad (5.10)$$

where x_0 is the given initial content of ~~water~~ ^{liquid} of the liquid-gas mixture. x_g is defined as the molar ratio of gas. The introduction of x_g becomes necessary if the expansion or compression crosses the dew line at $x_0 = x_{sat}$ and the process moves into the partly saturated 2-phase-area where $x_0 > x_{sat}$. x_g can be derived as follows: The molar ratio of "air" in the mixture is $(1 - x_0) = x_g(1 - x_{sat})$. Thus it follows:

$$x_g = (1 - x_0) / (1 - x_{sat}) \quad (5.11)$$

Table 5.3: the thermodynamic properties of the benzene and water [99]:
units: energies H in kJ/kg, volume V in m³/kg, entropies S in kJ/(kg.grad)
benzene

T(K)	p/(bar)	$V'.10^3$	$V''.10^3$	H'	H''	S'	S''
450	9.746	1.43	42.47	47.7	367.9	3.0095	3.7215
350	0.917	1.209	397.1	-160	239.7	2.4937	3.6357

water

T(K)	p/(bar)	$V'.10^3$	$V''.10^3$	H'	H''	S'	S''
450	9.32	1.123	210.883	747.7	2773.9	2.105	6.61299
350	0.41635	1.0272	3851.3	321.69	2638.4	1.0376	7.6575

The algorithm

In order to determine the isentropes of a vapor mixture water-benzene mixture I start with the equation of enthalpy $dH = VdP + TdS$. If we determine the isentrope it holds $dS = 0$. This constraint allows to find iteratively the isentrope from step to step if an initial point is given.

$$dH = VdP \quad \text{or} \quad H_{i+1} = H_i + V(P_{i+1} - P_i). \quad (5.12)$$

The principal program scheme to determine the isentrope is the following:

- calculate the initial values of the first point:
set N, T, x, P and calculate p_{sat}, x_{sat}, H, x_g
- **for** every i from the point 1 until to the endpoint index $N-1$
 - set P_{i+1}
 - solve $H_{i+1}(T_{i+1}) = H_i(T_i) + V(P_{i+1} - P_i)$ for T_{i+1} by iteration using the equation of state
 - determine the final values p_{sat}, x_{sat} of each point
- **next** point i

The calculation uses the tabulated values from table 5.2 and 5.3

The results of the stabile calculation

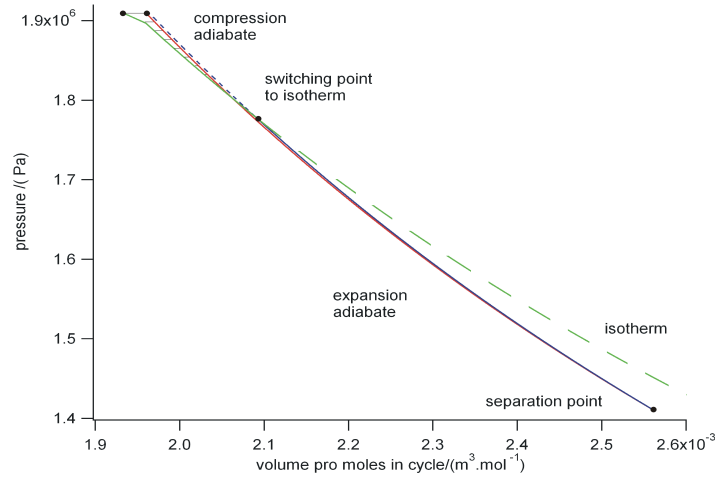
In the phase diagram, cf. fig. 5.11, the arrows indicate the region where Doczekal's cycle is proceeded. We calculate this cycle here for the equilibrium case because it gives an idea what Doczekal meant when he speaks about a dual effect. This equilibrium cycle follows the ~~rhythm~~ **large** cycle

- **large** isentropic expansion from the azeotropic point
- removal of liquid
- isentropic compression with the gas only until the boiler temperature is reached
- isotherm compression until the gas reaches the azeotropic point
- evaporation of all condensed liquid during the cycle

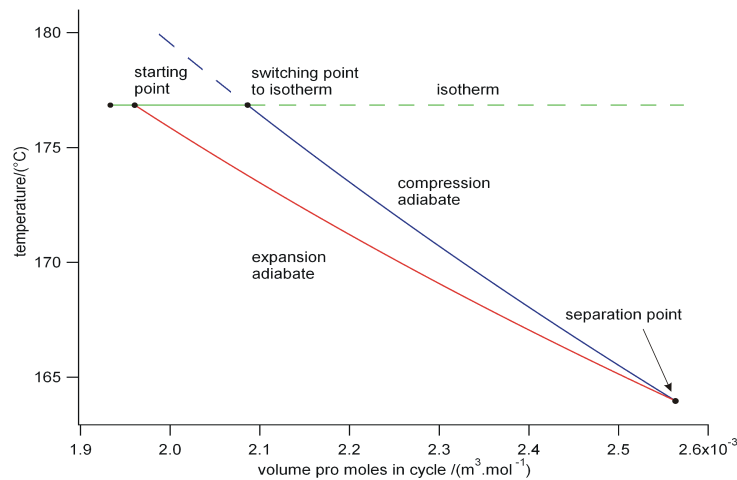
If the system is started at the upper temperature it contains a saturated water-benzene vapor mixture of N particles of the specific volume v_g whose total volume is $V_0 = v_g * N$. If the piston is expanded isentropically the gas is cooled down adiabatically. By this procedure only a ratio x_g of all N particles in the piston volume remains gaseous and a ratio $(1 - x_g)$ of (only) water liquid condenses. The benzene remains completely in the superheated state, cf. fig. 5.11. Then, the liquid water is separated off from the gas and is recompressed to the initial starting pressure by a pump, whose energy is neglected here in the following because this amount of energy is negligible compared with the gas compression. The results of the stabile equilibrium first order calculation for this model [9] are shown in fig. 5.12, fig. 5.13 and 5.14. A more exact second order calculation of h does not change the result significantly. Surprisingly the model for this crossed quasi-isothermic cycle yields a small second law violating net gain of energy per cycle which is contrary to other binary systems like water-air. This result could be enhanced if the gas is cooled back during the adiabatic compression by a heat exchanger with the condensed cooling liquid.

Nevermind, this overunity result is not significant enough and has to be tested by an more exact model calculation. Then we will see whether the result is real or a product of the simplifying model assumptions.

The gain efficiency per cycle (defined by energy gain / energy invested pro cycle) is quite small ($< 1\%$) if compared with standard Rankine cycles. The cycle efficiency is near to zero as it is expected from ideal gas adiabates without losses.

Figure 5.12: Doczekal's $p-v$ -cycle calculated

the cycle consists of: 1) an isentropic adiabatic expansion (red full line), 2) a separation of the phases, 3) an adiabatic isentropic compression of the gas to the switching point (blue full line) 4) an isotherm compression to the initial pressure (full green line) 5) an evaporation of the condensed fluid (on the full green line) Note the small net gain work area in the left upper corner of the diagram!

Figure 5.13: Doczekal's $T-v$ -cycle calculated

description and colors are the same as in the picture above on this page

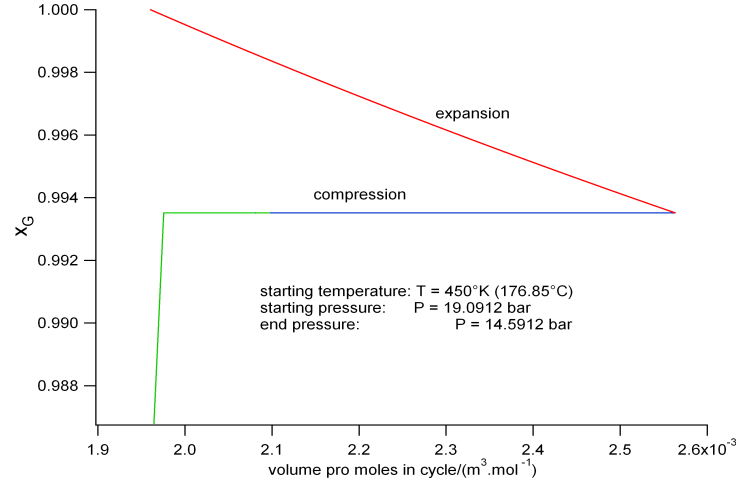


Figure 5.14: Doczekal's $x_G - v$ - cycle calculated

the cycle consists of: 1) an isentropic adiabatic expansion (red full line), 2) a separation of the phases, 3) an adiabatic isentropic compression of the gas to the switching point (blue full line) 4) an isotherm compression to the initial pressure (full green line) 5) an evaporation of the condensed fluid (on the full green line)

I calculated also the Rankine cycle efficiency of a cycle with water-benzene, see fig. 5.15. It is very near to the optimum Carnot efficiency. This result coincides approximately with the observations of Irinyi's referies. Irinyi's steam engine cycle is a quasi-Rankine cycle shown in fig. 5.15.

This cycle proceeds as follows:

point 1 \rightarrow 2: isobar + isotherm; point 2 \rightarrow 3: isentrope; point 3 \rightarrow 4: isobar;
point 4 \rightarrow 5 isobar + isotherm; point 5 \rightarrow 1: (for fluid) first isentropic then isobar ;

The states of the different points of the cycle can be calculated from the program

point 1: $T_1 = 176.85\text{ }^\circ\text{C}$, liquid state, $p_1 = 19.0912\text{ bar}$, $x = 0.5088$

point 2: $T_2 = 176.85\text{ }^\circ\text{C}$, saturated vapour, $p_2 = 19.0912\text{ bar}$, $x = x_{sat} = 0.5088$

point 3: $T_3 = 86.2093\text{ }^\circ\text{C}$, $p_3 = 1.3333\text{ bar}$, $x_G = 0.9394$, $x = x_{sat} = 0.5416$

point 4: $T_4 = 76.85\text{ }^\circ\text{C}$, saturated vapour, $p_4 = 1.3333\text{ bar}$, $x_{sat} = 0.68774$

point 5: $T_5 = 76.85\text{ }^\circ\text{C}$, saturated liquid state, $p_5 = 1.3333\text{ bar}$, $x = 0.5088$

point 6: $T_6 \approx 76.85\text{ }^\circ\text{C}$, liquid state, $p_6 = 19.0912\text{ bar}$, $x = 0.5088$

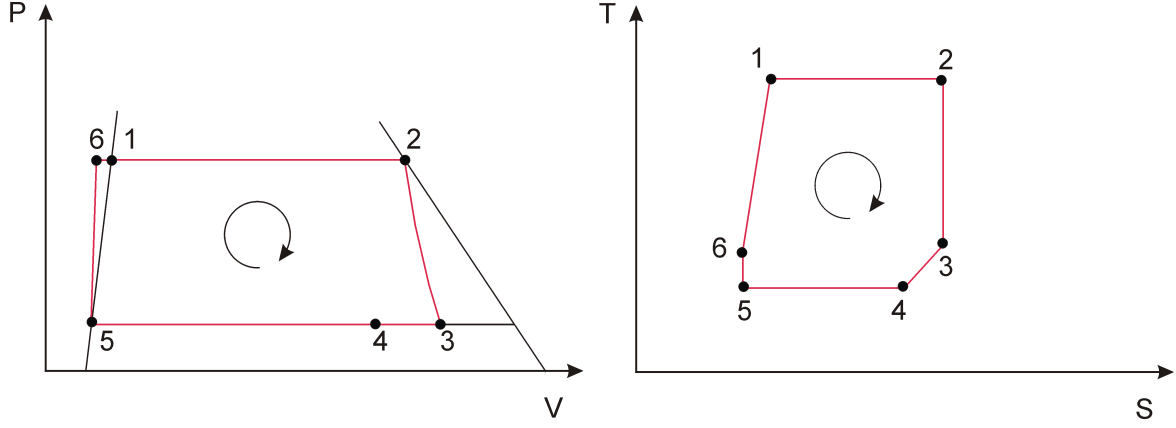


Figure 5.15: the Irinyi - Rankine cycle

The program routines developed so far can be applied also for the calculation of Irinyi's cycle, cf. [9]. Using these values, the tab. 5.3 and the h_{mol_ex} values calculated by the program we obtain the enthalpy differences between the points

point 1 \rightarrow 2: isobar evaporation: $\Delta h_{12} = 30.664 kJ/mol$ (data from tab. [99])

with $\Delta h_{12} \equiv h_2 - h_1 = x \cdot (H_{C_6H_6}'' - H_{C_6H_6}') M_{C_6H_6} + (1 - x) \cdot (H_{H_2O}'' - H_{H_2O}') M_{H_2O}$

point 2 \rightarrow 3: adiabatic expansion: $\Delta h_{23} = -8.6 kJ/mol$ (data calculated by program)

with $\Delta h_{23} \equiv h_3 - h_2$

point 3 \rightarrow 5 isotherm compression with condensation: $\Delta h_{35} = -34.0803 kJ/mol$

with $\Delta h_{35} \equiv h_5 - h_3 = h_5 - (h_1 + \Delta h_{12} + \Delta h_{23})$

and $h_{1/5} = x H_{C_6H_6} M_{C_6H_6} + (1 - x) H_{H_2O} M_{H_2O}$

point 5 \rightarrow 6 adiabatic compression: Δh_{56} is not necessary to be calculated here

point 6 \rightarrow 1: isobar heating: $\Delta h_{61} \approx 11.7 kJ/mol$ (estimative data for C_p from [99])

with $\Delta h_{61} = C_p T$ with $C_p = x C_p^{mol}(C_6H_6) + (1 - x) C_p^{mol}(H_2O)$

Due to $dh = vdp + TdS$ and $dp = 0$ we can identify $Q_{12} = \Delta h_{12} > 0$, $Q_{35} = \Delta h_{35} < 0$ and $Q_{61} = \Delta h_{61} > 0$ as exchanged heats. Therefrom we calculate the efficiency to be

$$\eta \equiv \frac{Q_{12} + Q_{61} + Q_{35}}{Q_{12} + Q_{61}} \approx 19.5\% < \eta_C \equiv \frac{T_{450} - T_{350}}{T_{450}} \approx 22.2\%. \quad (5.13)$$

According to this estimative calculation the Rankine cycle of the mixture yields efficiencies near to Carnot's maximum. This makes Irinyi's measurements believable, cf. tab.5.1, if one assumes some additional unknown loss channels.

May be that Doczekal's claimed "Over-Carnot - operation is due to uncontrolled cooling by the environment"

5.3.2 labile case

Introduction

In order to explain the non-equilibrium phenomena in section 5.2.2 we need the theory of spontaneous condensation of supersaturated gases. However, we have to note that the state of the theory is far from being accomplished still today. Only some basic of it are generally accepted. The generally accepted knowledge can be summarized as follows: In a clean atmosphere (with no germs) and if the gas is sufficiently supersaturated the condensation process starts spontaneously by a energy fluctuation over a defined activation barrier of droplet formation. These new born droplets at the top of the activation barrier are called "critical droplets". They are characterized by a critical radius r^* . This process is called spontaneous condensation. If the fluctuation has exceeded the activation barrier for the critical droplet then the critical droplets become a germ at which further condensation takes place in a supersaturated atmosphere. It is possible also that dust particles and aerosols are the germs for an condensation. This process is called heterogeneous condensation. It is excluded and

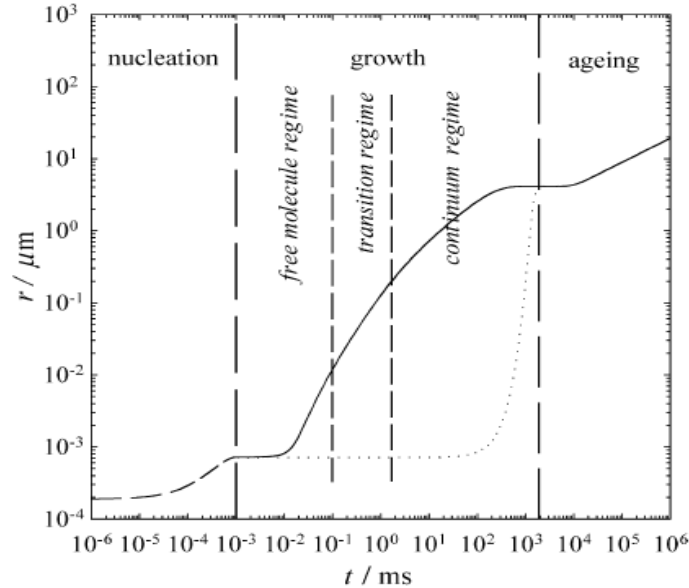


Figure 5.16: the growth phases of a droplet(from [102]); dotted line \equiv critical radius

Table 5.4: the theoretical literature of spontaneous condensation

year	authors	topic	ref.
1806	Laplace	mathematical theory of capillarity	[103]
1870	Kelvin	capillarity applied to droplets , critical radius	[104]
1875	Gibbs	free enthalpy of the critical droplet	[16]
1886	Helmholtz	correction of Kelvin critical radius	[105]
1886	Thomson	alternative droplet radius formula	[106]
1927	Farkas	almost complete formula of condensation rate	[107]
1929	Volmer	growth law; critical droplet = activated complex	[108]
1935	Becker/Doering	free enthalpy and condensation rate of a droplet	[109]
1939	Volmer	droplet radius as maximum of free enthalpy	[110]
1942	Oswatish	droplet growth limited by heat exchange	[111]
1950	Reiss	extension to mixtures	[112]
1951	Mason	droplet growth limited by mass transport	[113]
1951	Mason/Frisch	distinguishing kinetic and continuum regime	[114]
1958	Cahn-Hilliard	variational formulation of nucleation	[115][116][117]
1984	Bedeaux	application of non-equilibrium thermodynamics	[118][119]
2006	Horsch	application of molecular dynamics	[120]

is not discussed in this chapter, for further reading see [121]. For homogeneous condensation 4 growth phases are distinguished ($l \equiv$ mean path length), cf. fig.5.16

- 1) the kinetic regime: $r^* < l$
 - 2) the transition regime: $r^* \approx l$
 - 3) the continuum regime: $r^* > l$ controlled by diffusion
 - 4) the coagulation regime which is the fusion of the separate droplet to a bulk liquid
- In this chapter article we discuss only phases 1 until 3 .

A time table of the development of the theory of spontaneous condensation can be found in tabel 5.4. The tabel summarizes the authors who introduced new aspects first. Oftenly the discussion about the right opinion regarding the theme is going on until today. I will discuss the points of tabel 5.4 and will propose some new ideas.

the theory of capillarity of Young and Laplace

The Young-Laplace theory of capillarity from 1805 [122] and 1806 [103] describes quantitatively correct the additional pressure by surface tension which arise at the boundaries between different media [123]. The pressure P_r inside a liquid droplet [16] [124] is

$$P_r = P_d + \frac{2\gamma}{r} \quad (5.14)$$


where P_d is the pressure in the gas, γ the surface tension, r is the radius of the droplet and the indices d and r stand for vapor (d) and for the droplet (r). Gibbs derived this formula also by optimizing the inner energy [125, 126]. Modifications published [127].

the critical droplet

a) the concepts of reference pressure and temperature for deviations from equilibrium

The deviation of a gaseous state from the thermodynamic equilibrium is characterized by two additional variables which allow to characterize the distance from equilibrium. If a system has the non-equilibrium states P_d and T_d one defines a reference pressure $P_{ref} \equiv P_{sat}(T_d, v)$ which is the equilibrium pressure at T_d . For the non-equilibrium temperature T_d one defines the reference temperature $T_{ref} = T_{ref}(P_d, v)$ which is the temperature necessary so that P_d would be an equilibrium pressure, cf. fig.5.17.

This definition, however, is not so very clear as it will be shown in the following:

Conventionally it is assumed that the reference temperature is identical with the equilibrium temperature $T_{ref} = T_{sat}$ at P_d which can be determined by solving the equation of the dewline pressure equation [106]. Originally this definition was derived for germ formation in supersaturated solutions.  It was transferred to gases by Frenkel [128]. Any critical discussion about the limits of this method was not found in the literature. Because the application of this method did not yield reasonable numerical results in code programming I had to modify the conventional procedure here. So I calculate T_{ref} by solving the equation of state (EOS) at the present (labile) pressure P_d and the specific volume v_g in the gas in order to obtain the reference equilibrium state, cf. fig.5.17. For the empirical temperature T_d , however, the reference pressure is defined traditionally at $P_{ref} = P_{sat}$. In other words: I define the reference states to be deter-

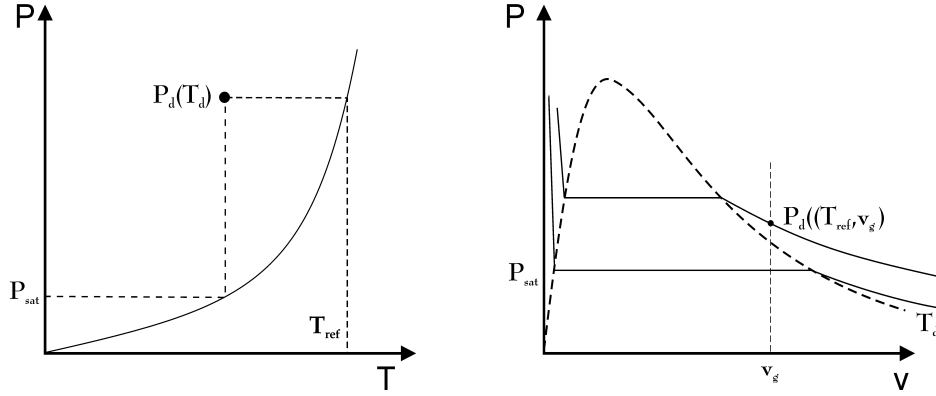


Figure 5.17: the definition of P_{sat} and T_{ref} for any labile supersaturated state $P_d(T_d)$
 conventional definition left pic: for a labile point $P_d(T_d)$ the reference pressure P_{sat} lays on the vapor pressure curve at T_d , the reference temperature $T_{ref} = T_{sat}$ is at P_d .
 alternative definition right pic: for a labile point $P_d(T_d)$ the reference equilibrium pressure P_{sat} lays on the saturated pressure curve at T_d , the reference temperature $T_{ref} = T_{sat}$ can be found at the on the EOS-line at P_d at the actual (labile) specific gas volume v_g

mined by the projection points of the labile state onto the equilibrium function.

Two different situations of non-equilibrium exist, cf. table 5.5:

supersaturation and undersaturation. Supersaturation or undercooling entrains the phenomena of homogeneous or heterogeneous condensation. Undersaturation or over-heating entrains the phenomenon of evaporation and boiling.

b) the definition of the critical radius

Kelvin derived a first order phenomenological derivation of the formula which allows to derive the so called critical radius r^* of embryonic droplets which start to develop in a undercooled supersaturated gas atmosphere [104]. Originally Kelvin assumed the gas to be ideal and applied the hydrostatic law of the liquids for a gas instead of using the barometric formula for a gas atmosphere. Robert v. Helmholtz [105] corrected the approximation and improved so Kelvin's formula. On another manner - but applying the ideal gas law for the real gas state- he obtained the today so called Kelvin - Helmholtz formula

$$r^* = \frac{2\gamma v_{fl}}{RT_d \log(P_d/P_{sat})} \quad (5.15)$$

Table 5.5: labile thermodynamic states

	pressure	temperature	reference state
supersaturation	$P_d - P_{sat} \geq 0$ or	$T_d - T_{ref} \leq 0$	dew line
& undercooling	$\log(P_d/P_{sat}) \geq 0$		or gaseous EOS
undersaturation	$P_d - P_{sat} \leq 0$ or	$T_d - T_{ref} \geq 0$	boiling line
& overheating	$\log(P_d/P_{sat}) \leq 0$		or liquid EOS

Here is v_{fl} the specific volume of the liquid droplet, R is the Avogadro constant, P_d is the empirical supercooled vapor pressure and P_{sat} is the equilibrium reference pressure of the gas calculated at the actual non-equilibrium temperature T_d . One should note that a corrected Kelvin derivation applying the barometric pressure law contains the ideal gas law as an approximation. Therefore 5.15 should fail for very real and condensing fluids especially near to critical points.

Nevertheless, the droplet formula 5.15 is a good approximation for the most purposes and it is still today the state of the art.

Newer definitions define the critical radius of a droplet to be situated at the maximum (or saddle point) of the total free enthalpy G of a droplet [129], cf. fig. 5.18 below. This idea goes probably back to [110] and was spread out by [128]. The advantage of this method is that it can be extended for multi-component droplets as proposed by Reiss [112]. If we formulate an equation for the free enthalpy G of a droplet with N component and with the radius r_j we obtain for each droplet phase[130]

$$G_j = \left(\sum_{i=1}^N n_i \int_{p_i^g}^{p_i^{fl}} v_i^g dp_i \right)_j + 4\pi\gamma r_j^2 + \left(\left(\sum_i n_i \right) v^{fl} (P_d - P_{sat}) \right)_j \quad (5.16)$$

The integral of this equation is abbreviated here as chemical potential difference $\mu_i \equiv \int v_i dp_i$ of a component i . Note that v_i of the labile gas phase is still unknown. Most authors solve this by applying again the mentioned ideal gas approximation $v_i = RT/p_i$ which yields $\Delta\mu_i = -RT \log(p_i^d/p_i^{sat})$. So, applying the ideal gas formula for only one component and Laplace's capillarity formula 5.14, using the approximation $P_d \approx (P_d - P_{sat})$ and setting $(dG/dr = 0)$ one can solve for r which results in 5.15.

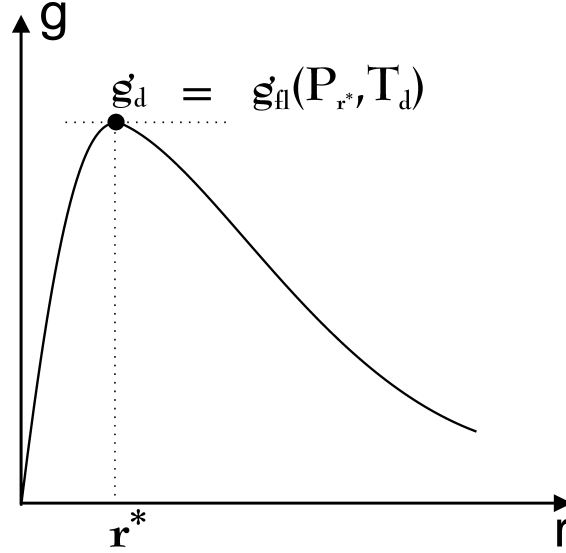


Figure 5.18: Free enthalpy g (per mass or mol) of a droplet vs. radius r

c) the Thomson critical radius formula

Gibbs free enthalpy g of the liquid (index fl) and the labile vapor phase (index d) can be equilibrated for every critical droplet according to [110]

$$g_d(T, P_d) = g_{fl}(T, P_r) = g_{fl}(T, P_d + 2\gamma/r) = g_{fl}(T, P_d) + 2\gamma v_{fl}/r \quad (5.17)$$

where the droplet pressure P_r is defined according to the Laplace law, i.e.

$P_r = P_d + 2\gamma(T)/r$. According to Volmer [110] this assumption holds for a (labile) optimum of the Gibbs enthalpy at the critical radius r^* of a droplet, cf. fig.5.18.

According to Hedbäck [124] an expansion of the droplet free enthalpy g_d and g_{fl} at any radius r_0 yields for vapor and liquid each

$$\begin{aligned} g_d &= g_d(T_{r_0}, P_d) + \Delta T(r_0) \frac{\partial g_d}{\partial T} \\ g_{fl} &= g_{fl}(T_{r_0}, P_{r_0}) + \Delta T(r_0) \frac{\partial g_{fl}}{\partial T} + \Delta P(r_0) \frac{\partial g_{fl}}{\partial P} \end{aligned} \quad (5.18)$$

Here is $\Delta T(r_0) \equiv T_r - T_{r_0}$ and $\Delta P \equiv (P_r - P_d) - (P_{r_0} - P_{d_0})$. Differing to Hedbäck I modify the last term in ΔP the second equation by including the actual vapor pressure P_d defined by $P_d \equiv \sum_i p_d(i)$. If $r_0 = r^*$ holds then eq. 5.17 and both sides of eq. 5.18

can be equated and it follows

$$(T_r - T_{r_0}) \frac{\partial g_d}{\partial T} = (T_r - T_{r_0}) \frac{\partial g_{fl}}{\partial T} + (P_r - P_d - (P_{r_0} - P_{d_0})) \frac{\partial g_{fl}}{\partial P} \quad (5.19)$$

After division with $(T_r - T_{r_0})$ follows

$$(P_r - P - (P_{r_0} - P_0)) / (T_r - T_{r_0}) = \frac{\frac{\partial g_d}{\partial T} - \frac{\partial g_{fl}}{\partial T}}{\frac{\partial g_{fl}}{\partial P}} = - \frac{s_d - s_{fl}}{v_{fl}} \quad (5.20)$$

Here s_d and s_{fl} are the entropies of the vapor and the liquid respectively. Another equation can be obtained if the left side of 5.20 is calculated taking the limes $r \rightarrow r_0$ and applying Laplace's law cf. eq. 5.14

$$\begin{aligned} & \lim_{r \rightarrow r_0} [(P_r - P_d - (P_{r_0} - P_{d_0})) / (T_r - T_{r_0})] \\ &= \frac{\partial}{\partial T} (P_r - P_d) = \left(\frac{2\gamma}{r} \frac{\partial \gamma}{\partial T} - \frac{2\gamma}{r^2} \frac{\partial r}{\partial T} \right) \end{aligned} \quad (5.21)$$

So with eq.5.20 and eq.5.21 the final differential equation for critical droplets is

$$\frac{\partial T}{\partial r} = \frac{2\gamma}{2r \frac{\partial \gamma}{\partial T} + r^2 (s_d - s_{fl}) / v_{fl}} \quad (5.22)$$

Hedbäck gave already an approximative solution of this equation. I found out that the equation can be solved generally. Therefore I change the independent variable from r to x by using the definition $x \equiv 1/r$

$$\frac{\partial x}{\partial T} = - \frac{2x \frac{\partial \gamma}{\partial T} + (s_d - s_{fl}) / v_{fl}}{2\gamma} \quad (5.23)$$

The analytical solution of eq. 5.23 is

$$x_H = - \frac{1}{2\gamma} \int_{T_{ref}}^{T_d} \frac{s_d - s_{fl}}{v_{fl}} dT \quad (5.24)$$

So the inverted critical droplet radius $x_H = 1/r_H$ is obtained.

The principal result 5.24 (but without integration) is old [106]. It can be anticipated from an another ansatz: Frenkel [128] found out that a critical droplet can be interpreted as a fluctuation of free enthalpy for which holds $dg = vdP + (s_d - s_{fl})dT = 2\gamma v_{fl}dx + (s_d - s_{fl})dT = 0$. Applying 5.14 and solving for x yields eq. 5.24.

d) modifications of the Kelvin-Helmholtz critical radius formula

I propose here another procedure which can avoid the ideal gas equation usually applied in labile state theories. I assert that a critical droplet arises from a spatial fluctuation of the gas density at an extremum of inner energy u . This takes place in the volume v in the gas atmosphere around the birth of a droplet. There it holds $du = -pdv + Tds = 0$. So it follows

$$v - v_0 = p^{-1} \int T ds = p^{-1} \int_{T_{ref}}^{T_d} C_v dT \quad (5.25)$$

with $v_0 = v_0(P_{sat}, T_d) = RT_d/P_{sat}$. Writing down the conventional and the alternative equation two possibilities exist for the chemical potential of the gas state

$$\Delta \mu_i = \int_{p_i^{sat}}^{p_i^d} v_i dp_i = -RT \log(p_i^d/p_i^{sat}) \quad I) \quad (5.26)$$

$$\Delta \mu_i = \int_{p_i^{sat}}^{p_i^d} v_i dp_i = v_{0i}(p_i^{sat}, T)(p_i^d - p_i^{sat}) + \int_{p_i^{sat}}^{p_i^d} \left(\int_{T_{ref}}^T C_v dT/p \right) dp \quad II) \quad (5.27)$$

The first equation I) 5.26 is the conventional formula which applies the ideal gas law. The second equation II) 5.27 represents the alternative - i.e the maximum state of inner energy ($du = 0$). One can suppose that this state exists in the homogeneous gas at some distance from the critical droplet.

For a demixed droplet of water-benzene the general formula 5.16 can be simplified to

$$\begin{aligned} G_j &= n_j \Delta \mu_j + 4\pi \gamma_j r_j^2 + n_j v_j^{fl} (P_d - P_s) \\ &= n_j \Delta \mu_j + 4\pi \gamma_j \left(\frac{3n_j v_j^{fl}}{4\pi} \right)^{2/3} + n_j v_j^{fl} (P_d - P_s) \end{aligned} \quad (5.28)$$

where n_j are the mol numbers in a droplet of one component. For binary mixtures Reiss [112] developed a general method to solve these problems. It was known from [131] that the maximum or the saddle point of the droplets free enthalpy separates the growing from the decaying droplets. The calculation showed that the critical radius can be obtained by solving for the optimum, i.e. by setting the derived partial free enthalpies to zero and solving the equations

$$\frac{dG_j}{dn_i} = 0 \quad (5.29)$$

In our simplified case of a demixed liquid and if both species of droplets are condensing we obtain critical radiuses r^* for water (W) and benzene (B) (with $\rho_i \equiv 1/v_i \equiv$ density and $n_i \equiv 4\pi r_i^{*3}/v_i^{fl}$)

$$r_W^* = \frac{2\gamma_W}{-\rho_W^{fl}\Delta\mu_W - (P_d - P_s)} \quad (5.30)$$

$$r_B^* = \frac{2\gamma_B}{-\rho_B^{fl}\Delta\mu_B - (P_d - P_s)} \quad (5.31)$$

with

$$\mu_i = RT(p_i - p_i^{sat})/p_i^{sat} + \log(p_i/p_i^{sat}) \int_{T_{ref}}^T C_v dT \quad (5.32)$$

The maximum of free enthalpy of each critical droplet follows to be

$$G_{max} = -\frac{4}{6}\pi r^{*3}[(P_d - P_s) + \rho^{fl}\Delta\mu] = \frac{4}{3}\pi\gamma r^{*2} \equiv \frac{1}{3}\gamma A \quad (5.33)$$

As shown by Volmer [132] the free enthalpy of the critical droplet G_{max} can be interpreted as surface energy minus compression energy. This can be casted in the formula $G_{max} = \gamma A - 4\pi(P_r - P_d)r^{*3}/3$, where the surface area A is $A \equiv 4\pi r^{*2}$. It coincides with Gibb's original result [125].

The rate formula of spontaneous condensation

According to Volmer's classical theory [108] the formation energy G_{max} of a droplet has to be interpreted as the activation energy of the droplet growth process. Hence nucleation rate I (in mol germs per volume) can be derived to

$$I = C \exp(-G_{max}/(kT_d)) \quad (5.34)$$

Here C will be explained below, k is the Boltzmann factor and T_d is the (undercooled) temperature of the vapor with

$$G_{max} = \frac{1}{3}\gamma A \quad (5.35)$$

The expression coincides with the maximum free enthalpy valid for the critical droplet as shown in eq.5.33. This classical old version is the most simple accepted form of

description and is applied here only. The most common formulation of the complete prefactor C here has been derived by Zeldovich [133]. It is described by

$$C = f * A * Z / v_d \quad (5.36)$$

where the droplet surface A is $A = 4\pi r^{*2}$, v_d is the specific volume of the gas, the non-equilibrium factor Z is

$$Z = \left(\frac{\Delta G}{3\pi k T_d} \right)^{1/2} \frac{3v_{fl}}{4\pi r^{*3}} \quad (5.37)$$

and the frequency factor f is

$$f = \frac{P_d}{(2\pi m k T_d)^{1/2}} \quad (5.38)$$

The rate equation has been modified by Feder[134]. For miscible mixtures it has been generalized by Reiss[112]. It was applied practically by Zahoransky [130].

the growing droplet

a) Introduction

In order to describe the enthalpy of the whole labile transient condensing process one has to determine temperature and radius of each class of grown-up droplets at each time moment. Generally, the growth of droplets can be described by systems of coupled time stepper ODE's [135], of which we sketch here the general mathematical form

$$\begin{aligned} \frac{\partial T}{\partial t} &= f(t) & (I) \\ \frac{\partial r}{\partial t} &= g(t) & (II) \\ \frac{\partial T}{\partial r} &= f(t)/g(t) = h(t) & (III) \end{aligned} \quad (5.39)$$

If the relevant relations are found these equations can determine the growth of droplets born at any time interval during the process. So one obtains at every moment the "droplet spectrum". It allows to sum up the enthalpy of the whole system at any time t . This is needed to determine the non-equilibrium isentrope of expansion or compression.

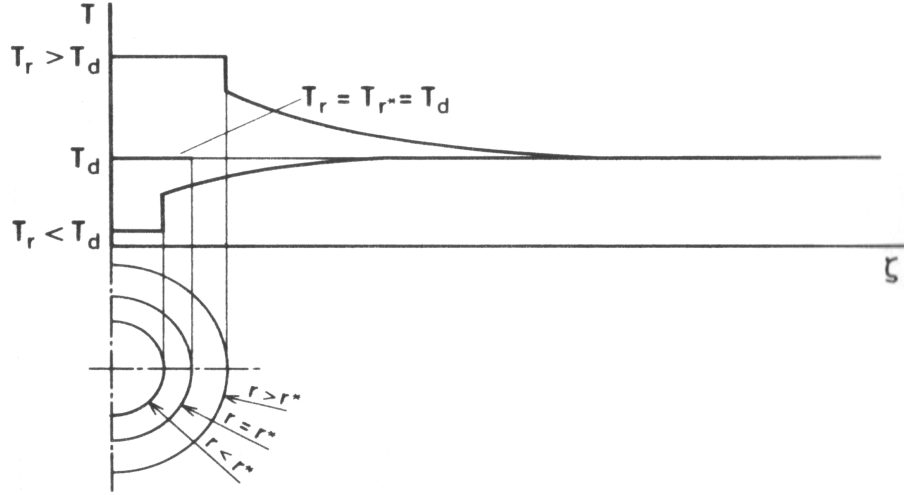


Figure 5.19: Hedbäck's model temperature distribution at a condensing droplet, from [124]

b) The droplet growth equation determined by the non-equilibrium transport field

If the boundary conditions at the droplet surface are known then the equation system of non-linear thermodynamics in the gas can be solved which yields the space-time profiles of temperature, specific density and the advection field around a droplet in an non-equilibrated gas atmosphere. This is very complicated. So I apply here the simplified ansatz from Hedbäck's thesis [124] because it can be programmed with my possibilities. In appendix 5.6 it is shown in the appendix that this ansatz contains a coupled boundary condition for heat exchange and mass at the changing liquid - gas interface and can be reconciled with the formalism of non-equilibrium thermodynamics under some simplifying assumptions.

Hedbäck derives an equation for heat exchange at the boundary of the droplet, cf. fig. 5.19

$$\begin{aligned}
 \frac{1}{4\pi r^2} \frac{\partial Q}{\partial t} &= \alpha_r (T_r - T_d) \\
 &= \alpha_m (T_r - T_i) \\
 &= \alpha_k (T_i - T_d) = \dot{H}_z - \dot{H}_b - \dot{H}_0 = \dot{r} \left((W_k - \frac{r}{3} W_b) / v_r - W_0 \right)
 \end{aligned} \tag{5.40}$$

The symbols in 5.40 are defined in fig.5.19 and in the text below as follows:

$$\dot{H}_z \equiv 4\pi r^2 \dot{r} W_k / v_r \tag{5.41}$$

is the enthalpy contribution to the droplet due to the mass transport and the phase transition. W_k is calculated to

$$W_k = H_b^0 + T_r(s_d(T_d, P_d) - s_f(T_r, P_r)) - \frac{C_p^g(T_r - T_d)}{1 + \alpha_m/\alpha_k} + g^\Delta \quad (5.42)$$

where the original equation had to be corrected here by g^Δ which is defined in fig.5.20. The symbols are: α_r is the total heat transfer number which defined as $\alpha_r \equiv (1/\alpha_k + 1/\alpha_m)^{(-1)}$ consisting of two serial resistors $1/\alpha$ of heat transfer due to conduction $\alpha_k = \lambda/r$ ($\lambda \equiv$ heat conduction coefficient of the mixture vapor, cf. [81]) and mass transport α_m . This number is calculated by $\alpha_m = C_p^g(\sqrt{P_d/(2\pi v_i)} - (\partial r/\partial t)/v_r)$ where v_i is the specific volume (per mass unit) of the vapor molecules to be condensed. Note that v_i is the value situated directly at the droplet boundary and has a different value than the mean value v_{Di} in a far distance from the droplet. α_m is explained by the kinetic model of heat exchange in the next neighborhood of the droplet[124].

$\dot{H}_b = 4\pi r^2 \dot{r}(H_b^0 + W_b \cdot r/3)/v_r$ is the enthalpy contribution due to the growing mass of the droplet. W_b is calculated to (we have corrected here Hedbäck's κ_T by $\kappa_T \equiv v_r$)

$$W_b = (C_p^{fl} + v_r \frac{2}{r} \frac{\partial \gamma}{\partial T}) \frac{\partial T}{\partial r} + v_r \frac{2\gamma}{r^2} \quad (5.43)$$

$\dot{H}_0 = 4\pi r^2 \dot{r} W_0$ is the enthalpy contribution due to the surface enthalpy. W_0 is calculated here as

$$W_0 = (\frac{2\gamma}{r} + \frac{\partial \gamma}{\partial T} \frac{\partial T}{\partial r})_r \quad (5.44)$$

From eq. 5.40 an equation of the growth of a droplet radius can be derived

$$\frac{\partial r}{\partial t} = \frac{\alpha_r(T_r - T_d)v_r}{W_k - \frac{r}{3}W_b - v_r W_0} \quad (5.45)$$

This formula will become an element of the ODE system of a growing droplet, cf.sec.5.6.

c) the equation of the temperature of a growing droplet dependent from the radius

As mentioned already in the introduction of this section an important ingredient for the numeric calculation of spontaneous condensation problems is an equation for the temperature of the growing droplets as function of the radius. As long as the temperature of the droplet T_r is different from the global temperature T_d the droplet is not in equilibrium with its environment and grows or shrinks. A first approximative relation of such a equation was developed by Gyarmathy [136]. He derived

$$T_r - T_d = \left(1 - \frac{r^*}{r}\right)(T_{ref} - T_d) \quad (5.46)$$

This relation can be derived also as a special case from the differential equation by Hedbäck [124] if the entropies s_d and s_{fl} and the surface tension γ are set to be constant with respect to temperature. Hedbäck's differential equation 5.22 has been derived already above

$$\frac{\partial T_r}{\partial r} = \frac{2\gamma}{2r \cdot \partial\gamma/\partial T + r^2(s_d - s_{fl})/v_{fl}} \quad (5.47)$$

Originally Hedbäck claimed that this equation is a general solution for $\partial T_r/\partial r$ valid for all droplets. However, it is wrong to apply 5.47 for growing droplets because the equation 5.47 asserts that the mother eq. $g_d(T_r, P_d) = g_{fl}(T_r, P_r)$ cf. eq. 5.17 is valid always. This holds only at the labile extremum (saddle) point of the free enthalpy G_j of a droplet of species j . In order to solve this problem for the growing droplet I generalize eq. 5.17 and 5.47 by adding a compensating difference of free enthalpy (per mass or mol) g_j^Δ in order to obtain an equation, namely, cf. fig. 5.20.

$$g_j^\Delta \equiv g_d^j(T_r, P_d) - g_{fl}^j(T_r, P_r) \quad (5.48)$$

This term g_j^Δ will be evaluated in the following.

It can be rewritten, cf. fig. 5.20

$$g_j^\Delta \equiv \frac{G_{j,max}(T_r)}{4\pi r^{*3}/v_{fl}} - \frac{G_j(T_r)}{4\pi r^3/v_{fl}} \quad (5.49)$$

Here $G_{j,max}$ and $G_j(T_r)$ stems from eq. 5.33 and eq. 5.28 . Along the line of the derivation in sec. 5.3.2 one obtains a differential equation as solution for any droplet

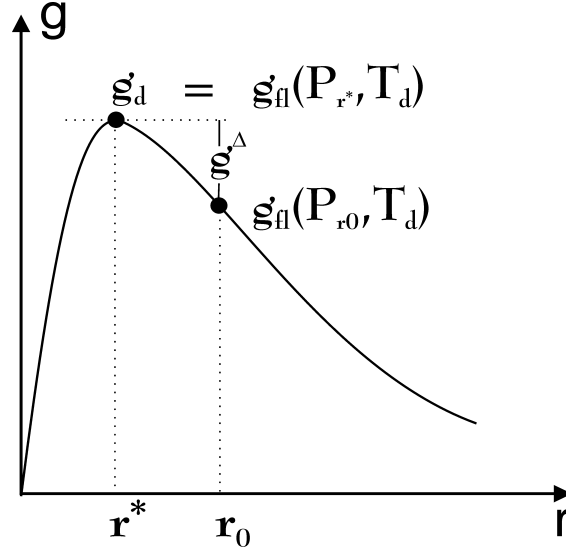


Figure 5.20: Free enthalpy g (per mass or mol) of a droplet vs. radius r
 g^Δ is defined as difference specific enthalpy between the real growing droplet minus specific free enthalpy (per mass or mol) of the critical droplet, cf. text.

written dependent either in terms of r or x

(I assume for simplicity that $v_{fl} = \text{const.}$ So $\Delta v_{fl} \approx \partial g^\Delta / \partial P = 0$ can be neglected)

$$\frac{\partial x}{\partial T} = - \frac{2x \cdot \partial \gamma / \partial T + (s_d - s_{fl} + \partial g^\Delta / \partial T) / v_{fl}}{2\gamma} \quad (5.50)$$

$$\frac{\partial T}{\partial r} = \frac{2\gamma}{2r \partial \gamma / \partial T + r^2 (s_d - s_{fl} + \partial g^\Delta / \partial T) / v_{fl}} \quad (5.51)$$

with the solution

$$\frac{1}{r} \equiv x = - \frac{1}{2\gamma} \int_{T_{sat}}^{T_r} \frac{s_d - s_{fl} + \partial g^\Delta / \partial T}{v_{fl}} dT \quad (5.52)$$

For better handling and programming some transformations are useful.

Inserting eq. 5.28, 5.30 and 5.33 in eq. 5.49 yields

$$g_j^\Delta(T_r) = 3v_{fl}\gamma \left(\frac{1}{r^*(T_r)} - \frac{1}{r} \right) = 3v_{fl}\gamma (x_K(T_r) - x) \quad (5.53)$$

From eq. 5.48 follows with eq.5.17

$$g_j^\Delta(T_r) = g_d^j(T_r, P_d) - g_{fl}^j(T_r, P_r) = 2v_{fl}(x_H(T_r) - x) \quad (5.54)$$

From eq.5.53 and 5.54 follows

$$x = 3.x_K - 2.x_H \quad (5.55)$$

Using eq.5.53 and 5.55 we can write

$$g^\Delta = 3.\gamma(T_r)v_{fl}[2x_H - 2x_K] = 6\gamma(T_r)v_{fl}[x_H - x_K] \quad (5.56)$$

the full equation system and the solving algorithm

The solving algorithm contains two main elements:

- 1) a routine solving for the actual critical radiuses in the state of supersaturation
- 2) If the supersaturation is high enough and if the amount of condensation is quantitatively relevant then the so called droplet spectra routines are switched on each for water or benzene droplets. Then at any moment the growth rate is calculated for each present droplet class which were born at any preceding iteration step before. The (simple version) equation system to be solved for T_r and r of every class of droplets (in continuous or in discrete version) is

$$\frac{\Delta T_r}{\Delta t} = \frac{\partial T_r}{\partial r} \frac{\partial r}{\partial t} \quad \text{or} \quad \frac{T_r^i - T_r^{i-1}}{t_i - t_{i-1}} = \frac{\partial T_r}{\partial r} \frac{\partial r}{\partial t} \quad I) \quad (5.57)$$

$$1/x = \int_0^t \frac{\partial r}{\partial t} dt \quad \text{or} \quad 1/x_i = 1/x_{i-1} + \frac{\partial r}{\partial t} \Delta t \quad II) \quad (5.58)$$

Eq. 5.57 I) contains eq. 5.50 and eq.5.45 , eq. 5.58 II) contains eq. 5.56 and eq.5.45. If the temperatures and the radiuses of all droplet classes are calculated the composition of gases and liquids in both phases can be determined. The obtained data allow to add up the enthalpy of the mixture. In order to be able to solve the complete problem numerically with own means it is assumed here that the gas phase is always spatially homogeneous for pressure, temperature and density. This assumption is also a preliminary simplification to test out whether the system can be calculated numerically. Then the enthalpy of the combined vapor-liquid system is

$$h = X_G x_D^W h_g^W + X_G (1 - x_D^W) h_g^B + \sum_j \Delta X_{fl}^W(j) h_{fl}^W + \sum_j \Delta X_{fl}^B(j) h_{fl}^B \quad (5.59)$$

Here we define x_0 to be $x_0 \equiv$ the initial and total molar ratio of water in volume, $X_{fl}^W \equiv \sum_j \Delta X_{fl}^W(j)$ total molar ratio of liquid water as sum of the different droplet classes j of same radius. Similarly is $X_{fl}^B \equiv \sum_j \Delta X_{fl}^B(j)$ the total molar ratio of liquid benzene with $X_{fl}^{W/B}(j) = v_g^{W/B}(t_i) I_j \Delta t_i r_{ij}^3 4\pi L / v_{fl}^{W/B}$ being the molar liquid content of a class j of droplets of water or benzene at the moment t_i born before at the moment t_j in the volume. Then it follows it is $X_G \equiv 1 - X_{fl}^W - X_{fl}^B \equiv$ molar gas content in the volume. $x_D^W = [x_0 - (1 - x_G) X_{fl}^W / (X_{fl}^B + X_{fl}^W)] / x_G$ is the molar ratio of water steam in the gas (due to mass conservation) and $v_g^{W/B} \equiv x_D^{W/B} X_G v(t_i)$ follows which is calculated according to the simplifying assumption from the beginning.

The expansion and compression of the cylinder proceeds as follows: The expansion is started at an equilibrium point. The time profile of expansion + eventually compression $v(t)$ is set by the formula $v(t_i) = v(t_1) + v_{hub}(1 - \cos(2\pi t_i))$. v_{hub} is calculated from the given maximum compression factor $\chi_{comp} \equiv v(t_{endpoint})/v(t_1)$ by $v_{hub} = v(t_1)(\chi_{comp} - 1)/2$.

The total solving algorithm of the non-equilibrium expansion proceeds as follows:

In the initial phase - as long as the condensation rate is low enough - the droplet spectrum is switched off: This means $X_{fl}^W = 0$, $X_{fl}^B = 0$. Only the critical radiuses and the very low ineffective spontaneous condensation rate are calculated.

If one species of droplet only becomes supersaturated and can condense, the system to be solved is dependent only from the unknown variables temperature T_d and labile partial pressure P_d . Then the final equation system to be solved consists of the equations

$$v = \frac{\partial h}{\partial P_d} \quad x_K = x_H \quad (5.60)$$

The second equation states that the reciprocal critical droplet radius is the same regardless whether it is calculated according to Volmer / Frenkel or according to Kelvin / Helmholtz . If two pure species are supersaturated the system to be solved is dependent from the unknown variables T_d , P_d (water) , and P_d (benzene).

Then, the system to be solved is

$$\begin{aligned} v &= \frac{\partial h}{\partial P_d} \\ \text{for water :} \quad x_K &= x_H \\ \text{for benzene :} \quad x_K &= x_H \end{aligned} \quad (5.61)$$

So the algorithm solves for the transient thermodynamic pathway of the labile mixture:

- calculate the first point $i=1$ from the initial values:
 set N, T, x, P and calculate p_{sat}, x_{sat}, h, x_g
- **for** every i from the point 2 until to the endpoint index N
 - set new volume $v(t_i)$ and starting values P_d and T_d of the iteration
 - if sufficient droplets exist already - determine their growth using eq. 5.58
 - add up the enthalpy eq. 5.59
 - solve equation system eq. 5.60 or eq. 5.61
 - calculate and store all relevant values of the actual point
- **next** point i

For the integration the Euler-Heun procedure is used. At the moment only equidistant time intervals are used with a maximum number of 4600 time points. The numerical calculation of the supersaturated states (without condensation) works well, the droplet condensation, however, breaks down after some iterations due to missing memory. All calculations are done by a small 2 GHz Pentium 4 notebook.

The longest time per run to perform a simulation is about a day.

Results

The first numerical results of the simplified model discussed are shown in fig. 5.21. They show that the difference between labile state and equilibrium curves are not too large if no liquid condenses. Surprisingly the supersaturated pressures are higher than the equilibrium isentrope line which is contrary to all textbooks. It is clear that the method is still not matured enough with respect to quantitative correctness in order to make statements regarding the Second Law.

Furthermore it is also clear that Doczekal's pressure values, cf. fig. 5.5 are far off from any curve calculated here and therefore seem to be doubtful.

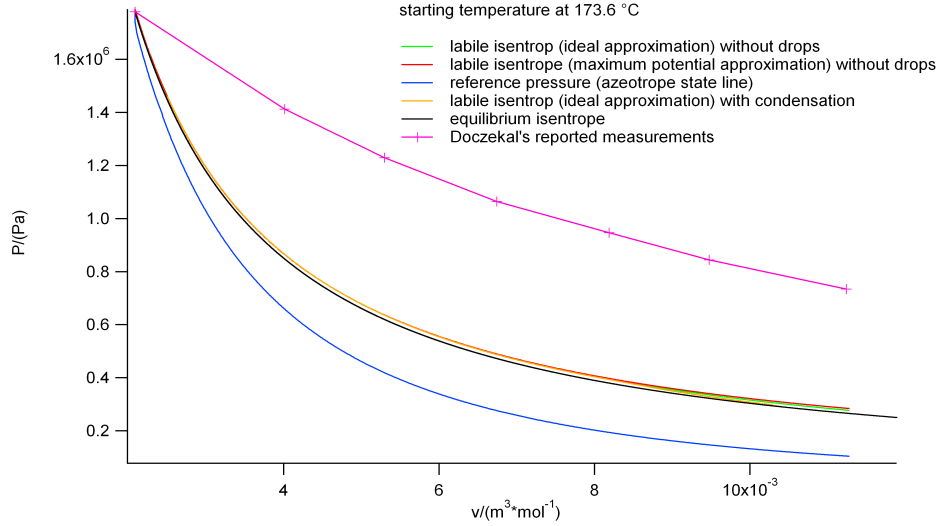


Figure 5.21: P-v- expansion water-benzene calculated according to different methods
 main results: 1) the supersaturated expansion is at higher pressures than the isentrope
 2) Doczekals experimental data show much higher pressures than the other curves calculated

Possible Improvements

Before I describe the possible improvements of my current algorithm I write down the thermodynamic equations valid for real gases [52]

$$\begin{aligned}
 \bar{H} &= \sum_{i=1}^n x_i (\bar{H}_{0i} + \int_{T_0}^T C_{P_i}^0(T) dT) \\
 &\quad + (Z_M - 1)RT + \int_v^\infty (P - T \frac{dP}{dT}) dv \\
 \bar{S} &= \sum_{i=1}^n x_i (\bar{S}_{0i} + \int_{T_0}^T \frac{C_{P_i}^0}{T} dT + R \log x_i) \\
 &\quad - R \log(\frac{RT}{P_0 v}) + \int_0^\rho (\frac{R}{\rho} - \frac{1}{\rho^2} \frac{dP}{dT}) d\rho \\
 C_P &= C_V + \frac{T}{\rho^2} \frac{(\frac{dP}{dT})_V^2}{(\frac{dP}{d\rho})_T} = C_V - \frac{T(\frac{dP}{dT})_V^2}{(\frac{dP}{dv})_T}
 \end{aligned} \tag{5.62}$$

My present non equilibrium-algorithm still applies caloric equilibrium data of the vapor. The long term aim is to apply real gas quantities C_p , C_v , H and S in the

labile state obtained numerically during the simulation without any extrapolation by an equilibrium EOS. In order to achieve this for $(\partial P/\partial T)_v$, $(\partial P/\partial v)_T$ and C_v I propose the following method:

At each iteration step vary the volume slightly by Δv to $v' = v \pm \Delta v$. Perform the varied iteration at v' as done for v already ! These varied iterations produce the additional data which allow to extrapolate numerically the next values in the numerical calculation of $(\Delta P/\Delta T)_v$ and $(\Delta P/\Delta v)_T$ (in the labile state).

Then C_v can be estimated numerically from the differential $dS(T, v) = \partial S/\partial T dT + \partial S/\partial v dv$. Applying the Maxwell relation $(\partial S/\partial v)_T = -(\partial P/\partial T)_v$ one obtains

$$C_v dT \equiv T \left(\frac{\partial S}{\partial T} \right)_v dT = T \left(\frac{\partial P}{\partial T} \right)_v dv + T dS \quad (5.63)$$

where the heat $dQ = TdS$ is nonzero if liquid condenses or evaporates, or if heat exchange with the environment takes place, cf. eq. 5.40.

If liquid condenses significantly then the problem complicates:

Then the differential quotients $(-\Delta P/\Delta T)_v = (\Delta S/\Delta v)_T$ and $-(\Delta P/\Delta v)_T$ and their differences $\Delta S_T, \Delta P_v, \Delta P_v$ and Δh_T have to be determined for C_p numerically for each class of droplets. In order to solve for the local specific gas volume v_i around the droplet the additional equation to be solved is:

$$v_i = \frac{\Delta h - T \Delta S}{\Delta P} \quad (5.64)$$

Therefrom for each step the labile real gas contributions for C_P in eq.5.62 at every t_i

$$\int_{v_n}^{v_{n-1}} (P - T \frac{dP}{dT}) dv \quad \text{and} \quad \int_{\rho_{n-1}}^{\rho_n} (\frac{R}{\rho} - \frac{1}{\rho^2} \frac{dP}{dT}) d\rho \quad (5.65)$$

can be determined for the gas phase. They can be added up to the full integral and help to determine the labile values of eq.5.63. This procedure may allow to remove the initial approximation $v_i = v_g^{W/B}$ by summing up over the self-organized spatial profiles of gas density and temperature around the droplets.

5.4 How to replace the Second Law

Today the name "Second Law" suggests that there should exist a law which describes something which is meant that the Second Law should be. Actually, however, in reality there exists no Second Law but a zoo of Second Laws [59, 137] and even for a "normal" scientist it is normally not clear at all whether and in which sense these version are equivalent, what they mean exactly and which is the generally valid real version.

In the following I will present some of these different versions and will compare them with the statements of nonlinear dynamics. It is clear that independently from the mathematical rhetorics each of these theories should come essentially to the same result in the end for the same physical system. However, in fact, this is not the case as it will be shown below.

The most known versions of the Second Law are:

- I) Clausius integral version II) Kelvin's ban on 100% efficiency heat to work converter.
- III) Gibb's stability criterion IV) Prigogine's principle of minimum entropy dissipation.

To I) In 1854 Clausius introduced the expression dQ/T and he formulated the ban on perpetuum mobiles of 2nd kind in terms of dQ/T for closed cycles with irreversible parts [138]. In 1865 he defined $dS \equiv dQ/T$ and created the term entropy for S [15]. So he derived for a closed cycle with irreversibilities

$$\oint dS \geq 0 \quad (5.66)$$

I call this formulation the integral formulation of the Second Law (version I)

Due to energy conservation (i.e. $\oint dU = T \oint dS + W = 0$) it follows as a special case that under isothermal conditions - if only one heat bath is present - it holds

$$\begin{aligned} W &= - \oint p dV \geq 0 \\ W &= - \int \oint P dE dV \geq 0 \text{ all equations at } T = \text{constant} \\ W &= - \int \oint M dH dV \geq 0. \end{aligned} \quad (5.67)$$

The electro-magnetic versions of eq. 5.67 rely on the fact that the currently best state of the art electric engines convert electric energy to mechanical energy by an efficiency near to 100% .

To II) Another well known formulation of the Second Law from 1851 goes back to Kelvin [139] p.174 ff. It bases on Carnot's prediction (proven by Clausius[140]) of a maximum (Carnot) efficiency for any steam engine [141] which is regarded as an equivalent to the Second Law. It is equivalent also to Clausius statement from 1850[140], which means, that no machine can transport heat against a temperature difference by itself. It is concluded therefrom by Kelvin that a cyclic machine does not convert heat to work with an efficiency of 100%. This is the classical thermodynamical ban on perpetuum mobile of 2nd kind (version II). It means that any machine can consume only (and does not deliver) mechanical or electro-magnetic energy after a closed cycle if it is in contact with one heat bath only.

To III) In 1875 Gibbs applied the Second Law in order to define the stability behavior of a system [125]. He formulated the Second Law in differential form

$$dS \geq 0 \quad (5.68)$$

I call this version the differential version (version III)

Therefrom the principles of mechanical and thermal stability are derived

$$\kappa_S \equiv -\frac{1}{V} \left(\frac{dV}{dp} \right)_S > 0 \quad c_v > 0 \quad c_p > 0 \quad \kappa_T > 0 \quad (5.69)$$

To IV) In the 20th century the Second Law has been transferred to non-equilibrium thermodynamics by the Brussel school of Prigogine [142]. They reformulated the Second Law as the principle of minimum entropy production with the aim to have a principle of stability for systems out of equilibrium.

$$\frac{dS}{dt} - > \text{minimum} \quad (5.70)$$

They extended the thermodynamics also to non-linear systems. Therefore the new mathematical methods of non-linear dynamics were applied. These methods allow to describe qualitative different systems like bistable, chaotic and oscillating ones which all were not covered by thermodynamics so far. Stability behavior is analyzed here by linear stability analysis, cf. tab.5.6.

They showed that thermodynamic stability (i.e stability conditions based on minimum entropy production) can be proved by linear stability analysis as stable fixpoints of a dynamical system. Furthermore they weakened the concept of stability by introducing

Lyapunov stability and applied these new methods in order to characterize the stability of dissipative oscillating systems.

It should be emphasized that all the axioms mentioned do not create a consistent situation automatically. So Muschik [143] postulates that the constitutive equations have to be restricted in order to fulfil the Second Law. Otherwise violations are possible.

From the beginning of thermodynamics not everybody liked the narrow axiomatic depressive philosophy behind the Second Law(s) and its consequences. So J.J. Thomson wrote a book [106] already in 1888 in order "to endeavour to see what result can be deduced by the aid of .. dynamical principles without using the Second Law of Thermodynamics." I will show by comparison with the features of the thermodynamics how non-linear dynamics can be applied.

Therefore I regard a nonlinear dynamic FitzHugh-Nagumo equation

$$\dot{v} = v - v^3 - w + I_{ext} \quad \dot{w} = v - a - bw \quad (5.71)$$

It is well known that this system can have stable, bistable and oscillating solutions dependent from the control parameter $q = (a, b)$. Principally this system can be mirrored if the moving coordinate $x = (u, v)$ is exchanged for instance by the mapping $x^* = (u, v^*) = (u, -v)$. It is clear that the orientation of a cycle in a (q, x) plane is reversed in the mirrored (q, x^*) plane space. The stability behaviour remains unchanged under this operation. So it is mathematically shown that the orientation of any quasi-stationary path in a (q, x) -(working) diagram is independent from the stability behavior of the system. Transferred to physics terminology this means:

Table 5.6: comparison of thermodynamics vs. non-linear dynamics concepts, cf. [142]

	Non-linear dynamics	thermodynamics
stability:	by linear stability analysis	minimum entropy dissipation
Second Law check	by check of orientation of quasistationary cycle	by constitutive equation and material test criteria
variable	control parameter	extensive variable (??)
variable	dependent variable	intensive variable (??)

1) the maximum entropy principle (version III) is a existence condition of any stable thermodynamic system. It is a purely mathematical statement contrary to the other versions of Second Law. The condition is necessary - but not sufficient for existence of the Second Law. Therefrom I conclude:

Even if stability exists and if the maximum entropy principle is fulfilled - the ban on a perpetuum mobile of second kind can be violated if stable inverted fixpoint curves exist which have control variables as independent parameters.

2) the constitutive equations of the material determine the orientation of a thermodynamic cycle finally. They describe whether a substance behaves according to the Second Law (version I or II) or not [9]. In the model with Doczekal's system one can regard the vector $q = (N, V)$ as the control parameter - and the $x = (P, T)$ - vector corresponding to the moving variables (u, v) of the differential equation system. Further Second Law violating candidates due to such a appropriate (or inappropriate) constitutive material behavior can be found under the key word "inverted hysteresis"

3) May be that the inverted cycles have to do something with a phenomenon known from non-linear dynamics called labile fixpoint stabilization. This means that a labile equilibrium point can be stabilized if the system is brought near to the labile equilibrium and if a periodic forcing is applied for stabilization. Known examples for such phenomena are known from the artists in the circus cf. fig. 5.22 or in science [144] and engineering. These principles are known as inverted pendulum in mechanics [145] [146] , they are applied in simple quadrupole mass spectrometer or in more sophisticated higher pole setups to trap molecules [147]. They are perhaps unnoticed in Ruthenocuprate-system [148]. So in the labile state space around these labile maxima "the thermodynamic rules of the world" may be reversed for inverted hysteresis non-dissipative material properties. Then permanent oscillatory states can be stabilized.

So I summarize:

It is known that the different versions of the Second Law are not equivalent [137]. The most real versions of the Second Law may be the criteria which coincide with the stability analysis of non-linear dynamics. These formulations have a clear mathematical foundation and can not die if new physical observations are made.

If we are more radical we can say that the old version of the Second Law should be replaced by correct and complete dynamically constitutive equations of the material which contain the physical information of the system exclusively. This alternative



Figure 5.22: the inverted pendulum

pragmatic formulation of the "Second Law" is of course quite contrary to the quasi-religious intentions of Clausius who wanted to establish the Second Law as a natural law independent from the individual material and the processes applied [57].

For a dynamical system an axiom about the Second Law compatibility is obsolete because the question is answered by the mathematical solution of the dynamical system. As shown by the Doczekal cycle the classical ban on perpetual mobiles could be violated if the cyclic processes are proceeded inversed outside of the small subspace reserved for the well known thermodynamic cycles of Clausius's theory or Prigogines chemical oscillators.

5.5 Summary

- 1) The equilibrium calculation of the water-benzene system confirms the typical efficiency of Irinyi's steam engine measured by independent referies.
- 2) A new non-equilibrium theory of spontaneous condensation introduces the following improvements for the calculation methods of adiabatic expansion and compression:
 - a) it calculates labile expansions and compressions in cylinders forced by a piston.
 - b) no EOS extrapolation or ideal gas assumption is necessary for the labile gas phase. Instead of this a new equation is introduced which bases on the postulate that the critical radius of droplet formation has to be always the same - regardless whether it is calculated according to a Kelvin-like or a Thomson-like prescription.
 - c) The conventional definition of reference equilibrium temperature of the labile state is modified in order to be able to describe mixtures.
 - d) the theory can be based on conventional non-equilibrium thermodynamics, it applies new boundary conditions at the droplet boundary and has the real perspective to be extended to general mixtures.
- 3) The calculated pressures of an adiabatically expanded water-benzene vapour are much lower if they are compared with the claimed measurement of Doczekal.
- 4) Despite of the many new features of the theory the method is still not matured and has to be improved by varying and precisising the implemented approximations.
- 5) The Second Law is a heuristic helping tool of the 19th century in order to predict the direction of irreversible processes. Today, if we are able to formulate the problems in terms of non-linear dynamics, this method can be avoided.

5.6 Appendix

In this section it is discussed to which extent Hedbäck's equation 5.40

$$\alpha_r(T_r - T_i) = \dot{r}((W_k - \frac{r}{3}W_b)/v_r - W_0)$$

is compatible with non-equilibrium thermodynamics. We will see that the equation is a combined boundary condition for heat and mass at the liquid-vapor droplet interface. The derivation of 5.40 implies many not mentioned simplifying assumptions. The theoretical framework of our discussion can be found in the textbook by Baranowski[22]. First we neglect any force fields on the particles and set the momentum equation (i.e. viscous effects and pressure tensor) to zero for simplification.

So, if the momentum balance in [22], p.50, equ.(4.42), is omitted the following reduced balance equation system consisting of the mass balance [22], p.36, equ.(3.30), and the enthalpy balance [22], p.180, eq.(12.119),

$$\frac{\partial c_i}{\partial t} + v \cdot \nabla c_i = -\nabla J_i - c_i \nabla v \quad (5.72)$$

$$\rho c_p \frac{\partial T}{\partial t} + c_p v \cdot \nabla T = \sum_{i=1}^{n-1} D_i Q_i^* \nabla x_i + \nabla T - \sum_{i=1}^n J_i \cdot \nabla \bar{h}_i \quad (5.73)$$

is the starting point of the consideration here. The symbols are: c_i the molar concentrations of a species, v the velocity (if specied with an index specified for a species), J_i is the molar current pro surface, D_i is the diffusion constants of the species i , Q_i^* is the cross diffusion coefficient (Dufour effect = inversion of thermodiffusion !), and \bar{h}_i is the enthalpy density of a component i . The generalized thermodynamic fluxes J_i are described generally by Onsager's linear approach to describe transport phenomena, i.e.

$$J_i = \sum_{j=1}^{n-1} L_{ij}(X_j - X_n) + L_{in}Q^*X_q \quad (5.74)$$

$$J_q = \sum_{j=1}^{n-1} L_{jq}Q^*(X_j - X_n) + L_{qq}X_q \quad (5.75)$$

where X are the thermodynamic forces which drive the fluxes. The appropriate definition of the forces X is given below in the context of this article. The L_{ij} are Onsager's

linear thermodynamic coefficients which make the equation numerically correct. The equations 5.72 and 5.73 describe the thermodynamic field around the condensing droplet. If they are solved the spatial profile of mass and heat is obtained. However, because the inhomogeneous structuring of the gas phase is neglected in our work, cf. sec 3.3.5, these equations are not solved explicitly. I am interested only in the boundary conditions of the heat and mass at the droplet vapor liquid interface. In order to describe the heat balance around the droplet the Gibbs fundamental equation

$$T \cdot \frac{d\bar{s}}{dt} = \frac{d\bar{u}}{dt} + p \cdot \frac{d\bar{v}}{dt} - \sum_i \bar{\mu}_i \frac{dx_i}{dt} \quad (5.76)$$

has to be written down. Then, if the balance equations of inner energy density \bar{u} and x_i are inserted and after many calculation steps described by Baranowski in [22] p.83-87, he obtains in the end the known non-equilibrium entropy balance equation of entropy of the form (which we multiplied by the test volume ΔV)

$$\frac{\partial(\Delta V \rho \bar{s})}{\partial t} = (-div J'_{\rho \bar{s}} + \sigma_{\rho \bar{s}}) \cdot \Delta V \quad (5.77)$$

where the variable $J'_{\rho \bar{s}}$ in the divergence term is defined by (with $v^* \equiv$ transformed velocity, see definition below)

$$J'_{\rho \bar{s}} = \rho \bar{s} v^* + \sum_i \bar{s}_i J_i + \frac{J_q}{T} \quad (5.78)$$

with the shorted entropy source term definition

$$\sigma_{\rho \bar{s}} \equiv \frac{1}{T} J_q \cdot X_q + - \sum_i J_i \cdot X_i \quad (5.79)$$

and with the thermodynamic forces X defined here by

$$\begin{aligned} X_i &= -\nabla \left(\frac{\bar{\mu}_i}{T} \right) \\ X_q &= -\frac{\nabla T}{T} \end{aligned} \quad (5.80)$$

The growth of a droplet is controlled by the rate of heat or/and mass exchange with the gas environment. This is characterized by the boundary conditions at the phase border. The growth of a droplet is controlled by the rate of heat or/and mass exchange with the

gas environment. This is characterized by the boundary conditions at the phase border. For the boundary condition of mass the oldest rule stems from Smoluchowski[149]. He stated $c = 0$. As a consequence it was calculated then that this rule lead to a growth law for purely diffusive system which shows an infinite stream into the sink when the condensation process starts. Therefore Collins and Kimball [150] improved the boundary condition and found arguments for a boundary condition of the form, $ck = D \cdot \nabla c$. If both side of the equation are multiplied by $4\pi r^2$ and having Fick's first law in mind (at no convection) the rule can be interpreted that a diffusive influx of gas leads to the growing of the droplet into the opposite direction. This rule was applied by Collins [151] and Frisch and Collins [114]. They calculated analytically the growth law therefrom for a purely diffusive system. The result shows already the well known separation between the kinetic regime and the continuum regime around the droplet. Collins' boundary condition however has a problem. It does not include the known convective Stefan flow. Another more general boundary condition is proposed here. This new boundary condition for mass exchange includes the convective flow

$$c_{fl} \cdot \dot{r} = D_g \frac{\partial c_g}{\partial r} - c_g(v - \dot{r}) \quad (5.81)$$

This boundary condition is a continuity equation taken at the moving gas vapor interface of the droplet. In order to be able to compare equation 5.78 with Hedbäck's heat balance eq. 5.40, we change 5.78 to a moving coordinate making a spatial coordinate transformation $\xi \rightarrow \xi^*$ where the origin of the new coordinate system is sitting now at the droplet boundary interface. The coordinate transformation is

$$\xi^{*'} = \xi - r(t) \quad v^* = \dot{\xi} - \dot{r}(t) \quad (5.82)$$

The transformed balance at droplet boundary is

$$T \frac{\partial(\rho \bar{s} \Delta V)}{\partial t} - T \sigma_{\rho \bar{s}} \Delta V = -T \cdot (\text{div}(\rho \bar{s}(v - \dot{r}) + \sum_i \bar{s}_i J_i + \frac{J_q}{T}) \cdot \Delta V \quad (5.83)$$

The left side of the transformed equation represents the inner of the droplet, the right side represents the outer influx of the gas. Now we want to identify the terms of the last equation by comparing them with Hedbäck's derivation eq.5.40. In order to do so we remember our first boundary condition for mass eq. 5.81, we assume $\bar{s} = \bar{s}_i$

to be valid in our case and we apply the Gauss integral theorem (integrating variable $\Delta V = 4\pi r^2 \Delta r$) for the second and third equation then we can identify the terms of 5.83 by the following equations

$$\begin{aligned}
 T \frac{\partial(\rho \bar{s} \Delta V)}{\partial t} &= 4\pi r^2 (W_0 + \frac{r.W_b}{3v_r} + \frac{T \bar{s}_{fl}}{v_r}) \dot{r} & I) \\
 -T(\rho_g \bar{s}_g(v - \dot{r}) + \sum_i \bar{s}_{ig} J_i) &= T \rho_{fl} \bar{s}_g \dot{r} = \dot{r}(W_k + T \bar{s}_{fl})/v_r & II) \\
 4\pi r^2 J_q &= -4\pi r^2 \lambda grad T = \alpha_m(T_r - T_i) & \dots III)
 \end{aligned} \tag{5.84}$$

The first equation describes the change of enthalpy or heat in the liquid droplet under quasi-isobaric conditions, the second describes the material heat/enthalpy transport by the energy contained in the gas to be condensed and the third represents the diffusive heat transport away from droplet. It holds $eq.III = eq.II - eq.I$. On the left side this is eq. 5.83 integrated (where $\sigma_{\rho \bar{s}} = 0$), on the right side we obtain exactly Hedbäck's original boundary condition. We see that the entropy source term has been set to $\sigma_{\rho \bar{s}=0}$ because it has no pendant in Hedbäck's eq. 5.40.

I summarize: Hedbäck's heat transport equation at the droplet interface is equivalent to a combined non-equilibrium thermodynamical boundary condition of heat and mass valid for cases where the following simplifications can be applied:

- 1) pressure differences and chemical effects in the gas are neglected in the calculation
- 2) Any entropy production is regarded to be negligible with respect to other energy exchanges. This means physically that any temperature differences in the liquid droplet are neglected in the entropy balance. Note that other models show that the temperature differences may exist [118][119].

It should be mentioned that according to Baranowski [22] the calculation here using the classical set of formulas is not fully correct. He presents a corrected set of equations which is more complicated and which is skipped here. It may become relevant if one extends the theory to multi-component droplet condensation.

Chapter 6

Beyond the Second Law

6.1 Systems driven by Fluctuations

I will give here a short incomplete view on a field of science which is relevant in the context of overunity systems. This section is written in order to give some keywords in order to ease the access to the primary official scientific literature.

6.1.1 Introduction

In section 2.2.2 vortex systems in fluctating media were discussed. These theoretical model objects were invented by Smoluchowski [152] and are better known under the name "ratchets" today. Feynman popularized them in his famous textbook[153]. He argued from the thermodynamics doctrine (without any material information input)

that it is impossible to violate the second law with these systems because a nano-ratchet system itself behaves as a thermally fluctuating object. So he developed a theoretical thermodynamic model which prevents any precise ratchet working.

However, it is clear that vortex systems (see fig.2.1) work even if they are driven by a fluctuating noise field which of course has to match to the system. Therefore it is interesting to find out the conditions and the limits at which these systems work. Then the question of the second law compatibility can be answered more precisely.

It is shown here by standard model considerations how this problem can be tackled: A ratchet system element may be in a spatial (and/or time) fluctuating noise field $\tilde{\mathbf{E}}$. It exerts the generalized torque T by the coupling of the fluctuating field $\tilde{\mathbf{E}}$ to the the generalized charge (or resistance) matrix density $\hat{\mathbf{Q}}$ integrated by the volume $d\mathbf{x}'^3$

$$\mathbf{T} = \int (\hat{\mathbf{Q}}(\mathbf{x}', \mathbf{x}) \cdot \tilde{\mathbf{E}}(\mathbf{x}', \mathbf{x})) \times \mathbf{x} d\mathbf{x}'^3 \quad (6.1)$$

The torque \mathbf{T} is exerted on the arms of a wheel as shown in fig.2.1 and is can produce work. We describe the energy transfer in first order by the equation

$$T = \Theta \cdot \ddot{\varphi} + \gamma \cdot \dot{\varphi} \quad (6.2)$$

where φ is the angular coordinate, γ damping constant Θ the moment of inertia of the generalized mass and T the fluctuating generalized torque from the environment.

So, generally, in order to build any system driven by any noise source we have to answer the following questions:

What is the amplitude of the driving noise ? What is the noise spectrum? What is the spatial distribution ? Can the noise couple to the system or it is damped out ?

Here I will give a short incomplete overview of the state of the art.

6.1.2 Noise Driven Systems

While application of the ratchet principle at a larger length scale is standard technology today, nano-ratchets are current topics of research of scientific groups worldwide. Such system are named also as Brownian motors or quantum motors dependent from the source of fluctuations. A collection of typical examples are described in Applied Physics 75A in 2002. These are non-equilibrium systems with a periodic potential

which are driven additionally by a weak periodical noise source. So a flow is generated which can be harvested. Some of these system are built experimentally showing particle separation. The energy balance question is discussed seldomly. Most interesting is this question for AC - driven ratchets because they can circumvent the thermal effects in the model and produce DC offset current due to quantum noise [154].

Stochastic resonance can be a candidate for overunity efficiencies also. Haenggi discusses these system under this aspect, however his opinion is not too optimistic [155]. Very interesting is an "inverted hysteresis" ratchet model with two noise sources [156], see also sec. 6.2. The discussion of the system in the article is purely formal. The question remains whether it can be applied for electro-magnetic variables connected to a thermal and a quantum noise source.

6.1.3 van der Waals Force and Zero Point Energy

In the overunity scene the concept of zero point energy (ZPE) is a central hypothesis. It suggests that the energy balance problem can be resolved for overunity systems by a noise energy influx. Here I refer to the "official" current state of discussion, cf. [157]. The application of this hypothesis was initiated by Casimir[158] and Polder[159] in 1948. They assumed the vacuum to be full of zero point noise waves which have their origin from the Heisenberg uncertainty. They are present at absolut zero temperature. These waves can be shielded or reflected by metal boundaries So flat metal parallel plates are pressed together from outside if they are very near. (An analogous effect is well known from ships which must not pass nearly because they are attracted together if the waves in the sea are high). Interestingly the identical result for the same system was derived later by assuming a spatial distributed source of a electromagnetic background noise field [160]. Later this assumption was justified again by quantum electrodynamics [161]. In these papers the effect could be interpreted also as a van-derWaals interaction. The attracting part were the quantum-mechanically fluctuating (London-)forces [162, 163] between instantaneously induced dipoles.

Although the results of all methods coincide, the natural philosophy of the approaches is opposite: London's vanderWaals dispersion forces are explained by forces caused from inside of the molecules, Casimir forces seem to be generated from the outside

field. The natural philosophy of the last model suggests generally that the structures of matter may be stabilized by a fluctuating input field from outside. The idea is founded by quantum field theory and is called zero point energy field.

So proposals came up to apply this for the explanation of gravitation[164], or as well to implement it as a new physical force for the construction of propulsions [165, 166] and -(perhaps because of infinite energy integrals appearing in the calculation)- for second law violating gain cycles [167, 168]. A later paper [169] discusses Casimir forces in terms of the equilibrium thermodynamics of a photon gas. It concludes that most thermodynamic changes of this ZPE system are unstable. A newer articles tries to explain the selfcharging of piezoelectric crystal batteries and capacitances [170].

The main problem of ZPE energy research, however, is, that the proved force effects discussed are tiny, see cf.[157]. They are accessible experimentally by the AFM [171]. So the energy exchanges of the speculated or proved overunity cycles are still small and far off from any economic relevance.

6.2 Inverted Hysteresis Systems

6.2.1 Introduction

Inverted hysteresis exists if the orientation of the hysteresis loop of a magnetic or dielectric material is opposite to the well known loss hysteresis. According to the Poynting theorem of electrodynamics[172, 173] the existence of an inverted hysteresis area means that the material performs electromagnetic work under isothermal conditions. Inverted hysteresis systems are candidates for cycles beyond the Second Law.

Articles describing such effects exist since the thirties of the last century [174].

However, the phenomenon itself has been overlooked or not mentioned for long time. In the sixties it is found that the ferroelectric hysteresis loop of DNA is inverted partially[175]. In the seventies magnetic layer systems are investigated as storage elements. The inverted hysteresis is rediscovered as a surface effect interesting for magneto-optic storage discs[176]. 1977 the first magnetic metal layer system is discovered and shows a still unstable inverted hysteresis [177]. In 1990 the systems are

more stable at room temperature. It can be shown that the inverted hysteresis effect is measured as a global effect[178] although it is attributed to an interface coupling[179]. In 1994 Aharoni[180] remarks in a theoretical article that inverted hysteresis might violate the second law of thermodynamics.

Inverted electric hysteresis can be found in the gate capacitance of semiconductor storage elements[9]. Typical examples are the Yusa-Sakaki FET[181, 182], MFIS capacitances[183] as used in industrially produced DRAM cells[184].

Any discussion of the energetic aspect in the references about inverted hysteresis is seldom, only one article was found which sheds doubts on the effects measured therefore[185]. Another article shows up possible problems of the measurement with inverted magnetic hysteresis systems[186]. But despite of this, every year some articles about inverted hysteresis systems are published until today[187].

Tabel 6.1 gives a short overview for the different types of literature about inverted hysteresis systems from the beginning up to today. For magnetic layer systems especially with Cobalt there exist some coincidences between the different articles. For electric systems many references report an inverted hysteresis of some FET designs.

The last references found in Tab.6.1 are singular and still have to be confirmed or disproved.

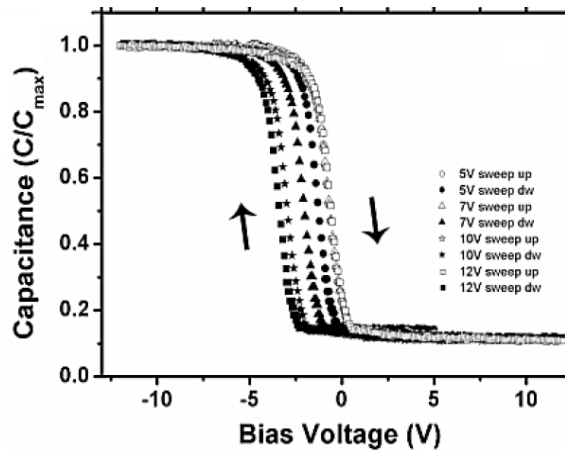


Figure 6.1: typical asymmetric inverted gate capacitance of a p-MFIS-FET, cf.[183]

Table 6.1: Typical references of inverted hysteresis systems

system	work	year	reference
Cu-Co layer	exp.	1990	[178]
Pd-Ni-multilayer	exp./theor.	1996	[188]
CoFeAlO thin film	exp.	2005	[189]
Co-MOVCD-film	exp.	2006	[190]
Co:CoO core nanoclusters	exp	2008	[191]
$Pr_{0.7}Ca_{0.3}MnO_3/SrRuO_3$ Superlattices	exp.	2011	[187]
Yusa-Sakaki-FET	exp./theor.	1997	[181, 182]
MFIS-FET	exp.	2005	[183]
DRAM-FET	exp.	2005	[184]
Ni-Fe wire	exp.	1938	[174]
bulk Rhodrosite	exp.	2004	[192]
bulk Ruthenocuprates	exp.	2002	[148]
Fe-Cu composite	exp.	2007	[193]

6.2.2 Basics for Hysteresis Measurements

the Maxwell Equations

If one follows the history of electromagnetism the first mathematical descriptions of magnetism were formulated as effects originating from current wires [194]. After Faraday introduced the field concept Maxwell could summarize quite generally most of the knowledge of electromagnetism of his time in a set of partial differential equation describing the fields in space [195–197]. In order to maintain the consistency of Ampere’s law with the continuity equation of electric charges the electric displacement current was added. After Maxwell’s death, in the course of time, especially the constitutive equations of the materials complicated the Maxwell theory. Therefore, Maxwell’s equations are reproduced here in a modified general updated form, cf. [198]:

$$\begin{aligned}
-\oint \mathbf{E} \, ds &= \frac{1}{c} \frac{d\phi}{dt} = \frac{1}{c} \frac{d}{dt} \sum_i \int \mathbf{B} \, d\mathbf{A}_i \\
\oint \mathbf{H} \, ds &= \frac{1}{c} \frac{d\theta}{dt} = \frac{1}{c} \frac{d}{dt} \sum_i \int \mathbf{D} \, d\mathbf{A}_i
\end{aligned} \tag{6.3}$$

$$\begin{aligned}
-\nabla \times \mathbf{E} &= \frac{1}{c} \frac{\partial \mathbf{B}}{\partial t} + \sum_i \left(\frac{4\pi}{c} \rho_{Hi} \mathbf{v}_i - \nabla \times \left(\frac{\mathbf{v}_i}{c} \times \mathbf{B} \right) \right) \\
\nabla \times \mathbf{H} &= \frac{1}{c} \frac{\partial \mathbf{D}}{\partial t} + \sum_i \left(\frac{4\pi}{c} \rho_{Ei} \mathbf{v}_i - \nabla \times \left(\frac{\mathbf{v}_i}{c} \times \mathbf{D} \right) \right)
\end{aligned} \tag{6.4}$$

$$0 = \dot{\rho}_H + \sum_i \nabla \mathbf{j}_H(i) \qquad 0 = \dot{\rho}_E + \sum_i \nabla \mathbf{j}_E(i) \tag{6.5}$$

$$\text{div} \mathbf{B} = 4\pi \rho_H \qquad \text{div} \mathbf{D} = 4\pi \rho_E \tag{6.6}$$

The definitions of the symbols are from Jackson[172], cf. also appendix 6.4.4. The summation symbol in the lines of 6.3 and 6.4 takes into account that different species of charges with different velocities can exist at any point in the field. In the equations 6.4 the Lorentz force [199] and the Rowland effect [200][201] are accounted for. In the induction law the magnetic charges are written out in order to include magnetic currents and charges, cf. experiments. [202–206]. Therefrom follow the energy and moment conservation of systems with electromagnetic charges, cf. appendix 6.4.2.

The Maxwell equations are the Helmholtz decomposition of the electromagnetic field, cf. section 2.2. Note that the equations 6.4 are directly derived from the equations 6.3. The mathematical calculation is from [207]. The derivation is reproduced in appendix 6.4.1. The continuity equations 6.5 follow from 6.4 by applying the div-operator.

In the next section the very important decomposition of the terms $\dot{\rho}$ or \dot{D} or \dot{B} into two parts will be introduced namely $\dot{\rho} = \dot{\rho}_S + \dot{\rho}_P$ or $\dot{D} = \dot{D}_S + \dot{D}_P$ or $\dot{B} = \dot{B}_S + \dot{B}_P$, cf. [208]. The index P denotes the contributions originating from charge polarisation, the index S denotes the "new" source term, cf. [209], which describes charge separation in the medium, maybe due to ionisation, charged particle generation, photo effect or interband hopping into the conduction band. The analogous source terms for magnetism describe self-polarisation maybe due to a phase transition at a Curie point.

the Definitions for Inductivity and Capacitance

The concepts of inductivity and capacitance are older than Maxwell's theory. They are defined by the old simplified and incomplete precursor versions of Maxwell's field equations which were formulated in terms of I and U . The equations (6.7) below

$$\begin{aligned} -\nabla \times \mathbf{E} &= \frac{1}{c} \frac{\partial}{\partial t} (\mathbf{B}_P + \mathbf{B}_S) & -U &= L\dot{I} + \dot{\phi}_S \\ -\nabla \mathbf{j}_E &= \dot{\rho}_{EP} + \dot{\rho}_{ES} & I &= C\dot{U} + I_S \end{aligned} \quad (6.7)$$

show the (shorted) Maxwell field equations and aside the adequate old style versions. The technical possibilities or restrictions of measurement lead to the prescription that inductivity L and capacitance C have to be defined as slopes $L \equiv \frac{d}{dI}\phi(I; t)$ and $C \equiv \frac{d}{dU}Q(U; t)$. Inductivity $L(I)$ and capacitance $C(U)$ can be measured so locally either by a AC signal and a phase measurement or by a pulse experiment each with a small amplitude. Due to the method of measuring the source terms $\dot{\phi}_S$ or I_S are not detected under stationary conditions of I or U . The constitutive material functions of $\dot{\phi}_S$ or I_S have to be found to reconstruct the information loss of the measurement.

Fig. 6.1 shows a typical diagram of a capacitance with inverted hysteresis. It suggests that after a closed cycle the system should be charged up because it holds $\Delta Q = \oint dQ/dU dU \neq 0$ [210]. However, in reality it is observed after a cycle that the whole system is again in the same initial charge state when the cycle was started. This fact can be explained by including the source term in the continuity equations.

I discuss here the two basic theoretical possibilities in order to reconstruct the lost integration constants after introducing $L \equiv \frac{d}{dI}\phi(I; t)$ and $C \equiv \frac{d}{dU}Q(U; t)$:

1) If $\Delta Q_{ES} = 0$ it holds $\Delta Q_{ES} = \int \int \dot{\rho}_{ES} dt dV = - \int \int (\nabla j + \dot{\rho}_{EP}) dt dV = 0$. Then, if the hysteretic cycle area is non zero we have a "polarisation jump" or "voltage jump". This case corresponds to the birth of an inner dielectric double layer.

2) If $\Delta Q_{EP} = \int \int \dot{\rho}_{EP} dt dV = - \int \int (\nabla j + \dot{\rho}_{ES}) dt dV = 0$ holds after the cycle Δt , the polarization state can be described by a (unique) state function. Therefrom it follows that the inverted hysteresis charge area, i.e. the effect of the integrated charge source term I_S in equation 6.7 is measured by the integration of the ∇j -offset current. This I call a "charge jump" which can explain the electric case.

For magnetic systems "magnetic charges" are introduced as an analogon to electricity. This approach can be tested by asymmetric magnetic hysteretic materials [193].

So we can conclude: Any energetic description of nonlinear capacitances or inductivities with hysteresis must include source terms like $\dot{\phi}_S$ or I_S because inverted hysteresis capacitance or inductance diagrams do not represent the complete information of the system. Such systems can behave as if they are supplied by a source of additional charge or voltage "from inside". The direct physical cause of these source terms are the birth and the death of charge pairs for electric phenomena and for magnetic phenomena self-polarisation effects by a changing magnetic density.

If source terms are present additional equations outside of electrodynamics (maybe from thermodynamics or quantum mechanics) must describe any outer influx sources.

6.2.3 Magnetic Systems

Magnetic inverted hysteresis is demonstrated generally by a $\mathbf{M} - \mathbf{H}$ diagram which at first sight contains the full energy information of the sample measured quasistatically. An alternative diagram exists which shows susceptibility χ vs. magnetic field \mathbf{H} . It contains less information because it is derived from the slope of the $\mathbf{M} - \mathbf{H}$ - diagram. Normally the $\mathbf{M} - \mathbf{H}$ diagram shows a point symmetry. Then the "magnetic charge area" (indicated indirectly by $\oint \chi dH$) is zero. So any net flow of magnetic charges is excluded and the hysteresis is explained only by polarisation changes.

Four methods are applied in order to measure inverted hysteresis.

- 1) MOKE (magneto-optic Kerr effect) 33 references found
- 2) VSM (vibrating sample magnetometry) 38 references found
- 3) AC-detection (alternating current detection) 6 references found
- 4) TM (torque magnetometry by a torsion balance) 1 reference found

to 1) The magneto-optic Kerr effect is only surface sensitive. This method only gives no answer to questions about the energetics of the whole probe.

So all these references are neither cited nor discussed here.

to 2) The vibrating sample magnetometer gives a better answer about the energetic behaviour of the probe. It was invented in 1959 [211] and is a standard method today.

It is very sensitive and can be used for thin film samples. Today superconducting coils and SQUIDS are build in oftenly. Then the results of measurements at field strengths $H_C < 20 \text{ Oe}$ can be critical because the superconducting coils can have persistent coil currents which falsify the instrument's readout [186] and can suggest so an inverted hysteresis. Therefore 11 from 19 references are omitted because it is not clear whether the authors is accounted for this problem.

to 3) The AC-detection is applied seldomly in the context of inverted hysteresis.

It is less sensitive if compared with VSM. It is applied mainly for bulk probes.

to 4) The torque magnetometry is the oldest method [212] in order to measure inverted hysteresis but today it is applied quite seldom.

A selection of the experimental articles about inverted hysteresis gives Tab. 6.2.

There exist about 8 articles analyzing inverted hysteresis theoretically.

Generally the theory of magnetic materials describes the inner field M of any material by a combination of five basic theoretical effects or energies [213]:

- 1) the external (Zeeman-) field energy due the interaction with an external H -field.
- 2) the (Weiss-) demagnetisation field energy due to the self-interaction of the field.
- 3) the exchange energy. This is a potential energy associated with gradients in the orientation of the magnetization field. Or- it is due to the internal interaction energies in or at the sample at boundaries.
- 4) the anisotropy energy. It describes the dependence of the potential energy on the orientation of the magnetization field relative to the crystal axes.
- 5) the magnetostrictive energy. It describes the influence introduced by strains in the crystal lattice on the magnetization field energy.

The experimental inverted thin film systems normally have a hard and a soft magnetic axis. Only one direction of them can show inverted hysteresis. Therefore, most theoretical articles discuss the anisotropy energy (point 4) as cause of inverted hysteresis: Aharoni[180] and O'Shea + al-Sharif [179] discussed the early two-layer film systems. Aharoni's model reproduces inverted hysteresis due to finite dimensions and pores.

The model of O'Shea and al-Sharif includes a simple Stoner-Wohlfarth-(SW) model [214] (i.e. Zeeman- plus exchange terms) for each layer plus an exchange term describing the interaction between the two adjacent films. Both want to explain the

Table 6.2: the currently most significant measurements of magnetic inverted hysteresis

system	method	$-H_C/(G)$	T/(K)	references
<i>thin films:</i>				
Zr ₄₀ Cu ₅₀ Mn ₁₀	VSM [215]	80k	77	[177]
Co-Cu-thin film	VSM	4k	300	[178]
CoFeAlO thin film	VSM	160	300	[189][216]
CoFe/LaCoFeO thin film	VSM	80	300	[217]
$La_{0.7}Sr_{0.3}MnO_3/SrRuO_3$	SQUID	160k	5	[218]
Fe _{0.78} Pd _{0.22}	VSM	8k	300	[219]
<i>Cobalt systems:</i>				
Co-MOCVD	VSM [220]	200k	300	[221] [190]
Co:CoO clusters	SQUID	160k	300	[191]
Co clusters	SQUID	800	125	[222]
<i>multilayers:</i>				
Co-Cu-multilayer	VSM	4k	300	[223][224]
Pd-Ni-multilayer	VSM/TM[225]	8k	300	[226]
Co/Pt/Gd/Pt multilayer	SQUID	8k	4,5	[227]
Fe/Ho multilayer	VSM	16k	80k	[228]
<i>sandwich structures:</i>				
MnIr/CoFe/Ru/CoFe/MnIr	SQUID	1k	300	[229]
SiN/GdFeCoSi/SiN	VSM	1k	300	[230]
Ta/NiFe/Ta	VSM	1,2k	300	[231]
Ni/TbFeCo/Ni trilayer	SQUID	8k	300	[232]
<i>bulk materials:</i>				
SrIIIGdIIHexacyanochromateIII	SQUID	800	2	[233]
bulk Rhodrosite	AC	?	≤ 34	[192]
bulk Fe-Cu composite	AC	10k	300	[193]
$Fe_{1-x}Co_xSi$ bulk	SQUID	20	4	[234]
<i>miscellaneous:</i>				
bulk labile Ruthenocuprates	VSM/AC	?	300	[148]
Ni-Fe wire	AC	?	300	[174]

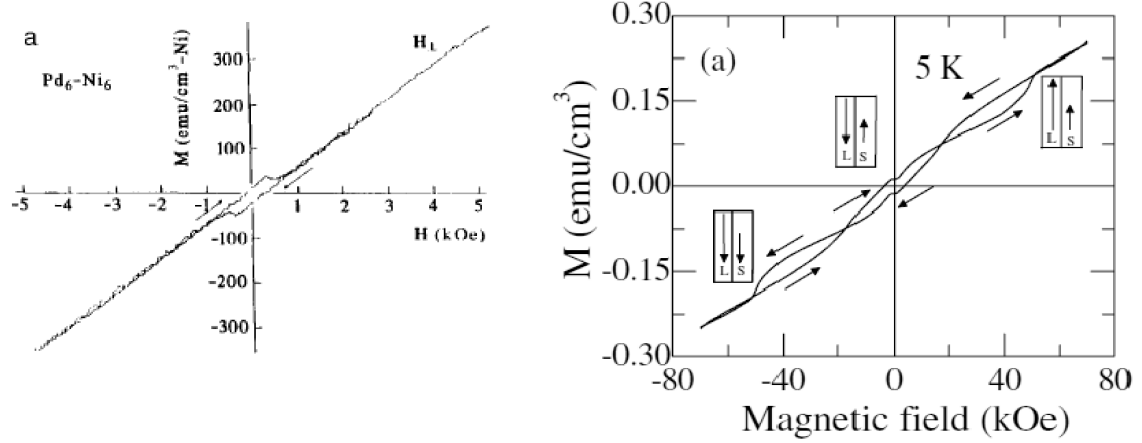


Figure 6.2: typical M-H diagrams of different types of inverted hysteresis
left insert: inverted single loop [188]; right insert: partially inverted loop cf.[238]

single inverted loops as measured by [178] and [224], but obtain a 3 - loop systems with an inverted loop in the middle, cf. fig. 6.2. A similar result is obtained by Geshev [235] for a mixture of cubic magnetocrystalline and a uniaxial components. Y.-J. Nam and S.H. Lim [236] simplify this ansatz again and extract from the improved classical Stoner-Wohlfarth (SW) model[237] (with two uniaxial anisotropies) an phase diagram of material parameters which allows to simulate an inverted middle loop of a 3 loop hysteresis system but no single inverted loop.

Byeon et al. [238] modify the SW model and assume an only slightly oblique "perpendicular" magnetic axis. The result is again a very small inverted hysteresis of the middle loop in a 3-loop hysteresis system which they confirm experimentally, cf. fig. 6.2 . Further theoretical paper exist discussing inverted loops in terms of the Heisenberg formalism. The results of [239] resemble the experimental result of [240]. Another article [241] discusses Prussian blue as possible inverted hysteresis bulk material similar to a previous reported bulk substance [233].

Poulopolos et al.[188], cf. fig. 6.2, investigate a 2-component Pd-Ni or Pt-Co magnet film system consisting of two antimagnetically coupled layers. They discuss a single observed inverted hysteresis loop which appears if the sample is not saturated magnetically. In their simulation they include a quadratic anisotropy contribution from [242] and an interlayer exchange energy. So they fit the experimental data to the single

inverted hysteresis loop. They mention that the cycles have a metastable pathway. They do not believe in second law violations by arguing that elastic crystal energies compensate the observed effect. In deed, elastic effects are not accounted for in the model. But this is justified because there is no elastic energy exchange in their experiment [243]. They obtained their data by VSM and torque magnetometry[225].

This means:

According to the Poynting energy conservation an magnetic energy outflux per cycle represented by the hysteresis area is really observed for their experiments.

So far the following questions regarding physics and technology remain open for me:

- 1) Can inverted hysteresis be caused by a magnetoelastic oscillation in the VSM ?
Today modern equipment tries to avoid the elastic input by appropriate design [244].
- 2) Is inverse hysteresis possible at higher frequency and at a higher amplitude of H ?
Quite all methods detect the loop by small test signals and "slow" detection speed.
- 3) What is the lifetime of the samples ? Can the quality be improved ?

Information of the sample lifetimes is seldom, in [177] and [223] it is about some days.

- 4) There exist only few bulk systems oftenly at very low temperature. How do magnetic cores of this material behave ?

- 5) Are inverted minor loops always possible, especially for 3-loop-systems ?

Two references [231] [188] were found so far mentioning explicitly that inverse hysteresis minor loops are obtained. Contrary, for spring exchange magnets (oftenly realized by 3 loop systems) minor loops are not possible always, see [245] [246] [247] [187].

- 6) What are the long term effect if the material is permanently cycled in the field?

Do we see physical side effects like cooling or is the sample destroyed by the process ?

- 7) Can the samples be upscaled macroscopically in order to obtain electronic products?
Or more precise - can inverted hysteresis be transferred to tape wound metal cores ?

6.2.4 Electric Systems

Introduction - the Semiconductor Capacity

For our further discussion we present here three known electronic elements which generate a relevant semiconductor capacitance, see fig. 6.3:

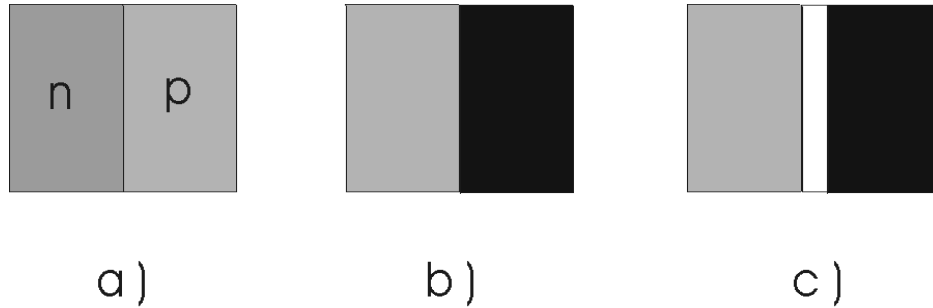


Figure 6.3: the different semiconductor capacities

a): p-n junction; b): Schottky metal(black)-semiconductor (grey);
 c): MIS-contact, i.e. metal(black)-insulator(white)-semiconductor(grey)

1) the Schottky diode. This is a metal - semiconductor contact. Its behaviour was explained qualitatively first by Schottky [248] [249].

2) the standard p-n diode. It consists of the p-n semiconductor junction. It was explained by Shockley (Nobel prize in physics 1956) [250] [249].

3) the FET . This invention goes back to Lilienfeld around 1925 [251] and Oskar Heil around 1934 [252]. After the development of pure materials the first industrial processable FET components were published in 1960 [253] [254]. This were MIS (metal-insulator-semiconductor) or MOS (metal-oxide-semiconductors) transistors.

The most simple FET capacity consists of three layers of different materials, cf. fig 6.3. A basis layer made from a doped bulky semiconductor connected to the electrical ground, an thin isolating layer oftenly consisting of an oxide and a top (thin)conducting metal layer. If the top metal layer is charged by the application of a voltage, charges are induced as well at the surface of the semiconductor. Then a current can flow along channel below the surface if contacts for drain and source exist on the semiconductor. The first successful theoretical description of the FET was the Pao-Sah model [255]. As it is done numerically today for every static semiconductor component they solved the Poisson equation of the charge species analytically. Additionally a thermodynamical equation holds in the semiconductor component which describes the chemical potentials equilibrated in space and determines the density of the charge species from the Fermi distribution. The model was made popular by Brews [256] who added the

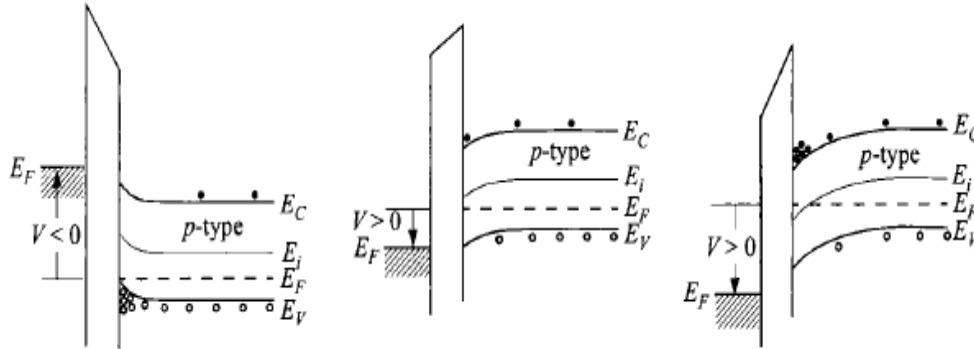


Figure 6.4: the different FET regimes dependent from voltage; from [249]
left: $V < 0$ accumulation; middle: $V > 0$ depletion; right: inversion $V \gg 0$

charge sheet approximation which allowed to estimate the charge and the (low frequency) capacity vs. voltage of the FET correctly. The theory differs three states of charging capacity dependent from voltage: accumulation, inversion and depletion, cf. fig.6.4. For the p-type semiconductor substrates we have accumulation (of holes) at the interface isolator- p-substrate at minus voltage bias. At moderate positive bias we have there depletion of holes and at higher positive bias we have an interface "inversion" layer of electrons(or a two dimensional electron gas 2DEG) plus depletion of holes. For n-type semiconductor substrates the situation is vice versa with electrons. Fig. 6.5 shows the calculated and measured C-U diagram for p-doted systems. Coincidence of the old theory [256] with the experiment can be obtained if low frequency AC-capacitance measurement are applied. If the frequency of the AC testing signal is too fast the inversion can not be detected because the buildup of the electrons of the inversion layer at the interface is too slow and can not follow the frequency of the testing AC voltage. This case coincides with the shape of many published C-V-diagrams of capacitances, cf. fig. 6.1.

As mentioned already, there exist the further complications by so called traps. At the beginning traps were only disturbing the technology, they shifted the C-V curves or deteriorated the quality of electronic components. But after understanding and mastering the processes behind, charge traps were applied systematically in order to build electronic storage elements, optical detector element(CCD) or other sensors. If

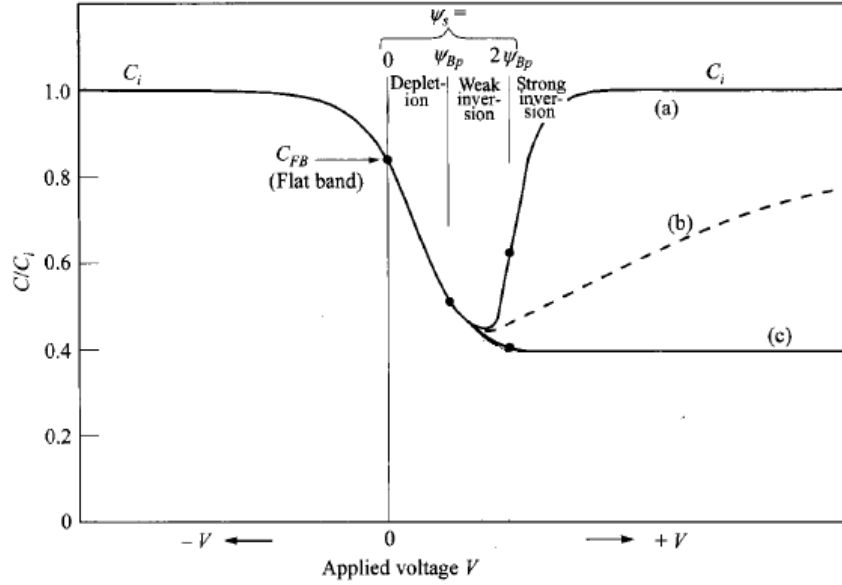


Figure 6.5: the MFIS capacities at the different voltage; modified from [249]
measurement at a) low frequency b) intermediate frequency, c) high frequencies

the traps in the isolating layer of a FET capacity are charged the capacitance curve shifts [257]. So a hysteresis is generated. Then the state of charged storage cell can be tested by the measurement of the drain current of a storage FET element.

Traps are locations and defects at the surface [258], [259] of the isolators or in the bulk of the electronic elements [260] where the charges can attach, cf. also Sze [249]. They are described similarly like donors and acceptor in the semiconductor [261]. They are regarded to be immobile (if compared with electrons and holes). One distinguishes interface traps at the surface, cristal defects or oxide traps in the bulk, ionic traps due to impurities in the bulk, and also today the well defined modern traps - the so called quantum dots. Each trap is characterized by an energy distance (or a spectrum of energies) from the valence or the conduction band and a time constant for generation or annihilation, cf. Sze [249].

Different methods exist for the diagnosis of these traps. An old method is a surface conductance measurement which can detect surface traps [262]. More precise information is obtained by newer methods which bake out the FET and measure quantitatively the current of the "desorbing" charge [263] [264].

The today state of the art is the dynamic capacitance spectroscopy [265–267] . Generally, storage elements based on electrically charged traps have a restricted data lifetime because any trapped charge diffuses with time. So the idea came up to apply the hysteresis state of a ferroelectric material instead of a trapped charge. The first MFIS (metal ferroelectric insulator semiconductor)- FETs were built in 1974 by Wu [268]. Today there exist different variations of the MFIS - FETs showing inverted hysteresis [268] [269] [183] [270] [184] [271] [272] [273].

The first theory article on MFIS FETs was published in 1992 [274]. After some improvements [275] the static Pao-Sah theory of MFIS FET's is today a standard instrument of modeling and some groups contribute to theme [276–279]. Traps are not included in these simulations. The simulations reproduce the inverted hysteresis [275] [278] which is a surprise for the author after some preliminary own initial numerical experiments. If these published results are true the missing integration constant from the C-V diagram (to the Q-V or **P-E** -diagram) can be identified here with the voltage jump of the ferroelectret.

No information was found so far about the dynamic behaviour of the components. Another very illustrative example of implementing traps systematically is the quantum dot FET invented by Yusa-Sakaki [181]. This structure is shown in fig. 6.6 . It consists of a modified FET-structure + a Schottky gate contact. As shown in fig. 6.7 the FET shows an inverted hysteresis. The cycle can be closed if the FET is irradiated by IR-photons. Then the bound electrons leave the potential traps again and the

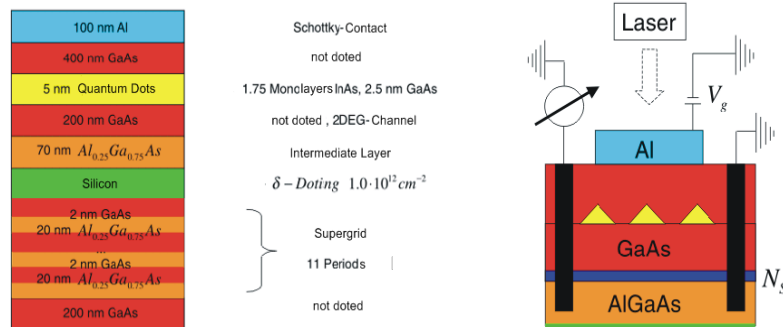


Figure 6.6: the Yusa-Sakaki FET ; from [209]

left: the layer structure of the FET; right: the electric circuit of the FET

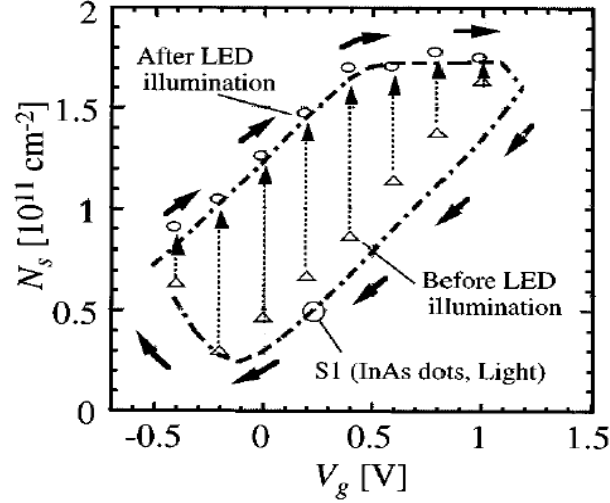


Figure 6.7: 2DEG-density seen by cyclotron resonance in the Yusa-Sakaki FET [181]

memory charge of the quantum dots (QD) is erased. The same effect can be achieved if a negative voltage is applied [280]. Normally conventional theoretical models assume a tunnel injection or lossy ohmic diffusion current as mechanism charging or discharging the traps. Rack et al. [182] propose a model for the Yusa-Sakaki FET which contains a source term suggesting an "internal" charging of the quantum dots. So they simulate an inverted hysteresis cycle of this FET, cf. 6.8.

Recently Marent et al. [267] published about an advanced hole storage element which shows also an analogous inverted hysteresis due to hole storage in the quantum dots. I discuss it below because the characteristic electronic values of the element allow the full simulation of a parametric oscillation near to reality.

The biggest memory window of inverted hysteresis -which I found- are FETs storing up alternatively electrons (after writing) or holes (after erasing) [281] [282].

Discussion - models for inverted capacitances

Rack's model of the electric cycle of the Yusa-Sakaki FET calculates an inverted hysteresis cycle, see fig. 6.8 and 6.9. In some sense the Yusa-Sakaki FET can be regarded

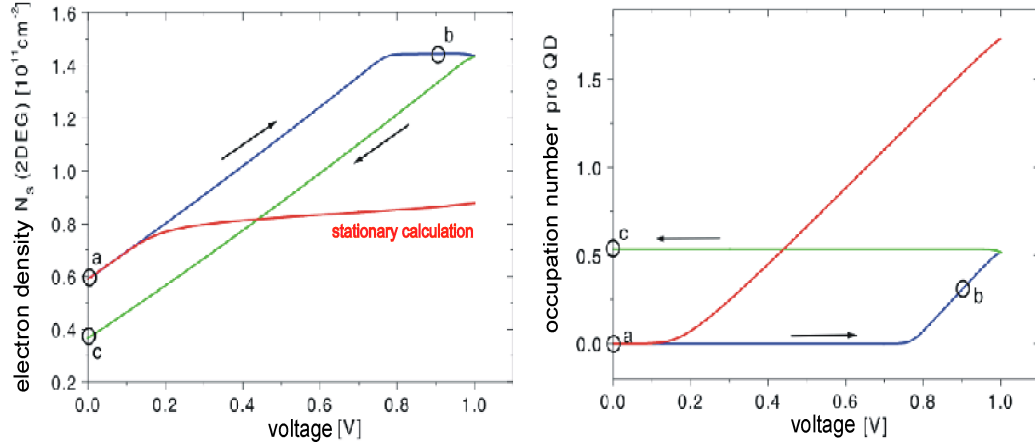


Figure 6.8: Electron density in the Yusa-Sakaki FET cycle calculated; from [209]
left: electrons in 2DEG vs. voltage; right: occupation of electrons in QD's vs. voltage

as a realization of Maxwell's demon. The stored electrons remain in the QD traps until collisions with photons of the ambient thermal radiation supply enough energy that the potential barrier can be overcome (Fowler emission). So, similarly like in a photocell, the QD-electrons select out the higher energetic part of the thermal energy and act as a Maxwell daemon. After closing the process the cycle can be repeated. Another (quantum mechanic) process helps to close the cycle as well: If a negative voltage is applied then the internal triangular potential barrier of the QD trap becomes thinner and the electrons can tunnel, cf. 6.9. So the cycle can also be closed even at temperatures about 10 K, cf. [267]. The equations of Rack's model [209] are

$$\begin{aligned}
0 &= e \partial_t n(z) = & \partial_z j_n(z) - e R_n(z) \\
0 &= -e \partial_t p(z) = & \partial_z j_p(z) + e R_p(z) \\
\rho_i(z) &= e \cdot [p - n + N_D^+ - N_A^- + p_{QD} - n_{QD}] \\
-\rho_i(z) &= \epsilon_0 \partial_z [\epsilon_z(z) \cdot \partial_z \phi_i(z)]
\end{aligned} \tag{6.8}$$

The first two equations are the generation law for electrons valid at every point in the semiconductor, it assumes that no charging takes place at the quantum dots, i.e. $\partial n / \partial t = \partial p / \partial t = 0$. The third equation is the total charge density composed by the different components like intrinsic charges p and n , the QD-charges p_{QD} and n_{QD} ,

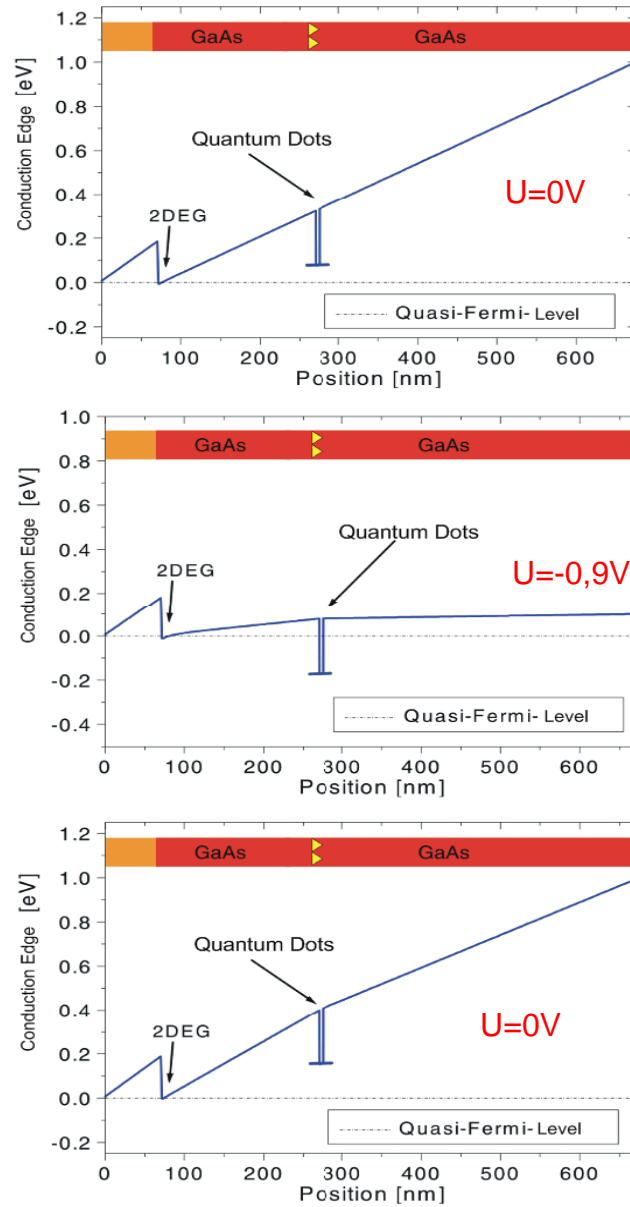


Figure 6.9: the conduction edge in the Yusa-Sakaki FET calculated; from [209]

and the acceptors N_A and donators N_D . The fourth equation of 6.8 is the Poisson equation of the semiconductor element. The solutions are shown in Fig. 6.9.

I differ slightly from Rack's interpretation of source term of the continuity equation: From his own simulation it is obvious that the charge density is built up at the quantum dot, i.e. $\partial n / \partial t \neq 0$. This is proven by the kink of the quasi-Fermi potential located at the quantum dots. There $\sigma = D_2 - D_1 \neq 0$ holds. I think that Rack's source term is identical with his selfcharging term. The source terms, however, are generally zero at the quantum dot for energetic reasons, otherwise we would have electron-hole pair generation similarly like in a photo cell. In Fig. 6.9 the slope of the conduction edge shows that the electrons of the QD's can flow in from the gate electrode where the sources of the electrons are located. If the gate electrode are loaded positive enough and if the QD's are below the Fermi potential, then the chemical potential of the QD helps the voltage source from outside to pull off electrons from the boundary at the Schottky contact. This can be interpreted as if inside the FET an internal voltage source is acting which is driven by the chemical potential of the traps. This charge separation is represented by Rack's source terms.

Note that this modified interpretation does not change Rack's numerical results.

So the processes in the Yusa-Sakaki FET can be explained at least formally by the following capacitive electric replacement circuit element in fig. 6.10.

The FET is modeled by a capacitance consisting of three electrodes which are located

- 1) at the boundary of the gate electrode
- 2) at the boundary of the 2DEG and
- 3) at the internal layer of the quantum dots.

The outer electrodes are at the system border. There, the system is experimentally accessible for measurements of voltage and current. The third inner electrode is electrically charged internally. Here the charging process may not be observable directly. It can be concluded indirectly by the non zero charge area of the hysteresis curve.

So the whole cyclic process is described a priori by an inconsistent mathematical mixture of the classical potential formalism with an Fowler or a (often thermally assisted) quantum mechanical tunnel emission process closing the cycle.

This inconsistency is the cause of the apparent non-conservative energy balance.

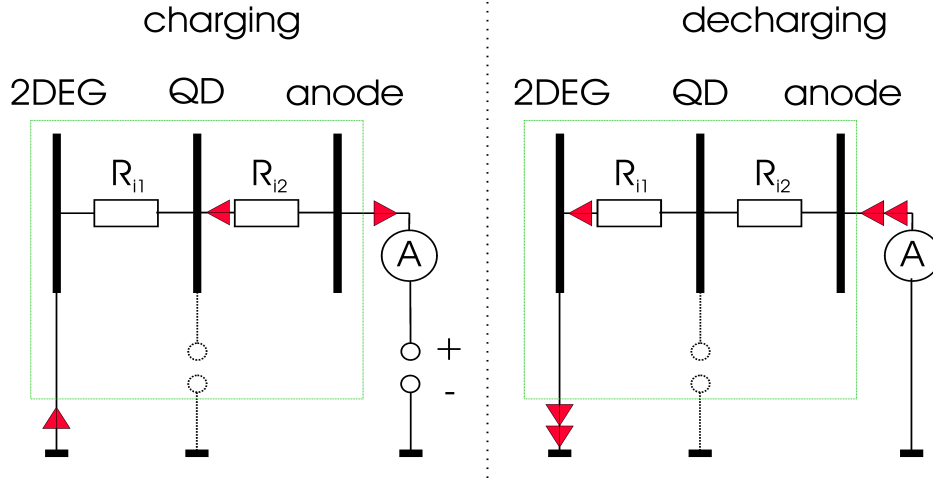


Figure 6.10: the electric circuits in the Yusa-Sakaki FET:(red arrows = electron fluxes)

Results - Parametric Oscillations with an Inverted Capacitance

The author here published under pseudonym in 2007 a simulation illustrating the idea that an electronic element with an inverted hysteresis may be applied for a self excited parametric oscillator [283] [284]. At this time not enough data were present to be able to judge the relevance of this speculation. In the meantime the data situation is better. Marent et al. [267] investigated an p-type quantum dot hole storage element which can be regarded roughly as a p-type analog to the Yusa-Sakaki storage n-FET setup. Its geometry is shown in fig. 6.11. Problems with the dynamics of the capacitance are avoided by the fast p-n junction. The quantum dots are embedded here in a diode, the dots itself are protected by a layer of pure GaAs on both sides, probably in order to reduce the Coulomb shielding at the quantum hole dots.

A typical (calculated) field situation is shown also in fig. 6.11. If the AC-capacitance is measured the setup shows an inverted hysteresis in the C-V-diagram, cf. fig. 6.12 . The cycle area $\Delta Q = \oint dQ/dU dU \neq 0$ indicates that there exists an influx of charge which suggests also an influx of energy. The so far missing integration constant of the corresponding $\mathbf{P}-\mathbf{E}$ diagram can be reconstructed from Marent's other measurements. The loss current of the storage diode is estimated to be few nA. The loading and erasing time of the storage element are less than 0.1 microseconds,

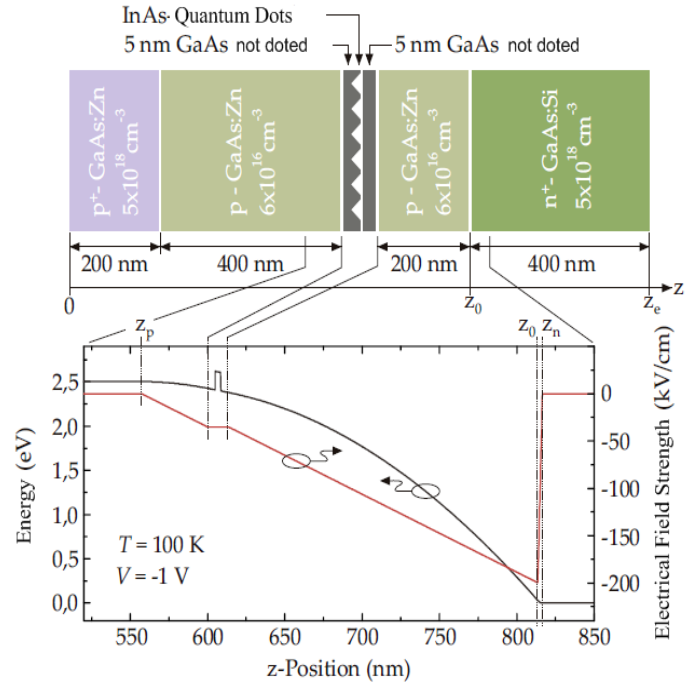


Figure 6.11: Structure of the capacitance TU5822; (from Marent [267])

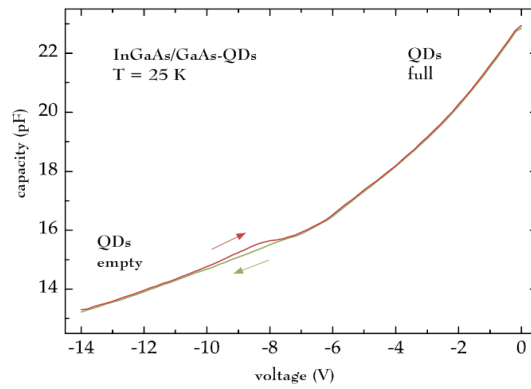


Figure 6.12: Capacitance vs. voltage of TU5822 (from Marent [267])

see [267]. The holes are loaded at voltages of typically $-1V$. They have to be erased at voltages lower than $-14V$.

The inverted hysteresis is similar in some respect to an illuminated photocell. However, it is not clear so far how the energy influx enters the system. Therefore, in order to clarify the relevance of the influx the following questions have to be answered:

- 1) Is the inverted capacitance energy area large enough in order to overcome the internal loss current in the diode in the time during the cycle ?
- 2) Are the charge and discharge processes fast enough in order to produce enough energy in the time of a cyclic process in order to maintain a selfexcited parametric gain oscillation driven by the inverted hysteresis as suggested in ref. [284].

Therefore I simulated the following circuit shown in fig. 6.13 . The circuit contains the diode capacitance TU5822 modeled by splines. The element is regarded as the combination of a current source plus a non-linear hysteretic capacitance as measured in the C-V - diagram. If the oscillation amplitude goes from $\approx 0V$ to negative voltages ($< -14V$) the green branch of the hysteresis has to be used, cf. fig. 6.12. If the negative peak (i.e. $< -14V$) is reached the erasing charge (i.e. the hysteresis area in fig.6.12) is "injected numerically" in our circuit model and the transition from the green to the red branch is done in the simulation. The advantage of this method is that we avoid a complicated solution of the Poisson PDE at every point, the disadvantage is that the solutions of model can be regarded to be valid only if the electric voltage oscillations at the capacitance TU5822 have a negative peak amplitude of U_c of $-16V < U_c < -20V$. Applying the definitions from fig. 6.13 a loop analysis[285] of this circuit yields the ODE system

$$\begin{aligned}\dot{Q} &= -((R_{cable} + R)Q + Q_z)/L \\ \dot{Q}_z &= Q/C + U_{QD} \\ \dot{Q} &= (U_{QD} + R\dot{Q}_{QD})/R\end{aligned}\tag{6.9}$$

The equations are derived in detail in appendix 6.4.3.

The initial conditions are $dQ_{QD}/dt(0) = 0$, $Q(0) = 8,4998 \cdot 10^{-6}$, $U_{QD}(0) = U_0$, $Q_{QD}(0) = -2,6238 \cdot 10^{-10}$, and $Q_z(0) = -(R_{cable} + R) * Q(0)$.

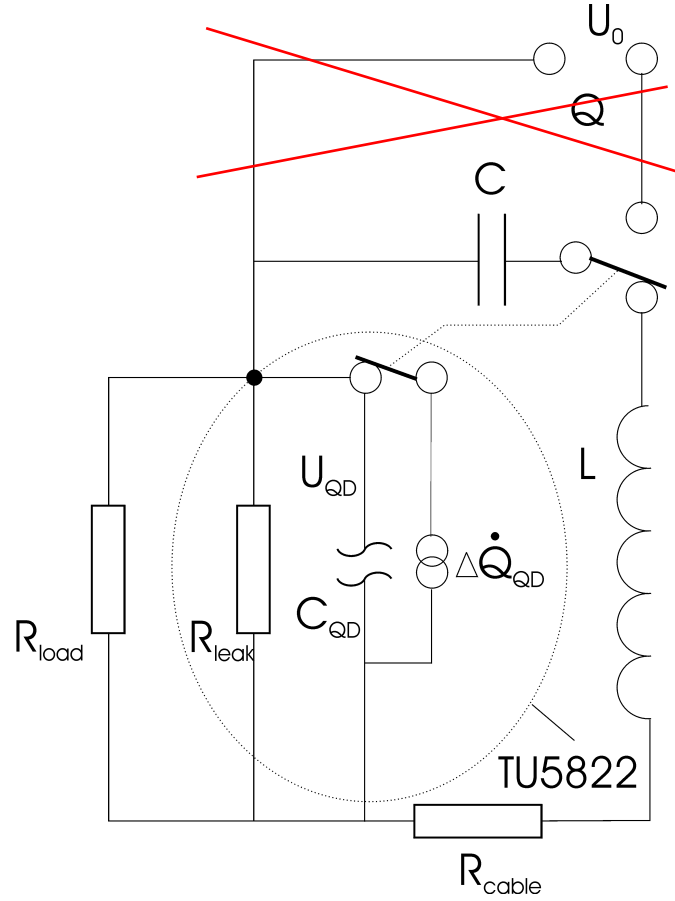


Figure 6.13: the capacitance TU5822 as replacement circuit in the oscillator circuit
 electrical data: $C = 10^{-6}$ F, $L = 0.235$ H, $R_{cable} = 2\Omega$, $R_{leak} = 5 \cdot 10^9\Omega$, $R_{load} = 10^7 \rightarrow 5 \cdot 10^8\Omega$, $R \equiv 1/(1/R_{load} + 1/R_{leak})$

The results of the simulation show that - under the present conditions - oscillations may selfexcite near to the limiting breakdown voltage specification ($= -20V$) of the element at typically $\leq -16V$ with a frequency of about 125 kHz.

The gained power per cycle is a little bit higher than about ten times the internal losses, cf. fig. 6.14.

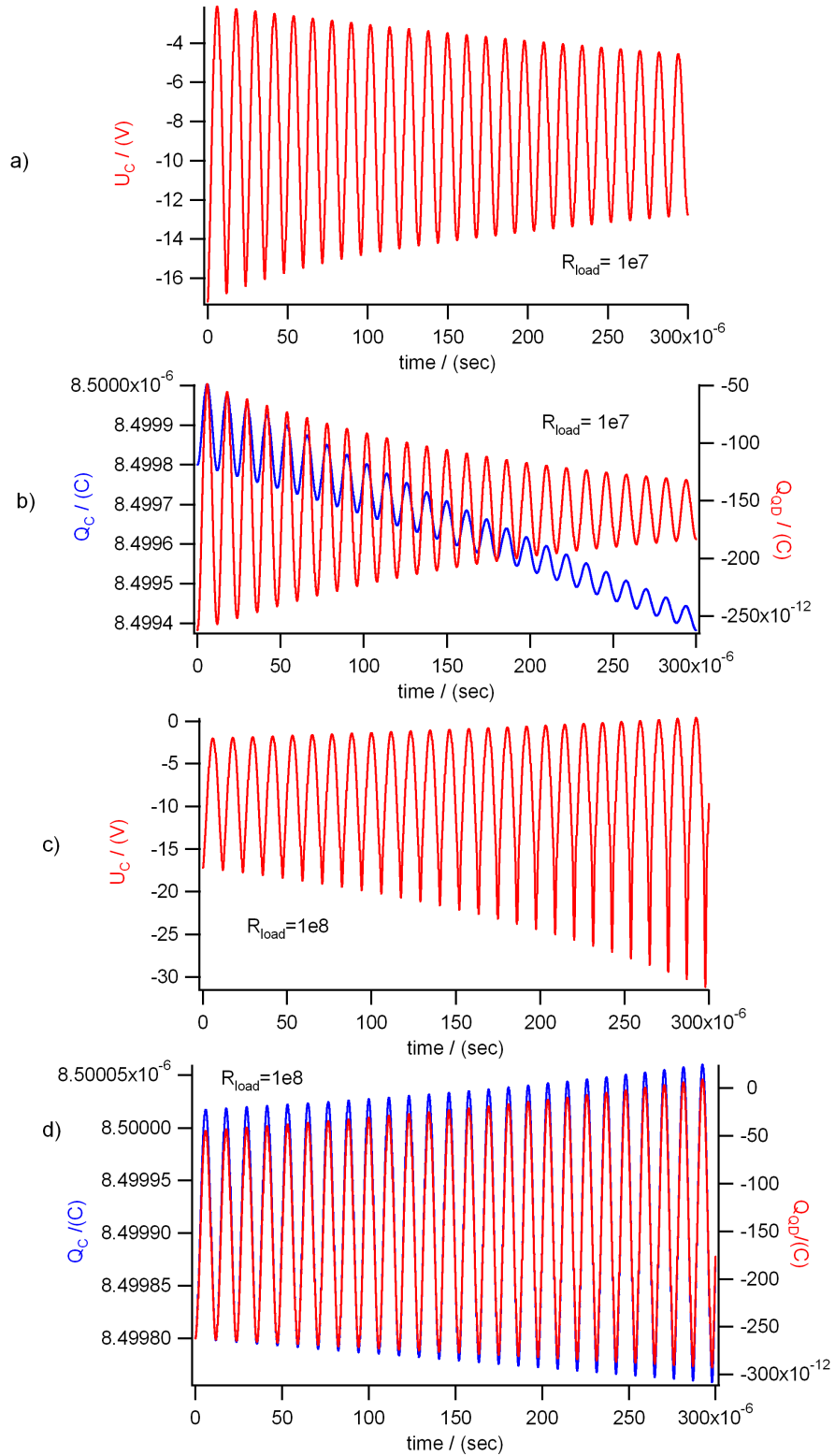


Figure 6.14: the oscillation signals of the above test circuit dependent from the load
a) + b) Relaxation: $R_{load} = 10M\Omega$; c) + d) Selfexcitation: $R_{load} = 100M\Omega$

Conclusions - Relevance and Outlook

Applying a recently published inverted capacitance FET model with available data I tested the energy balance. I showed that the consequent application of the model predicts that the energy from the inverted capacitance of the FET TU5822 can overcome the internal dissipation of the leakage current during an electric cycle. This can generate a parametric selfexcited oscillation on an offset DC-current, cf.[154]

The describing model itself is patched together by elements from different physical theories, i.e. quantum theory and electrodynamics. It would be very astonishing if one obtains a conventional consistent result in terms of energy under these conditions. An experimental test at the present stage I regard to be difficult but possible if the following list of engineering problems can be solved:

The load resistor of the circuit has a high impedance. The daily hum in the environment may be more intense than the signal which can be expected. Some hope may be future systems with higher capacitances and fast charging and erasing times. The conventional aims in the developments of new storage elements, (i.e. improvement of memory window and fast write and erasure times) are identical with a research for energy efficient capacitances. Therefore an additional energy measurement of these components should be a only a small investment at low risk.

Another perspective of research may be the analogous transfer of these new ideas here into electrochemistry, i.e. either to electrochemical systems or electrolytic capacitances. Only if an higher output can be achieved with any of these strategies it makes sense to couple out the gain by switched transformers (instead of the resistive load) in order to adapt to consumer loads.

It is still open whether the existence of the selfexcitation can be proved also for silicon technology. The lifetime under the oscillatory stress of these electronic elements is also a further critical question which can not be answered here finally. May be that the selfexcited high voltage peaks are responsible for the breakdown of the electronic elements. This could be avoided if electronic switching elements discharge the DC-energy in the circuit to a load before the breakdown voltage is reached.

6.3 Permanent Magnet Motors

6.3.1 Historical Permanent Magnet Motors

The oldest claim of a perpetual running permanent magnetic motor is by Peter Peregrinus from 1296 [286]. In the 19th century the Gary motor was patented [287, 288]. Other claims are from Minato [289–291], Johnson [292–295], Searl [296–299], which is partially confirmed by Godin and Roschin [300]. Today many claims can be found in the internet. Seldomly it is convincing that the machine cycle is closed with gain.

The actually most serious claim seems to be the Yildiz permanent magnet motor, [301, 302] which was shown at the university of Delft. In a Youtube video, selfacceleration can be observed. However, the principle of its working remained unrevealed.

This problem exists generally: even if any motor really seems to work - but if no (relatively simple) explanation and no engineering method exist - the development and fabrication of motors is impossible because the knowledge cannot be transferred.

So I will present here a simple analysis of permanent magnet motor principles suited for engineering applications. It is inspired by [303].

It is based on the magnetic analogy with the windwheel shown in section 2.2.2.

6.3.2 a Basic Mechanism of a Permanent Magnet Motor

Permanent running rotating motors are possible if the force or torque on the moving rotor cannot be derived from a conservative potential. So we need driving non-conservative force fields which are beyond the standard classical mechanics cf.[17] . They can be described neither by potentials ~~neither~~^{nor} by Lagrange or Hamiltonian energies. So one has to enlarge the ansatz or go back to the application of more general methods of mechanics i.e. either action-reactio or the principle of virtual work.

I suggested already in 1998 [304] that a ratchet potential coupled to a non-linear material property also makes non-conservative permanent motion possible. This idea is illustrated here by a simple mathematical model to be transferred to magnetic systems.

1.) I choose a coupling "charge" q dependent from $E(x)$ obeying the proportionality

$$q(E(x)) \propto \sqrt[2]{|E(x)|}$$

2) I move the "charge" in an asymmetric shaped periodic ratchet potential field $V(x)$. The generating field is then $E(x) = -\partial V/\partial x$. The periodic ratchet potential $V(x)$ may be modeled here by (with the cycle number ($n = 1, 2, 3..$) cf. fig. 6.15

$$V(x) = \begin{cases} \frac{1}{2}(x - 3n) & \text{for } 3n \leq x < 3n + 2 \\ 3 - (x - 3n) & \text{for } 3n + 2 \leq x < 3(n + 1) \end{cases}$$

Then the field $E(x)$ derived therefrom is

$$E(x) = \begin{cases} -\frac{1}{2} & \text{for } 3n \leq x < 3n + 2 \\ +1 & \text{for } 3n + 2 \leq x < 3(n + 1) \end{cases}$$

3) The force $F(x)$ of the field $E(x)$ on the charge $q(E)$ is $F(x) = q(E) \cdot E(x)$. (I set the proportional constant of $q(E(x)) \propto \sqrt[2]{|E(x)|}$ to be 1.)

In our numeric example the work $W(x)$ after one cycle is calculated to

$$W = \int_0^3 q(x)E(x)dx = \int_0^2 -\sqrt{|-1/2|}\frac{1}{2}dx + \int_2^3 \sqrt{|1|}(1)dx = -(\sqrt{1/2} - 1)$$

We see that W is non-zero indicating a periodic energy gain after the cycle if we choose a loss-free ~~magnet~~ ^{charged object} moving in the correct direction, cf. fig. 6.15

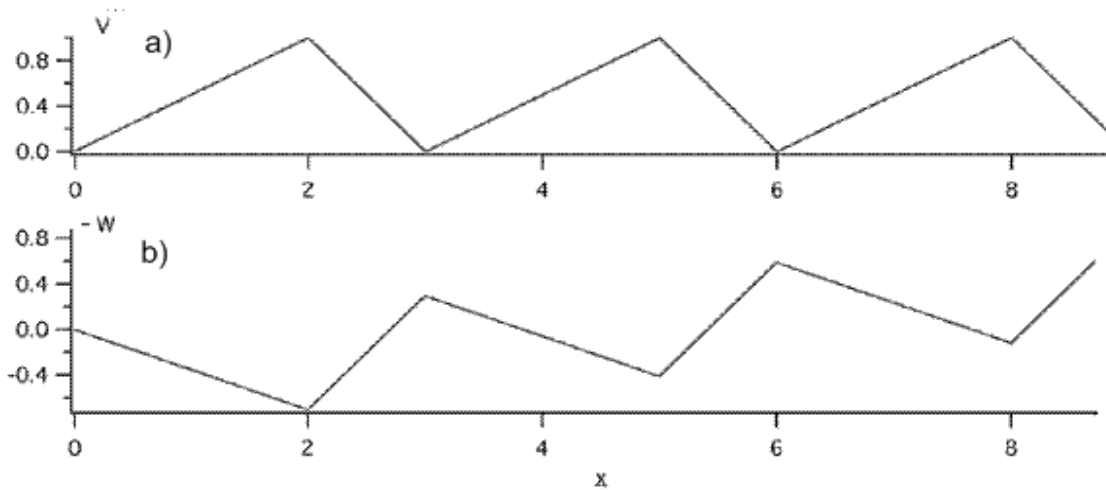


Figure 6.15: diagram a): generating potential $V(x)$ with periodic boundary condition
 diagram b): resulting work function $W(x)$ with no periodic boundary condition

6.3.3 the Simulation of a Permanent Magnet Motor

I transfer now the theoretical model mechanism from sec. 6.3.2 into a more real simulation near to a engineering situation. I take

1) a nonlinear magnetic material (i.e. a piece of Nickel(10mm \times 10mm \times height))
 2) an asymmetric magnetic field (by two Neodym magnets (50mm \times 8mm \times height)).
 The "charges" are the induced magnetic "North or South poles" at the moving Nickel piece (saturation 0,5 T). The generating field is the H -field between the Neodymium permanent magnets (saturation 1,2 T) The force at each position of the piece of Nickel is calculated at each step(step width 2.5 mm) by the Maxwell stress tensor. The simulated situation is illustrated in fig. 6.16. We have a Nickel metal pulled by an asymmetric magnetic field generated by two slightly tilted opposite strong planar Neodymium magnets. In order to enhance the asymmetry of the setup two Permalloy metal pieces (saturation 1,2 T) take off the magnetic field at one side of each magnet. The results are calculated with an open source 2D-simulation program FEMM 4.2 . They are shown in fig. 6.17 . We see that the gained work of the piece of Nickel is non-negative after passing the channel between the two Neodymium magnets horizontally. This means that this setup generates energy if the correct direction is chosen. From fig. 6.17 we read off an gain efficiency factor $\eta \equiv \text{gain}/\text{investment} \approx 0.7$ per cycle.

These results should be transfered to rotary systems.

According to the basics of mechanical engineering two conditions are necessary for mechanical stability of a rigid body: a balance of forces F_i and torques T_i [305]

$$\sum_i F_i = 0 \quad \sum_i T_i = 0 \quad (6.10)$$

If any permanent magnet motor rotation runs it is driven by non-compensated magnetic torques. The driving torque is generated by the stator field \mathbf{B} interacting with the magnetic moments \mathbf{m}_i of the rotor magnets.

$$\sum_i T_i = \sum_i \mathbf{m}_i \times \mathbf{B} \neq 0. \quad (6.11)$$

So the sum of all rotor torques acts on the rotor axis because any force couple (representing a torque) can be shifted parallel in a rigid body [305, 306].

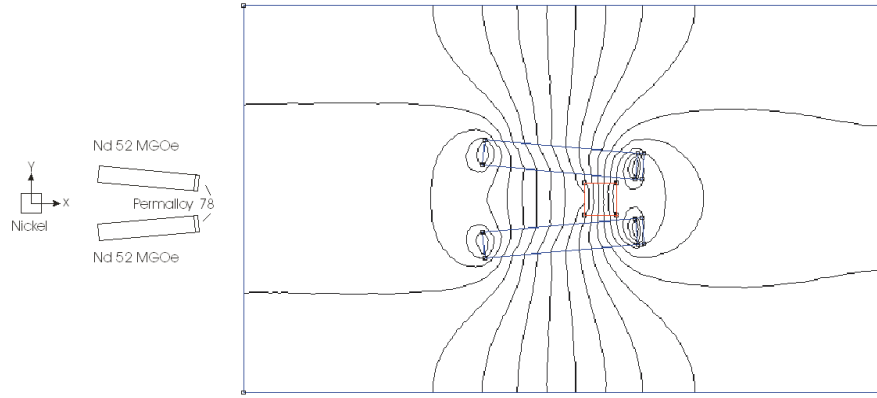
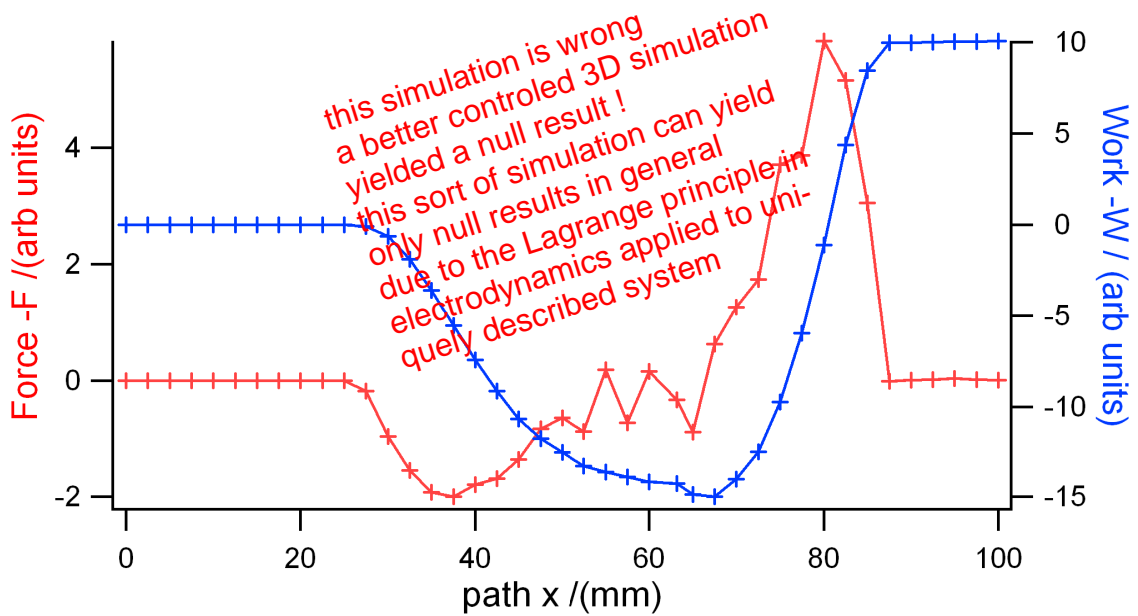


Figure 6.16: the experimental setup and field of the test system

left insert: the experimental setup

right insert: the calculated fields at a moment of the movement from left to right

Figure 6.17: force F and work W vs. path x of the Nickel piece in the setup of fig.6.17red line: force F vs. path x ; blue line: work $W(x) = \int_0^x F(x')dx'$ vs. path x

To obtain motor rotation seems to be difficult experimentally:

Oftenly magnetic forces and losses block the rotation. Furthermore any arising central forces are without effect because they do not contribute to a central torque [17].

So a systematic pre-simulation of the setup suggest a way to avoid these problems .

6.3.4 Discussion and Outlook

1) Conservative fields $F(x)$ are characterized by the condition $\nabla \times F = 0$ normally. A better alternative may be the integral version $W(\Delta x) = \int_0^{\Delta x} F(x') dx' = 0$. This means that $W(x) = \int_0^x F(x') dx'$ has a periodic boundary condition for the conservative systems moving along the cyclic path length Δx .

Note that the integral version holds also for one-dimensional systems, cf. fig. 6.15.

2) Note that the Nickel piece moves in a ~~labile equilibrium~~ with respect to the y-coordinate. The system is stabilized here by the realized constraint $y = \text{constant}$.

3) Note that the Poynting relation is without relevance here because it describes the work of the current. The Maxwell stress tensor determines here the mechanical forces and the mechanical work. This term is analogous to a pressure tensor.

4) If thermal effects are included the mechanical energy of these systems can be discussed only by non-equilibrium thermodynamics with non-conservative force fields. This approach is non-standard. The known thermodynamic approach applies only potential energies and describes the more simple situations.

~~5) Our results may be enhanced if we exchange~~

~~a) the Neodymium magnet by an electromagnet with iron cobalt core driven into saturation ($\approx 2T$) b) if we replace the Nickel by a iron saturation at $\approx 1,5T$~~

6) If the Nickel is exchanged by a permanent magnets as rotor magnets (instead of the passive Nickel piece) the non-linear part of the demagnetisation characteristics [307] determines the success. Note that long ago Searl applied special magnets with a nonlinear magnetic demagnetization similar to Alnico [296] .

~~7) All simulations still have to be controlled by high resolving professional programs.~~

~~8) It is clear that the simulation programs can be used for the optimization of design.~~

~~9) Our considerations might be transfered to ferroelectric materials in electric fields.~~

done

6.4 Appendix

6.4.1 the Derivative of the Electromagnetic Flux

In this section a mathematical vector relation is derived which helps to obtain Faraday's law and Ampere's law, cf. the equations 6.3 and 6.4.

I cite from the lecture script of H. Risken [207] , see also [172, 308].

The derivation starts in defining the space-time dependent vector field $\Gamma(x, t)$.

" A point $x(t)$ of the curve $C(t)$ moves to the point $x + v * \Delta t$ on $C(t + \Delta t)$. The velocity can vary." The flux of the vector field $\Gamma(x, t)$ through the area $F(t)$ at the time t is, cf. fig. 6.18

$$\Xi(t) = \int_{F(t)} \Gamma(x, t) df \quad (6.12)$$

The flux of $\Gamma(x, t + \Delta t)$ through the area $F(t + \Delta t)$ at the time $t + \Delta t$ is

$$\Xi(t + \Delta t) = \int_{F(t + \Delta t)} \Gamma(x, t + \Delta t) df \approx \int_{F(t + \Delta t)} \Gamma(x, t) df + \int_{F(t + \Delta t)} \frac{\partial \Gamma(x, t)}{\partial t} df \Delta t \quad (6.13)$$

From the last two equations follows

$$\Xi(t + \Delta t) - \Xi(t) \approx \int_{F(t + \Delta t)} \Gamma(x, t) df - \int_{F(t)} \Gamma(x, t) df + \int_{F(t + \Delta t)} \frac{\partial \Gamma(x, t)}{\partial t} df \Delta t \quad (6.14)$$

If the Gauss's integral theorem is applied to volume restricted by $F(t)$, $F(t + \Delta t)$ and the connecting hull surface between $C(t)$ and $C(t + \Delta t)$, cf. fig. 6.18 one obtains

$$\int_V \nabla \Gamma(x, t) dV = \int_{F(t + \Delta t)} \Gamma(x, t) df - \int_{F(t)} \Gamma(x, t) df + \int_{hull} \Gamma(x, t) df \quad (6.15)$$

If we insert eq. 6.15 in eq. 6.14 we obtain

$$\Delta \Xi \equiv \Xi(t) - \Xi(t + \Delta t) = \int_V \nabla \Gamma(x, t) dV - \int_{hull} \Gamma(x, t) df + \int_{F(t + \Delta t)} \frac{\partial \Gamma(x, t)}{\partial t} df \Delta t \quad (6.16)$$

On the hull surface holds, cf. fig. 6.19 left drawing

$$df = ds \times v \Delta t \quad (6.17)$$

For a volume element holds, cf. fig. 6.19 right drawing

$$dV = df * v \Delta t \quad (6.18)$$

Therefrom one reformulates the surface integral

$$\int_{hull} \Gamma(x, t) df = \oint_C \Gamma(x, t) (ds \times v) * \Delta t = \oint_C (v \times \Gamma(x, t)) ds * \Delta t \quad (6.19)$$

and the volume integral

$$\int_V \nabla \Gamma(x, t) dV = \int_S \Gamma(x, t) (v * df) \Delta t \quad (6.20)$$

In sum one obtains

$$\frac{d\Xi}{dt} = \lim_{\Delta t \rightarrow 0} \frac{\Delta \Xi}{\Delta t} = \int_{F(t)} \left(\frac{\partial \Gamma}{\partial t} + (\nabla * \Gamma) v \right) df - \oint_{C(t)} (v \times \Gamma) ds \quad (6.21)$$

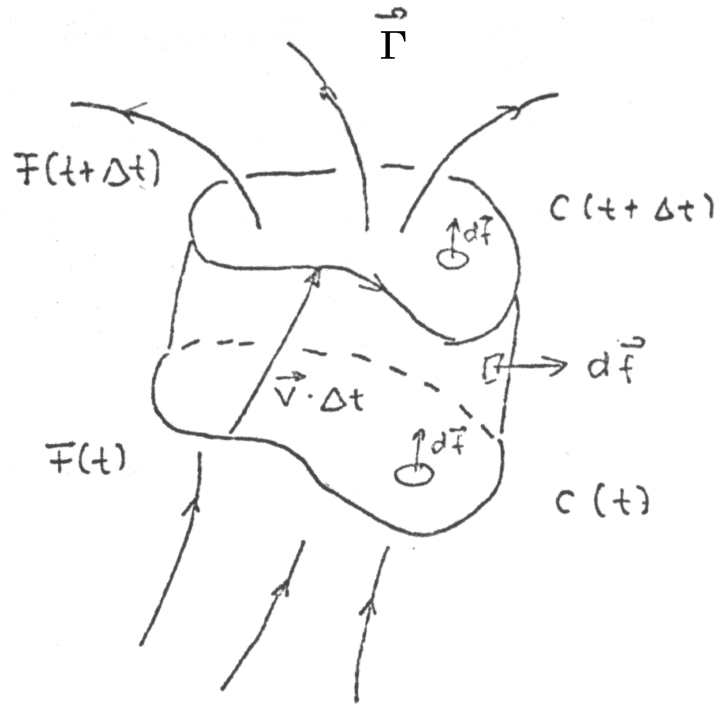


Figure 6.18: the geometry of the problem (from script[207] of H. Risken), cf. text

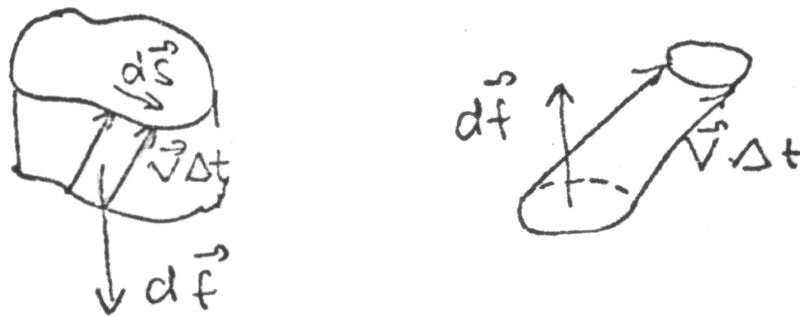


Figure 6.19: the coordinate transformations of the differentials (from [207]), cf. text

6.4.2 Moment and Energy Conservation of Charges

the Poynting relation

I start to write down the equations of the force F on a electric and a magnetic charge

$$\begin{aligned}\mathbf{F}_E &= q_E(\mathbf{E} + \frac{\mathbf{v}}{c} \times \mathbf{B}) \\ \mathbf{F}_H &= q_H(\mathbf{H} - \frac{\mathbf{v}}{c} \times \mathbf{D})\end{aligned}\quad (6.22)$$

In the popular derivation the mechanical work W on the charges each are written (the second terms of eq.6.22 are assumed to be perpendicular and are neglected)

$$\begin{aligned}W_E &= \int \mathbf{F}_E d\mathbf{s} = \int \mathbf{F}_E \cdot \mathbf{v} dt \\ W_H &= \int \mathbf{F}_H d\mathbf{s} = \int \mathbf{F}_H \cdot \mathbf{v} dt\end{aligned}\quad (6.23)$$

Now, I add both contributions and write down the total power involved P in field terminology

$$P \equiv \frac{\partial W}{\partial t} = \int (\rho_E \mathbf{v} \cdot \mathbf{E} + \rho_H \mathbf{v} \cdot \mathbf{H}) d^3\mathbf{x} \quad (6.24)$$

I write down the power density p of the electric and magnetic current

$$\begin{aligned}p_E &\equiv \mathbf{j}_E \cdot \mathbf{E} \equiv \rho_E \mathbf{v} \cdot \mathbf{E} = \frac{c}{4\pi} (+(\nabla \times \mathbf{H}) - \frac{1}{c} \frac{\partial \mathbf{D}}{\partial t}) \cdot \mathbf{E} \\ p_H &\equiv \mathbf{j}_H \cdot \mathbf{H} \equiv \rho_H \mathbf{v} \cdot \mathbf{H} = \frac{c}{4\pi} (-(\nabla \times \mathbf{E}) - \frac{1}{c} \frac{\partial \mathbf{B}}{\partial t}) \cdot \mathbf{H}\end{aligned}\quad (6.25)$$

Inserting eq.6.25 in eq.6.24 and applying the mathematical vector relation $\nabla \cdot (\mathbf{a} \times \mathbf{b}) = \mathbf{b} \cdot (\nabla \times \mathbf{a}) - \mathbf{a} \cdot (\nabla \times \mathbf{b})$ I obtain finally

$$\frac{\partial W}{\partial t} = \int (\rho_E \mathbf{v} \cdot \mathbf{E} + \rho_H \mathbf{v} \cdot \mathbf{H}) d^3\mathbf{x} = - \int \left[\frac{c}{4\pi} \nabla \cdot (\mathbf{E} \times \mathbf{H}) + \frac{1}{4\pi} (\mathbf{H} \frac{\partial \mathbf{B}}{\partial t} + \mathbf{E} \frac{\partial \mathbf{D}}{\partial t}) \right] d^3\mathbf{x} \quad (6.26)$$

Note that this extended Poynting energy conservation relation can describe also the energy exchange of permanent magnet currents (modeled by moving magnetic charge dipoles) in the field. This is not included in the conventional theory which describes the energy exchange exclusively with electric currents.

It must be mentioned that the Poynting energy conservation is incomplete and does not take into account for all possible energetic balance situations. Regarding

$$P \equiv \frac{\partial W}{\partial t} = \frac{\partial}{\partial t} \int \mathbf{F} d\mathbf{s} = \int \frac{\partial \mathbf{F}}{\partial t} d\mathbf{s} + \int \mathbf{F} d\mathbf{v} \quad (6.27)$$

the first term is not included in the historical derivation of the Poynting energy conservation, but it is relevant for the calculation of the betatron or of Nikulov's systems discussed in section 4.5.3. Other approaches are discussed in sec. 6.3.4.

the Maxwell stress tensor

I start writing down the total force \mathbf{F} of one species of electric and magnetic volume charge under the same quasi-stationary conditions as discussed at the end of sec. 6.26

$$\mathbf{F} = \mathbf{F}_{\mathbf{E}} + \mathbf{F}_{\mathbf{H}} = q_E(\mathbf{E} + \frac{\mathbf{v}}{c} \times \mathbf{B}) + q_H(\mathbf{H} - \frac{\mathbf{v}}{c} \times \mathbf{D}) \quad (6.28)$$

The charges $q = \rho \, d^3x$ and the currents j (consisting of $j = \rho \cdot v$) are eliminated by inserting the Maxwell equations 6.4 in 6.28. Integrating the object volume I obtain

$$\begin{aligned} \mathbf{F} = & \frac{1}{4\pi} \int (\nabla \mathbf{D} \cdot \mathbf{E} + \nabla \mathbf{B} \cdot \mathbf{H}) \, d^3\mathbf{x} \\ & + \frac{1}{4\pi} \int [(\nabla \times \mathbf{H}) \times \mathbf{B} + (\nabla \times \mathbf{E}) \times \mathbf{D}] \, d^3\mathbf{x} \\ & + \frac{1}{4\pi} \int (-\frac{1}{c} \partial \mathbf{D} / \partial t \times \mathbf{B} + \frac{1}{c} \partial \mathbf{B} / \partial t \times \mathbf{D}) \, d^3\mathbf{x} \end{aligned} \quad (6.29)$$

After applying the mathematical vector relation $\mathbf{a} \times \mathbf{b} = -(\mathbf{b} \times \mathbf{a})$ to the last term in last integral of eq. 6.29 the derivation can be completed by copying from standard textbooks. In tensor terminology the end result is (cf. [308] [207])

$$\begin{aligned} F_i = & + \frac{1}{4\pi} \int (E_i \cdot \partial D_j / \partial x_j + H_i \cdot \partial B_j / \partial x_j) \, d^3\mathbf{x} \\ & + \frac{1}{4\pi} \int \frac{\partial}{\partial x_j} (E_i D_j) - \frac{\partial E_k}{\partial x_i} D_k \\ & + \frac{1}{4\pi} \int \frac{\partial}{\partial x_j} (H_i B_j) - \frac{\partial H_k}{\partial x_i} B_k \, d^3\mathbf{x} \\ & - \frac{1}{4\pi c} \int \frac{\partial}{\partial t} \epsilon_{ijk} (D_k \cdot B_j) \, d^3\mathbf{x} \end{aligned} \quad (6.30)$$

(The Einstein convention and no simplification to linear materials are applied).

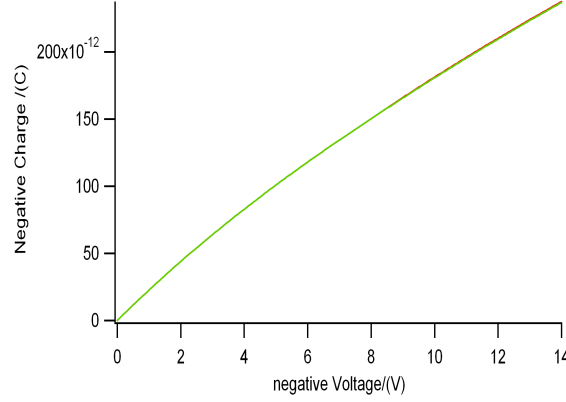


Figure 6.20: The Q-V diagram of the capacitance TU5822 integrated

6.4.3 the Derivation of the ODE of the Parametric Oscillation

The circuit to be calculated is motivated in section 6.2.4 and is shown in fig. 6.13 . First we explain the choice of the values of the electronic components. This allows us to estimate the behavior of the circuit. Then we derive the differential equation system describing more exactly the behaviour of the circuit.

We know that the capacitance TU5822 has a maximal erasing time of $0.1 \mu\text{sec}$ at -14 V , the writing time is still shorter (typical 6nsec at 0.5 V) [267]. This means: if we want to build in an inverted capacitance into an oscillation circuit, the cycle time should to be larger because the charging and discharging of the QD's is proceeded only in the peaks of the oscillation . We take arbitrarily a factor of $1/[(\text{oscillation frequency}) \times (\text{charging time})] \approx 100$ and choose $f=85 \text{ kHz}$ as working frequency. Because the mean capacity of the element is about 15 pF an inductance of 0.235 H follows from $f = 1/(2\pi\sqrt{L.C})$.

In order to estimate the offset current flowing out during one cycle we integrate numerically fig.6.12 by a tabel calculation program. If the up and the down curve of fig.6.12 are integrated we obtain fig. 6.20. From my numerical data of this diagram I read off a difference charge $\Delta Q = 5.55894 \times 10^{-13} \text{ C}$ per cycle between both curves at voltages $< -12 \text{ V}$ (hardly visible in fig. 6.20) This value represents the area between the up an down curve in fig. 6.12. This means: we expect a mean offset current

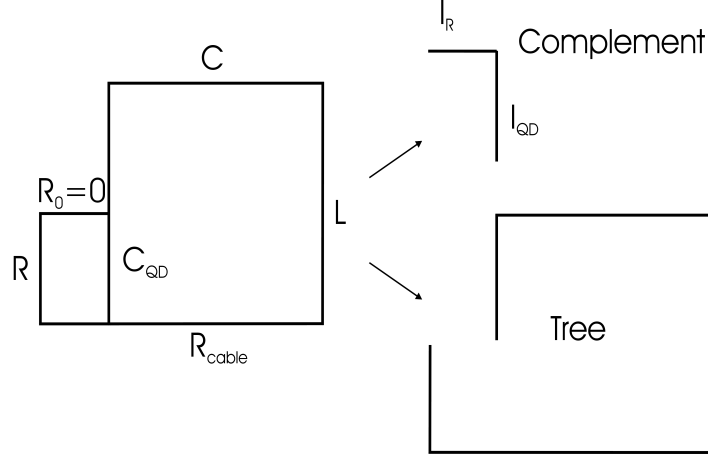


Figure 6.21: the decomposition of the network according to the loop analysis

$I \approx f \cdot \Delta Q$. This allows us to estimate a mean load resistance which is necessary in order to maintain the capacitance's mean voltage with the oscillation swinging around. If this load resistance is lower than the inner parasitic resistor of the capacitance itself, a selfexciting-oscillation should be possible. I estimate the bifurcating transition between selfexcitation and relaxation at an total inner resistance to be about $\approx 10 \text{ M}\Omega$.

In order to obtain the ODE system we use a loop analysis of the circuit [285] shown in fig. 6.13. For our calculation we decompose the network according to fig. 6.21. The complement leads us to select out the following independent mesh equations of the voltages of the two branches of the complement

$$\begin{aligned} L(\dot{I}_R + \dot{I}_{QD}) + (R_{cable} + R)(I_R + I_{QD}) + \frac{1}{C}(Q_R + Q_{QD}) + U_{QD} &= 0 \\ L(\dot{I}_R + \dot{I}_{QD}) + (R_{cable} + R)(I_R + I_{QD}) + \frac{1}{C}(Q_R + Q_{QD}) + RI_R &= 0 \end{aligned} \quad (6.31)$$

with $Q_R \equiv \int I_R dt$ and $Q_{QD} \equiv \int I_{QD} dt$.

$U_{QD}(Q_{QD})$ is numerically defined as the inverted function of $Q_{QD}(U_{QD})$, cf. fig.6.20 . It is integrated from the connecting splines of the pivot points obtained from fig.6.12 . In order to be able to compare with the experiment we introduce new variables and define $I \equiv I_R + I_{QD}$ and $Q \equiv Q_R + Q_{QD}$.

Applying this definition we rewrite eq. 6.31 in terms of I_{QD} and I or Q_{QD} and Q

$$\begin{aligned} L\dot{I} + (R_{cable} + R)I + Q/C + U_{QD} &= 0 \\ U_{QD} + RI_{QD} &= RI \end{aligned} \quad (6.32)$$

The next task is to make the equations handsome for programming.

Therefore we introduce the variable Q_z in order to decompose the first equation into two ODE's of first order this equation system. So we obtain

$$\begin{aligned} L\dot{Q} &= -(R_{cable} + R)Q - Q_z \\ \dot{Q}_z &= Q/C + U_{QD} \\ R\dot{Q} &= U_{QD} + R\dot{Q}_{QD} \end{aligned} \quad (6.33)$$

These equations are programmed. The initial conditions are

$Q(0) = 8.4998 \cdot 10^{-6}$, $dQ_{QD}/dt(0) = 0$, $U_{QD}(0) = U_0$, $Q_{QD}(0) = -2.6238 \cdot 10^{-10}$, and $Q_z(0) = -(R_{cable} + R) * Q(0)$.

6.4.4 List of Electromagnetic Symbols

bold symbols are vectors, normal symbols are normed scalars
 indices normally have the same meaning like symbols

name	symbol
area	\mathbf{A} or A
magnetic induction	\mathbf{B} or B
electric field	\mathbf{E} or E
electric displacement	\mathbf{D} or D
magnetic field	\mathbf{H} or H
current	I
current density	$\mathbf{j} \equiv \rho \mathbf{v}$ or j
hole density	p (in electrical context)
electron density	n
polarization	\mathbf{P} (in electrical context)
charge	Q
resistance	R
voltage	U
capacity	C
inductivity	L
path	\mathbf{s} or x
time	t
power	p (in mechanical context)
velocity	\mathbf{v} or v
volume	V or $d\mathbf{x}^3$
velocity of light	c
magnetic flux	ϕ
charge density	ρ
electric area charge	$\theta \equiv \oint \mathbf{D} d\mathbf{A}$

Chapter 7

Summary

If one thinks about what may be possible physically in the classical world two sorts of systems are offered by mathematics:

- 1) conservative ones to be found in mechanics and in thermodynamics obeying the classical laws of conservative energy conservation
- 2) non-conservative ones, which either depend from an additional parameter like time either are vortex systems distributed in space.

These systems are less popular in physics but they are more interesting for energy science because they are non-conservative with respect of energy. Under this aspect I discussed "overunity" systems in this book:

First I explained what energy conservation means regarded from the different common philosophic points of view. Then I referred to the classical second law violation claims of the isotherm stratification. I derived the (old) theory of this problems conventionally and completely by optimizing the internal energy of the thermodynamic system. I did not find "overunity" efficiencies contrary to some experimental second law violation claims discussed. Other systems which are outside of equilibrium thermodynamics are considered also in order to see the limits of standard thermodynamics. Temperature is proposed to be the fit parameter to any statistical distribution which can differ from the Gibbsian. This transcends the old empirical temperature concept.

I simulated also the historic Irinyi-Doczekal claim of a steam engine which applies a

water-benzene mixture as fluid. This system can be understood as a limit case of equilibrium thermodynamics. It has a high efficiency at low temperature but has no over-Carnot efficiency. I improved the labile continuum theory of spontaneous condensation applying an (ideal) mixture model in order to check the overunity claim by Doczekal. The theory does not need any extrapolation ansatzes because the set of non-linear equations is complete. The calculated results seem to be correct in the order of magnitude but they deviate strongly from the measurements of Doczekal. They give insight how thermostatics is embedded theoretically in non-equilibrium thermodynamics. The Second Law becomes obsolete with a non-equilibrium model because its purpose is taken over by the dynamics of the system.

Furthermore I sought for regimes "beyond" the Second Law. So I found as candidates for further investigation inverted hysteresis in magnet multilayer systems and in storage FETs. Following the measurements of the experimentalists I showed that the last systems can generate energy by cycling the inverted hysteresis. The energy gained of a discussed cycle is shown to be until 10 times the loss energy of the generating electronic part (a storage FET). These systems contain quantum mechanic elements in their cycle. This explains the inconsistency of the balance of energy.

Furthermore permanent magnet perpetuum mobiles are explained: they are shown to be analogous to wind wheels. They may be driven by a non conservative force field which is generated by a non-linear coupling of the rotor element to an asymmetric ratchet-like magnetic field, which even may be conservative. ~~Permanent running magnet motors are beyond equilibrium thermodynamics and beyond the Second Law. However, they are no contradiction to classical electrodynamics. First simulations indicate that they can be simulated by conventional standard finite element programs.~~

Bibliography

- [1] D. Meadows et al., *The Limits of Growth*.
University of Virginia: Universe Book, 1974.
- [2] H. Gruhl, *Ein Planet wird geplündert: die Schreckensbilanz unserer Politik*.
Frankfurt/M.: S.Fischer, 1975.
- [3] A. Ord-Hume, *Perpetual Motion - The history of an obsession*.
London: Allen & Unwin, 1977.
- [4] H. Dircks, *Perpetuum Mobile*, vol. 1. London: E.&F. Spon, 1861.
- [5] H. Dircks, *Perpetuum Mobile*, vol. 2. London: E.&F. Spon, 1870.
- [6] J. Collins, *Perpetual Motion: An Ancient Mystery Solved*.
Leamington Spa: Permo Publications, 1993.
- [7] H. Helmholtz, “Über Wirbelbewegungen,”
in *Ostwalds Klassiker der exakten Wissenschaften Nachdruck Vol.1,79,80*,
Frankfurt: Harri Deutsch Verlag, 1858, 2013.
- [8] I. Bronstein and K. Semendjajew, *Taschenbuch der Mathematik*.
Thun: Harri Deutsch, 20 ed., 1983.
- [9] F. Wiepütz, “Actual candidates for Second Law violations,”
NET-Journal, vol. 11, no. 1, pp. 18–21, 2006.
- [10] P. Haenggi, F. Marchesoni, and F. Nori, “Brownian motors,”
Ann. Phys., vol. 14, p. 51, 2005.

- [11] D. Cole and H. Puthoff, “Extracting energy and heat from the vacuum,” *Phys. Rev. E*, vol. 48, p. 1562, 1993.
- [12] W. Lucha and F. Schöberl, *Gruppentheorie*. Mannheim, Leipzig, Zürich: B.I. Wissenschaftsverlag, 1993.
- [13] K. Huang, *Statistical Mechanics*. New York: Wiley, 1963.
- [14] R. Mayer, *Die organische Bewegung in ihrem Zusammenhange mit dem Stoffwechsel - Ein Beitrag zur Naturkunde*. Heilbronn: C. Drechsler’sche Buchhandlung, 1845.
- [15] R. Clausius, “Über verschiedene für die Anwendung bequeme Formen der Hauptgleichungen der mechanischen Wärmetheorie,” *Ann. Physik Leipz.*, vol. 5, no. 5, pp. 353 – 400, 1865.
- [16] J. W. Gibbs, “On the equilibrium of heterogeneous substances,” *Trans. Conn. Acad. Sci.*, vol. 3, pp. 108–248, 108–248, 1875 - 1878.
- [17] F. Kuypers, *Klassische Mechanik*. Weinheim: Wiley, 5 ed., 1997.
- [18] H. Helmholtz, “Über die Erhaltung der Kraft,” in *Ostwalds Klassiker der exakten Wissenschaften Nachdruck Vol.1,79,80*, Frankfurt: Harri Deutsch Verlag, 1847,2013.
- [19] H. Störig, *Kleine Weltgeschichte der Philosophie*. Stuttgart: Verlag W. Kohlhammer, 1999.
- [20] P. K. Anastosovski, T. E. Bearden, C. Ciubotariu, W. T. Coffey, L. B. Crowell, G. J. Evans, M. W. Evans, R. Flower, S. Jeffer, A. Labounsky, B. Lehnert, M. Meszaros, P. R. Molnar, J. P. Vigier, and S. Roy, “Classical electrodynamics without the Lorenz condition: Extracting energy from the vacuum,” *Physica scripta*, vol. 61, pp. 532–535, 2000.
- [21] G. W. Bruhn, “No energy to be extracted from the vacuum,” *Phys. Scr.*, vol. 74, p. 535, 2006.

- [22] B. Baranowski,
Nichtgleichgewichts-Thermodynamik in der physikalischen Chemie.
Leipzig: VEB Deutscher Verlag für die Grundstoffindustrie, 1975.
- [23] A. G. Papathanasiou and A. Boudouvis, “Three-dimensional instabilities of ferromagnetic liquid bridges,” *Comput. Mech.*, vol. 21, p. 403, 1998.
- [24] L. Pontryagin, V. Boltyanskii, R. Gamkrelidze, and E. Mishchenko,
Mathematical Theory of Optimal Processes.
New York: Interscience Publishers, 1962.
- [25] J. Mayer, *Equilibrium Statistical Mechanics.*
Oxford, New York: Pergamon Press, 1968.
- [26] R. Courant and D. Hilbert, *Methods of Mathematical Physics*, vol. 1.
New York: Interscience Publishers, 1953.
- [27] C. Tsallis, R. Mendes, and A. Plastino, “The role of constraints within generalized nonextensive statistics,” *Physica A*, vol. 261, p. 534, 1998.
- [28] W. Dreyer, W. Müller, and W. Weiss, “Tales of thermodynamics and obscure applications of the Second Law,”
Continuum Mech. Thermodyn., vol. 12, p. 151 – 184, 2000.
- [29] J. Maxwell, “On the dynamical theory of gases,”
Phil. Trans. R. Soc. London, vol. 157, pp. 49 – 88, 1867.
- [30] J. Loschmidt, “Über den Zustand des Wärmegleichgewichts eines Systems von Körpern mit Rücksicht auf die Schwerkraft I,”
Wien. Sitzungsber. II, vol. 73, p. 128, 1876.
- [31] J. Loschmidt, “Über den Zustand des Wärmegleichgewichts eines Systems von Körpern mit Rücksicht auf die Schwerkraft II,”
Wien. Sitzungsber. II, vol. 73, p. 366, 1876.
- [32] J. Loschmidt, “Über den Zustand des Wärmegleichgewichts eines Systems von Körpern mit Rücksicht auf die Schwerkraft III,”
Wien. Sitzungsber. II, vol. 75, p. 287, 1877.

- [33] J. Loschmidt, “Über den Zustand des Wärmegleichgewichts eines Systems von Körpern mit Rücksicht auf die Schwerkraft IV,”
Wien. Sitzungsber. II, vol. 76, p. 209, 1877.
- [34] J. van der Waals, *Over de Continueit van den Gas- en Vloeistofoestand*.
PhD thesis, university Leiden, 1873.
- [35] R. von Dallwitz-Wegner, “Die atmosphärische Temperaturabnahme nach oben und ähnliche Erscheinungen als Wirkung der Schwerkraft, der Sama-Zustand der Materie,” *Zs. f. Phys.*, vol. 15, pp. 280 – 286, 1923.
- [36] R. von Dallwitz-Wegner, “Die Atmosphäre und der Samazustand,”
Zs. f. Phys., vol. 64, pp. 439 – 442, 1930.
- [37] W. Wagner, N. Kurzeja, and B. Pieperbeck,
“The thermal behaviour of pure fluid substances in the critical region - experiences from recent p, ρ, T - measurements on SF6 with a multi-cell apparatus,”
Fluid Phase Equilibria, vol. 79, pp. 151 – 174, 1992.
- [38] N. Kurzeja, T. Tielkes, and W. Wagner,
“The nearly classical behaviour of a pure fluid on the critical isochore very near the critical point under the influence of gravity,”
International Journal of Thermophysics, vol. 20, pp. 531 – 561, 1999.
- [39] R. Graeff, “Measuring the temperature distribution in gas columns,” in *Quantum Limits to the Second Law* (D. Sheehan, ed.), vol. 643, p. 125, AIP Press, 2002.
- [40] R. Graeff, “Gravity induced temperature difference device.”
Patent US2003014883, 2002.
- [41] R. Graeff, *My Path to Peaceful Energy*. Prof. -Domagk-Weg 7, D-78126 Königsfeld, Germany: Selfpublisher: ISBN 1451591861, 2010.
- [42] N. Roos, “Entropic forces in Brownian motion.”
<http://arxiv.org/abs/13104139.pdf>, 2013.
- [43] P. Fred, “Gravitation as resistance to the radial conduction of heat.”
selfpublished internet article, now withdrawn and revised, 2002.

- [44] P. Fred, “Is the sun? warmth gravitationally attractive?.”
vixra-0907.0018v4.pdf at <http://www.vixra.org>, 2009.
- [45] P. Shaw and N. Davy, “The effect of temperature on gravitative attraction,”
Phys. Rev., vol. 21, pp. 680–91, 1921.
- [46] N. Reiter, “Observation of an anomalous reversible weight change effect in a
system containing a thermo-electric Peltier device - initial report -160201a 18
feb. 2001.” <http://www.theavalonfoundation.org/docs/thermograv.html>.
- [47] N. Reiter, “Research update - the Peltier force effect 15 march 2001.”
<http://www.theavalonfoundation.org/docs/peltier.html>.
- [48] C. Liao, “Temperature gradient caused by gravitation,”
Int. J. Mod. Phys.B, vol. 23, pp. 4685 – 4696, 2010.
- [49] B. von Platen, “Method of recovering energy by means of a cyclic thermodynamic
process.” Patent US4084408, 1978.
- [50] G. Hielscher, *Energie im Überfluss*.
Hameln: Adolf Sponholtz Verlag, 1981.
- [51] W.D. Bauer and W. Muschik, “Second law induced existence conditions for
isothermal 2-phase region cyclic processes in binary mixtures,”
J. Non-Equilib. Thermodyn., vol. 23, no. 2, pp. 141–158, 1998.
- [52] W.D. Bauer and W. Muschik, “Kink conditions for isobars in binary v-x- phase
diagrams induced by Second Law,”
Archives of Thermodynamics, vol. 12, no. 3-4, pp. 59–83, 1998.
- [53] E. Holm, “Über den sogenannten Sama-Zustand I. vorherige Arbeiten,”
Ark. f. Mat., Astron. o. Fys. A, vol. 19, no. 34, pp. 1 – 19, 1926.
- [54] E. Holm, “Über den sogenannten Sama-Zustand II. Versuche an Gasen,”
Ark. f. Mat., Astron. o. Fys. A, vol. 20, no. 1, pp. 1 – 88, 1927.

- [55] E. Holm, “Über den sogenannten Sama-Zustand III:1. Versuche am Dampf der Diacetonxylose,” *Ark. f. Mat., Astron. o. Fys. A*, vol. 21, no. 12, pp. 1 – 72, 1928.
- [56] E. Holm, “Über den sogenannten Sama-Zustand III:2. Versuche am Dampf der Diacetoxylose und einer Lösung von 80 Prozent dieser Substanz und 20 Prozent Monomethylacetonxylose,” *Ark. f. Mat., Astron. o. Fys. A*, vol. 22, no. 20, pp. 1 – 65, 1931.
- [57] I. Müller, *A History of Thermodynamics - The Doctrine of Energy and Entropy*. Berlin: Springer Verlag, 2007.
- [58] D. Sheehan, J. Glick, T. Duncan, J. Langton, M. Gagliardi, and R. Tobe, “Phase space analysis of a gravitationally-induced steady-state nonequilibrium,” *Phys. Scr.*, vol. 65, pp. 430 – 437, 2002.
- [59] V. Capek and D. Sheehan, *Challenges to the Second Law of Thermodynamics*. Dordrecht: Springer, 2005.
- [60] D. Sheehan, J. Garamella, D. Mallin, and W. Sheehan, “Steady state non equilibrium gradients in hydrogen gas-metal system challenging the Second Law of thermodynamics,” *Phys. Scr.*, vol. T151, p. 014030, 2012.
- [61] X. Fu, Z. Fu, and S. Tong, “Realization of Maxwell’s hypothesis and experiment against the Second Law of thermodynamics.” www.arxiv.org under physics-0311104, 2003.
- [62] L. Ragni, “Nanocurrent oscillator indefinitely powered by a capacitor battery.” [arXiv:1211.6735v1](https://arxiv.org/abs/1211.6735v1) [physics.gen-ph] 28 Nov, 2012.
- [63] V. Gurtovoi, A. Ilin, A. Nikulov, and V. Tulin, “Could dissipationless current be observed at non-zero resistance?” [arXiv:1006.5346v1](https://arxiv.org/abs/1006.5346v1) [cond-mat.supr-con] 28 Jun, 2010.

- [64] S. Dubonos, V. Kuznetsov, and A. Nikulov, “Observation of DC voltage on segments of an inhomogeneous superconducting loop.”
arXiv:physics/0105059v1 [physics.gen-ph] 18 May, 2001.
- [65] V. Gurtovoi, S. Dubonos, A. Nikulov, N. Osipov, and V. Tulin, “Quantum oscillations of the critical current of asymmetric superconducting rings,” *Bulletin of the Russian Academy of Sciences: Physics*, vol. 71, no. 1, pp. 15 – 19, 2007.
- [66] A. Burlakov, V. Gurtovoi, S. Dubonos, A. Nikulov, and V. Tulin, “Little-Parks effect in a system of asymmetric superconducting rings,” *JETP Letters*, vol. 86, no. 8, pp. 517 – 521, 2007.
- [67] V. Gurtovoi, S. Dubonos, A. Nikulov, N. Osipov, and V. Tulin, “Magnetic dependence of the critical and persistent current of asymmetric superconducting rings.” arXiv:0903.3539v1 [cond-mat.supr-con] 20 Mar, 2009.
- [68] V. Gurtovoi, A. Ilin, A. Nikulov, and V. Tulin, “The DC voltage proportional to the persistent current observed on system of asymmetric mesoscopic loops.” arXiv:0910.5140v1 [cond-mat.supr-con] 27 Oct, 2009.
- [69] V. Gurtovoi, S. Dubonos, A. Nikulov, and V. Tulin, “Two permitted states of superconducting ring observed at measurements of its critical current.” arXiv:1102.5681v1 [cond-mat.supr-con] 25 Feb, 2011.
- [70] A. Burlakov, V. Gurtovoi, A. Ilin, A. Nikulov, and V. Tulin, “Experimental investigations of the change with magnetic flux of quantum number in superconducting ring.” arXiv:1103.3115v1 [cond-mat.supr-con] 16 Mar, 2011.
- [71] S. Dubonos, V. Kuznetsov, and A. Nikulov, “Segment of an inhomogeneous mesoscopic loop as a DC power source.”
arXiv:1112.6157v1 [cond-mat.supr-con] 28 Dec, 2011.
- [72] V. Gurtovoi, A. Burlakov, A. Nikulov, V. Tulin, A. Firsova, V. Antonov, R. Davis, and S. Pelli, “Multiple current states of two phase-coupled superconducting rings.” arXiv:1111.6882v1 [cond-mat.supr-con] 29 Nov, 2011.

- [73] A. Burlakov, V. Gurtovoi, A. Ilin, A. Nikulov, and V. Tulin, “A possibility of persistent voltage observation in a system of asymmetric superconducting rings.” arXiv:1207.0791v1 [cond-mat.supr-con] 2 Jul, 2012.
- [74] A. Nikulov, “Transformation of thermal energy in electric energy in an inhomogeneous superconducting ring.” arXiv:cond-mat/9901103 v1 12 Jan, 1999.
- [75] A. Nikulov, “About perpetuum mobile without emotions.” arXiv:physics/9912022 v1 10 Dec, 1999.
- [76] A. Nikulov, “Quantum force in a superconductor,” *PRB*, vol. 64, p. 012505, 2001.
- [77] A. Nikulov, “What is the azimuthal quantum force in superconductor.” arXiv:1104.4856v1 [cond-mat.supr-con] 26 Apr, 2011.
- [78] A. Nikulov, “The Meissner effect puzzle and the quantum force in superconductor,” *Physics Letters A*, vol. 376, p. 3392 - 3397, 2012.
- [79] E. Bender, “Die Berechnung von Phasengleichgewichten mit der thermischen Zustandsgleichung - dargestellt an den reinen Fluiden Argon, Stickstoff, Sauerstoff und ihren Gemischen,” Habilitationsschrift, Universität Bochum, 1986.
- [80] B. Platzter, *Eine Generalisierung der Zustandsgleichung von Bender zur Berechnung von Stoffeigenschaften polarer und unpolarer Fluide und deren Gemische*. PhD thesis, Fachbereich Maschinenbau, Universität Kaiserslautern, 1990.
- [81] R. Reid, J. Prausnitz, and B. Poling, *The Properties of Gases and Liquids*. New York: Mc Graw-Hill, 4 ed., 1987.
- [82] F.-N. Tsai and J.-H. Shuy, “Prediction of high-pressure vapor-liquid equilibria by the corresponding state principle,” *J. Chin. Chem. Engn.*, vol. 16, p. 157, 1985.
- [83] A. Polt, *Zur Beschreibung der thermodynamischen Eigenschaften reiner Fluide mit erweiterten BWR-Gleichungen*. PhD thesis, Maschinenbau, Universität Kaiserslautern, 1987.

- [84] K. Stephan and F. Mayinger, *Thermodynamik - Mehrstoffsysteme und chemische Reaktionen*, vol. 2. Berlin, Heidelberg: Springer Verlag, 1988.
- [85] W.D. Bauer, “the overunity theory website.”
<http://www.overunity-theory.de/firstlaw/firstlaw.htm>.
- [86] A. Irinyi, *Mischdampf-Krafterzeugung (Patent Arnold Irinyi)*.
Hamburg: Deutsches Institut für Energieforschung, 1931.
- [87] R. Doczekal, “Versuche über den Dual-Effekt bei Wasser-Benzin” , Wien 1941
unpublished document obtained indirectly by A. Urach.
- [88] R. Doczekal, “Verfahren zur Energieerzeugung mittels Verflüssigung von
Dampfgemischen aus zwei oder mehreren Flüssigkeiten.”
Patent no.155744, Deutschland / Nebenstelle Österreich, 1937.
- [89] R. Doczekal, “Das Problem des Perpetuum Mobile zweiter Art.”
Vortrag in Wien am 6.2.1940
(Nachdruck durch Werkstatt für dezentrale Energieforschung Berlin), 1989.
- [90] A. Urach, “Perpetuum mobile 2.Art (Energie aus Luftwärme).”
non registered self publisher, Wien, 1952 ?
- [91] B. Schaeffer, “Wärmekraftmaschine.” Offenlegungsschrift DE4101500A1, 1992.
- [92] B. Schaeffer and W.D. Bauer, *How to win energy with an adiabatic-isochoric-
adiabatic cycle over labile states of the P-V-diagram*. Berlin: WDB-Verlag, 1991.
- [93] A. Serogodsky, “Mit einem Kreisprozess arbeitende Wärmekraftmaschine.”
Offenlegungsschrift DE4244016A1, 1994.
- [94] G. Lerche and B. Schaeffer, “Die LESA story.”
from <http://www.lesa-maschinen.de>, 2005.
- [95] A. Irinyi, “Dampfkraftanlage.” Patent DE464301, 1928.
- [96] A. Irinyi, “Betriebsverfahren für Dampfmaschinen.” Patent AT116914, 1930.

- [97] B. Saleh, G. Kogelbauer, and M. Wendland, “Working fluids for organic Rankine cycles,” *Energy*, vol. 32, pp. 1210–1211, 2007.
- [98] B. Schaeffer, “Das Schaeffer Mischdampf Kraftwerk.” LESA Gmbh, Berlin, 2005.
- [99] N. Vargaftik, *Tables on the Thermophysical Properties of Liquids and Gases in normal and dissociated states*. New York, London, Sydney, Toronto: John Wiley, 1975.
- [100] U. Grigull, *Properties of Water and Steam in SI-Units*. Berlin, Heidelberg, New York, München: Springer-Verlag R. Oldenbourg, 1989.
- [101] J. Brock and R. Bird, “Surface tension and the principle of corresponding states,” *AIChE*, vol. 1, no. 2, pp. 174–177, 1955.
- [102] A. Fladerer and R. Strey, “Growth of homogeneously nucleated water droplets: a quantitative comparison of experiment and theory,” *Atmospheric Research*, vol. 65, pp. 161–187, 2003.
- [103] P. de Laplace, *Oeuvres completes de Laplace, Supplement a la theorie de la action capillaire*, vol. 4. Paris: Academie des sciences, 1880.
- [104] W. T. Thomson, “On the equilibrium of vapour at a curved surface of liquid,” *Phil. Mag.*, vol. 42, p. 448, 1871.
- [105] R. v.Helmholtz, “Untersuchungen über Dämpfe und Nebel, besonders solche von Lösungen,” *Wied. Ann.*, vol. 27, pp. 508–543, 1886.
- [106] J. Thomson, *Application of Dynamics to Physics and Chemistry*. London: MacMillan, 1888.
- [107] L. Farkas, “Keimbildungsgeschwindigkeit in übersättigten Dämpfen,” *Z. phys. Chem.*, vol. 125, pp. 236–242, 1927.
- [108] M. Volmer, “Über die Keimbildung und Keimwirkung als Spezialfälle der heterogenen Katalyse,” *Z. Elektrochemie*, vol. 35, no. 9, pp. 555–561, 1929.

- [109] R. Becker and W. Döring, “Kinetische Behandlung der Keimbildung in übersättigten Dämpfen,” *Ann. d. Phys.*, vol. 24, pp. 719–752, 1935.
- [110] M. Volmer, *Die Kinetik der Phasenbildung*.
Dresden, Leipzig: Theodor Steinkopf, 1939.
- [111] K. Oswatisch, “Kondensationserscheinungen in Überschalldüsen,”
ZAMM, vol. 22, no. 1, pp. 1–14, 1942.
- [112] H. Reiss, “The kinetics of phase transitions in binary systems,”
Journal of Chemical Physics, vol. 18, no. 4, pp. 840–848, 1950.
- [113] B. J. Mason, “Spontaneous condensation of water vapour in expansion chamber experiments,” *Proc. Phys. Soc. London Ser. B*, vol. 64, pp. 773–779, 1951.
- [114] H. Frisch and F. C. Collins, “Diffusional processes in the growth of aerosol particles II,” *J. Chem. Phys.*, vol. 21, no. 12, pp. 2158 – 2165, 1953.
- [115] J. W. Cahn and J. Hilliard, “Free energy in nonuniform system I. interfacial energy,” *J. Chem. Phys.*, vol. 28, p. 258, 1958.
- [116] J. Cahn, “Free energy in nonuniform system II. thermodynamic basis,”
J. Chem. Phys., vol. 30, p. 1121, 1959.
- [117] J. W. Campbell and J. Hilliard, “Free energy in nonuniform system III. nucleation in a two-component incompressible fluid,”
J. Chem. Phys., vol. 31, p. 688, 1959.
- [118] D. Bedeaux, E. Johannessen, and A. Rosjorde, “The nonequilibrium van der Waals square gradient model (I). the model and its solution,”
Physica A, vol. 330, pp. 329–353, 2003.
- [119] E. Johannessen and D. Bedeaux, “The nonequilibrium van der Waals square gradient model (II). local equilibrium on the Gibbs surface,”
Physica A, vol. 330, pp. 354–372, 2003.

- [120] M. Horsch, J. Vrabec, M. Bernreuther, S. Grottel, G. Reina, A. Wix, K. Schaber, and H. Hasse, “Homogeneous nucleation in supersaturated vapors of Methane, Ethane, and Carbon Dioxide by brute force molecular dynamics,” *J. Chem. Phys.*, vol. 128, p. 164510, 2008.
- [121] J. H. Seinfeld and S. H. Pandis, *Athmosperic Chemistry and Physics - From Air Pollution to Climate Change*. Hoboken, New Jersey: Wiley-Interscience, 2 ed., 2006.
- [122] T. Young, “An essay on the cohesion of fluids,” *Phil. Trans.*, vol. 95, pp. 65–86, 1805.
- [123] A. Rüger, “Die Molekularhypothese in der Theorie der Kapillarerscheinungen (1805-1873),” *Centaurus*, vol. 28, pp. 244–276, 2007.
- [124] A. J. W. Hedbäck, *Theorie der spontanen Kondensation in Düsen und Turbinen*. PhD thesis, ETH, Zürich, 1982.
- [125] J. W. Gibbs, *Collected Works*, vol. 1. New York: Longmans-Green, 1928.
- [126] J. Schmelzer, “Kinetics of condensation and boiling: Comparison of different approaches,” *J. Phys. Chem. B*, vol. 105, pp. 11595–11604, 2001.
- [127] R. Tolman, “The effect of droplet size on surface tension,” *J. Chem. Phys.*, vol. 17, pp. 333–337, 1949.
- [128] J. Frenkel, *Kinetic Theory of Liquids*. Oxford: Clarendon Press, 1946.
- [129] R. Becker, *Theorie der Wärme*. Berlin: Springer Verlag, 1966.
- [130] J. T. Zahoransky, *Experimentelle Untersuchungen zur homogenen Kondensation löslicher Binärgemische*. No. 70 in Fortschrittberichte der VDI-Zeitschriften Reihe 7: Strömungstechnik, Düsseldorf: VDI-Verlag, 1982.
- [131] H. Flood, “Tröpfchenbildung in übersättigten Äthylalkohol-Wasserdampfgemischen,” *Z. phys. Chem. A*, vol. 170, pp. 286–294, 1934.

- [132] M. Volmer and A. Weber, “Keimbildung in übersättigten Gebilden,” *Z. phys. Chem.*, vol. 119, pp. 277–301, 1926.
- [133] J. B. Zeldovich, “On the theory of new phase formation. cavitation,” in *Selected Works of Yakov Borisovich Zeldovich*, vol. 1, Princeton: Princeton University Press, 1992. contains English translation of JETP 12 (11) 1942, 525 - 538.
- [134] J. Feder, K. Russell, J. Lothe, and G. Pound, “Homogeneous nucleation and growth of droplets in vapours,” *Adv. Phys.*, vol. 1, pp. 111 – 178, 1966.
- [135] A. Ludwig, *Untersuchung zur spontanen Kondensation von Wasserdampf bei stationärer Überschallströmung unter Berücksichtigung des Realgasverhaltens*. PhD thesis, TU Karlsruhe, 1975.
- [136] G. Gyarmathy, “Zur Wachstumsgeschwindigkeit kleiner Flüssigkeitstropfen,” *ZAMP*, vol. 14, pp. 280–293, 1963.
- [137] W. Muschik, “Irreversibility and Second Law,” *J. Non-Equilib. Thermodyn.*, vol. 23, pp. 87 – 98, 1998.
- [138] R. Clausius, “Über eine veränderte Form des zweiten Hauptsatzes der Wärmetheorie,” *Poggendorf’s Annalen*, vol. 93, pp. 481 – 506, 1854.
- [139] W. T. Thomson, *Mathematical and Physical Papers*. Cambridge: Cambridge University Press, 1911.
- [140] R. Clausius, “Über die bewegende Kraft der Wärme und die Gesetze, die sich für die Wärmelehre selbst ableiten lassen,” *Poggendorf’s Annalen*, vol. 59, pp. 368, 500, 1850.
- [141] S. Carnot, “Reflexions sur la puissance motrice du feu, et sur les machines propres a developper cette puissance,” Paris, 1824.
- [142] P. Glansdorff and I. Prigogine, *Thermodynamic theory of structure, stability and fluctuations*. London: Wiley, 1971.
- [143] W. Muschik and H. Ehrentraut, “An amendment to the Second Law,” *J. Non-Equilib. Thermodyn.*, vol. 21, pp. 175 – 192, 1996.

- [144] V. N. Chelomei, “Mechanical paradoxes caused by vibrations,” *Sov. Phys. Dokl.*, vol. 28, no. 5, pp. 387–390, 1983.
- [145] B. vanderPol and M. Strutt, “On the stability of the solutions of Mathieu equation,” *Phil. Mag.*, vol. 5, pp. 18–38, 1928.
- [146] H. Smith and J. Blackburn, “Experimental study of an inverted pendulum,” *Am. J. Phys.*, vol. 60, no. 10, pp. 909 – 911, 1992.
- [147] J. vanVeldhofen, H. Bethlem, and G. Meijer, “AC electric trap for ground-state molecules,” *Phys. Rev. Lett.*, vol. 94, p. 083001, 2005.
- [148] I. Zivkovic, Y. Hirai, B. H. Frazer, M. Prester, D. Drobac, D. Ariosa, H. Berger, D. Pavuna, M. G., F. I., and O. M., “Ruthenocuprates $\text{RuSr}_2(\text{Eu,Ce})_2\text{Cu}_2\text{O}_{10-\text{Y}}$: Intrinsic magnetic multilayers,” *Phys. Rev. B*, vol. 65, p. 144420, 2002.
- [149] M. Smoluchowski, “Über die Brown’sche Molekularbewegung unter Einwirkung äusserer Kräfte und deren Zusammenhang mit der Diffusionsgleichung,” *Ann. d. Phys.*, vol. 48, p. 1103, 1915.
- [150] F. C. Collins and G. E. Kimball, “Diffusion-controlled reaction rates,” *J. Coll. (Interf.) Sci.*, vol. 4, pp. 425 – 436, 1949.
- [151] F. C. Collins, “Diffusion in the chemical reaction processes and in the growth of colloid particles,” *J. Coll. (Interf.) Sci.*, vol. 5, pp. 499 – 505, 1950.
- [152] M. Smoluchowski, “Über experimentell nachweisbare der üblichen Thermodynamik widersprechende Molekularphänomene,” *Phys. Z.*, vol. 13, p. 1069, 1912.
- [153] R. Feynman, R. Leighton, and M. Sands, *The Feynman Lectures - mainly Mechanics, Radiation and Heat*. Reading, Massachusetts: Addison Wesley, 1963.
- [154] H. Linke, T. Humphrey, A. Löfgren, A. Sushkov, R. Newbury, R. Taylor, and P. Omling, “Experimental tunneling ratchets,” *Science*, vol. 186, p. 2314, 1999.

- [155] P. Haenggi, M. Inchiosa, D. Fogliatti, and A. Bulsara, “Nonlinear stochastic resonance: The saga of anomalous output-input gain,” *Phys.Rev. E*, vol. 62, p. 6155, 2000.
- [156] P. Reimann, R. Kawai, C. Van den Broeck, and P. Haenggi, “Coupled Brownian motors: Anomalous hysteresis and zero-bias negative conductance,” *Europhys. Lett.*, vol. 45, pp. 545–551, 1999.
- [157] E. Elizalde and A. Romeo, “Essentials of the Casimir effect and its computation,” *Am J. Phys.*, vol. 59, p. 711, 1991.
- [158] H. Casimir, “On the attraction between two perfectly conducting plates,” *Proc. Kon. Ned. Acad. Wet.*, vol. 51, pp. 793 – 795, 1948.
- [159] H. Casimir and D. Polder, “The influence of retardation on the London-van der Waals forces,” *Phys. Rev.*, vol. 73, pp. 360 – 372, 1948.
- [160] E. Lifshitz, “The theory of molecular attractive forces between solids,” *JETP*, vol. 2, no. 1, pp. 73–83, 1956.
- [161] I. Dzyaloshinskii, E. Lifshitz, and L. Pitaevskii, “General theory of vanderWaals’ forces,” *Usp. Fiz. Nauk.*, vol. 73, pp. 381–422, 1961.
- [162] R. Eisenschitz and F. London, “Über das Verhältnis der van der Waalsschen Kräfte zu den homoepolaren Bindungskräften,” *Z. Phys.*, vol. 60, p. 491, 1929.
- [163] F. London, “Zur Theorie und Systematik der Molekularkräfte,” *Z. Phys*, vol. 63, p. 245, 1930.
- [164] B. Haisch, A. Rueda, and H. Puthoff, “Inertia as a zero-point-field Lorentz force,” *Phys. Rev. A*, vol. 49, no. 2, p. 678, 1994.
- [165] H. Puthoff, “Advanced space propulsion based on vacuum (spacetime metric) engineering,” *JBIS*, vol. 63, pp. 82 – 89, 2010.
- [166] R. Fateev, “Quantum flights.” arXiv:1309.3108v1 [physics.gen-ph] 12 Sep 2013.

- [167] R. Forward, "Extracting electrical energy from the vacuum by cohesion of charged foliated conductors," *Phys.Rev.B*, vol. 30, no. 4, p. 1700, 1984.
- [168] D. Cole and H. Puthoff, "Extracting energy and heat from the vacuum," *Phys. Rev. E*, vol. 48, pp. 1562 – 1565, 1994.
- [169] H. Mitter and D. Robaschik, "Thermodynamics of the Casimir effect," *Eur. Phys. J. B*, vol. 13, pp. 335 – 340, 2000.
- [170] L. November, "Crystal power: Piezo coupling to the quantum zero point." arXiv:1104.3813v1 [physics.gen-ph] 18 Apr 2011.
- [171] M. Bordag, *The Casimir Effect 50 Years Later*. Singapur: World Scientific, 1999.
- [172] J. Jackson, *Classical Electrodynamics*.
John Wiley & Sons, New York, second edition. ed., 1975.
- [173] J. H. Poynting, "On the transfer of energy in the electromagnetic field," *Phil. Trans.*, vol. 175, p. 277, 1884.
- [174] J. S. Webb, "Variation in the longitudinal incremental permeability due to a superimposed circular field," *Nature*, vol. 3600, p. 795, 1938.
- [175] J. P. Polonsky, P. Douzou, and C. Sadron, "Mise en evidence de proprietes ferroelectriques dans l'acide desoxyribonucleique (DNA)," *C.R. de Acad. Sci. (Paris)*, vol. 260, no. 3, p. 3414, 1960.
- [176] S. Esho, "Anomalous magneto-optical hysteresis loops on sputtered Gd-Co films," *7th conference on Solid State Devices, Supplement to Jap. Journ. Appl. Phys.*, vol. 15, pp. 93 – 98, 1976.
- [177] G. Gruzalski, *Magnetic and Electronic Properties of Amorphous Alloys*.
Dissertation, University of Lincoln, Nebraska, 1977.
- [178] C. A. Chang, "Magnetization of (100)Cu-Ni, (100)Cu-Co, and (100) Ni-Co superlattices deposited on Silicon using a Cu seed layer," *Appl. Phys. Lett.*, vol. 57, no. 3, pp. 297 – 299, 1990.

- [179] M. J. O'Shea and A. L. Al-Sharif, "Inverted hysteresis in magnetic system with interface exchange," *Journ. Appl. Phys.*, vol. 75, no. 10, pp. 6673 – 6675, 1994.
- [180] A. Aharoni, "Exchange anisotropy in films, and the problem of inverted hysteresis loops," *Journ. Appl. Phys.*, vol. 76, pp. 6977 – 6979, 1994.
- [181] G. Yusa and H. Sakaki, "Trapping of photogenerated carriers by InAs quantum dots and persistent photoconductivity in novel GaAs/n-AlGaAs field-effect transistor structures," *Appl. Phys. Lett.*, vol. 70, pp. 345 – 347, 1997.
- [182] A. Rack, R. Wetzler, A. Wacker, and E. Schöll, "Dynamic bistability of quantum dot structures: Role of the Auger process," *Phys.Rev. B.*, vol. 66, p. 165429, 2002.
- [183] J. Pak, K. Ko, and K. Nam, "Difference in electrical properties of Bi_{3.25}La_{0.75}Ti₃O₁₂-incorporated ferroelectric field-effect transistors with thermally oxidized SiO₂ layers prepared on n-type and p-type Si substrates," *Journ. Kor. Phys. Soc.*, vol. 46, no. 1, pp. 345 – 357, 2005.
- [184] T. Haneder, *Beiträge zum ferroelektrischen Transistor und dessen Integration in nicht-flüchtige Speicher*. Dissertation, University of Regensburg, 2005.
- [185] J. Hanmin, S. Dongsheng, G. Cunxu, and H. Kim, "Inverted hysteresis loops: Experimental artifacts arising from inappropriate or asymmetric sample positioning and the misinterpretation of experimental data," *J. Magn. Magn. Mat.*, vol. 308, no. 9, pp. 56 – 60, 2007.
- [186] G. Mastrogiacomo, J. F. Löffler, and N. Dilley, "Soft-magnetic materials characterized using a superconducting solenoid as magnetic source," *Appl. Phys. Lett.*, vol. 92, p. 082501, 2008.
- [187] M. Ziese, I. Vrejoiu, E. Pippel, E. Nikulina, and D. Hesse, "Magnetic properties of Pr_{0.7}Ca_{0.3}MnO₃/SrRuO₃ superlattices," *Appl. Phys. Lett.*, vol. 98, p. 132504, 2011. <http://arxiv.org/abs/1103.2299v1>.

- [188] P. Pouloupoulos, R. Krishnan, and N. K. Flevaris, “Antiferromagnetic-like coupling evidence in a Pd-Ni multilayer with inverted hysteresis features,” *Journ. Mag. Magn. Mater.*, vol. 163, pp. 27 – 31, 1996.
- [189] N. D. Ha, T. S. Yoon, E. Gan’shina, M. H. Phan, C. G. Kim, and C. O. Kim, “Observation of reversed hysteresis loops and negative coercivity in CoFeAlO magnetic thin films,” *J. Magn. Magn. Mat.*, vol. 295, pp. 126 – 131, 2005.
- [190] M. Chioncel and P. Haycock, “Cobalt thin films deposited by photoassisted MOCVD exhibiting inverted magnetic hysteresis,” *Chem. Vap. Deposition*, vol. 12, pp. 670 – 6789, 2006.
- [191] X. Wei, R. Skomski, Z. Sun, and S. D.J., “Proteresis in Co:CoO core shell nanoclusters,” *Journ. Appl. Phys.*, vol. 103, p. 07D514, 2008.
- [192] A. Kosterov, T. Frederichs, and T. vonDobeneck, “An observation of inverse hysteresis in rhodrosite,” *Geophysical Research Abstracts.*, vol. 6, p. 04183, 2004.
- [193] A. N. Cherkasov, B. A. Beloshenko, V. Z. Spuskanyuk, V. Y. Dmitrenko, and B. A. Shevchenko, “Low-frequency magnetic susceptibility of fiber FeCu composites,” *The Physics of Metals and Metallography*, vol. The Physics of Metals and Metallography, no. 2, pp. 136 – 141, 2007.
- [194] R. A. R. Tricker, *Frühe Elektrodynamik*. Vieweg, Braunschweig, 1974.
- [195] R. A. R. Tricker, *Faraday und Maxwell*. Akademie-Verlag, Berlin, 1974.
- [196] J. C. Maxwell, “On physical lines of force,” *Phil. Mag.*, 1861.
- [197] J. C. Maxwell, “A dynamical theory of the electrodynamic field,” *Phil. Trans. Roy. Soc. London*, vol. 155, pp. 459 – 512, 1864.
- [198] W.D. Bauer, “Magnetic monopoles in theory and experiment.” <http://arxiv.org/physics/0401151>, 2004.
- [199] H. A. Lorentz, *Versuch einer Theorie der electrischen und optischen Erscheinungen in bewegten Körpern*. Leiden: E.J. Brill, 1895.

- [200] H. A. Rowland, *The physical papers of Henry Augustus Rowland*.
Baltimore: Faculty of John Hopkins University, 1902.
- [201] E. Whittaker, *A History of the Theories of Aether and Electricity -*
Vol.1 The Classical Theories. New York: Humanities Press, 1973.
- [202] F. Ehrenhaft, "Über die Photophorese, die wahre magnetische Ladung und die
schraubenförmige Bewegung der Materie in Feldern - erster Teil,"
Act. phys. austr., vol. 4, p. 461, 1951.
- [203] F. Ehrenhaft, "Über die Photophorese, die wahre magnetische Ladung und die
schraubenförmige Bewegung der Materie in Feldern - zweiter Teil,"
Act. phys. austr., vol. 5, p. 12, 1952.
- [204] M. Gingras, "Observing monopoles in a magnetic analog of ice,"
Science, vol. 326, p. 375, 2009.
- [205] D. Morris, D. Tennant, S. Grigera, B. Klemke, C. Castelnovo, R. Moessner,
C. Czternasty, M. Meissner, K. Rule, J.-U. Hoffmann, K. Kiefer, S. Gerischer,
D. Slobinsky, and R. Perry,
"Dirac strings and magnetic monopoles in the spin ice $\text{Dy}_2\text{Ti}_2\text{O}_7$,"
Science, vol. 326, p. 411, 2009.
- [206] T. Fennell, P. Deen, A. Wildes, K. Schmalzl, D. Prabhakaran, A. Boothroyd,
R. Aldus, M. D.F., and S. Bramwell, "Magnetic coulomb phase in the spin ice
 $\text{Ho}_2\text{Ti}_2\text{O}_7$," *Science*, vol. 326, p. 415, 2009.
- [207] H. Risken, "Vorlesungsskript Elektrodynamik."
Universität Ulm Selbstverlag, 1976.
- [208] W.D. Bauer, "Future energy enews - iri / sept 9, 2006."
<http://www.zpenergy.com>, 2006. from a letter written to A. Schneider.
- [209] A. Rack, "Modellierung von bistabilen Quantenpunktstrukturen,"
Master's thesis, Technische Universität Berlin, 2002.
- [210] T. Ludwig. personal communication.

- [211] S. Foner, “Versatile and sensitive vibrating sample magnetometer,” *Rev. Sci. Instr.*, vol. 30, no. 7, pp. 548 – 557, 1959.
- [212] R. Bozorth, *Ferromagnetism*. New York: van Nostrand, 1951.
- [213] T. Gilbert, “A phenomenological theory of damping in ferromagnetic materials,” *IEEE Transactions on Magnetics*, vol. 40, no. 6, pp. 3443– 3449, 2004.
- [214] E. Stoner and E. Wohlfarth, “A mechanism of magnetic hysteresis in heterogeneous alloys,” *Trans. Roy. Soc A*, vol. 240, pp. 599 – 642, 1948.
- [215] J. Gerber, W. Burmester, and J. Sellmyer, “Vibrating sample magnetometer,” *Rev. Sci. Instrum.*, vol. 53, pp. 691 – 693, 1982.
- [216] K. Lee, T. Phan, N. Ha, M. Phan, S. Yuc, and C. Kim, “Electrical and magnetic properties of CoFeAlO thin films,” *Journ. Mag. Magn. Mat.*, vol. 304, pp. e201 – 203, 2006.
- [217] L. Tho, C. Kim, and C. Kim, “Investigation of negative coercivity in one layer formation of soft and hard magnetic materials,” *J. Appl. Phys.*, vol. 103, pp. 2666–2675, 2008.
- [218] S. NarayanaJammalamadaka, J. Vanacken, and V. V. Moshchalkov, “Exchange bias and training effects in antiferromagnetically coupled La_{0.7}Sr_{0.3}MnO₃/SrRuO₃ superlattices,” *EPL*, vol. 98, p. 17002, 2012.
- [219] C. Wang, K. Kuo, C. Lin, and G. Chern, “Magnetic anisotropy in Fe_xPd_{1-x} (x =30, .44, .55, .67, and .78) alloy film grown on $SrTiO_3(001)$ / and $MgO(001)$ by molecular beam epitaxy,” *Solid State Communications*, vol. 149, pp. 1523 – 1526, 2009.
- [220] P. Haycock, M. Chioncel, and J. Shah, “Remanence studies of cobalt thin films exhibiting inverse hysteresis,” *J. Mag. Magn. Mat*, vol. 242, pp. 1057 – 1060, 2002.
- [221] M. Chioncel, *Cobalt thin films produced by conventional and photo-assisted metal-organic chemical vapour deposition*. Dissertation, School of Chemistry and Physics, University of Keele, 2000.

- [222] J. Yang, J. Kim, J. Lee, S. Woo, J. Kwak, and J. Hong, “Inverted hysteresis loops observed in a randomly distributed cobalt nanoparticle system,” *Phys. Rev. B*, vol. 78, p. 094415, 2008.
- [223] C. Gao, *Co based hard magnets, thin films and multilayer*. Dissertation, Kansas State University, 1991.
- [224] C. Gao and M. J. O’Shea, “Inverted hysteresis loops in CoO-based multilayer,” *Journ. Mag. Magn. Mater.*, vol. 127, pp. 181–189, 1993.
- [225] P. Pouloupoulos, R. Krishnan, N. K. Flevaris, and M. Porte, “Methods of determining magnetization and uniaxial anisotropy of multilayers by means of torque magnetometry,” *Journ. Appl. Phys.*, vol. 75, pp. 4109 – 4113, 1994.
- [226] N. Flevaris and R. Krishnan, “Modulation-induced effects in magnetic multilayers: perpendicular anisotropy, reversed hysteresis and magnetisation enhancement,” *J. Mag. Magn. Mat.*, vol. 104-107, pp. 1760 – 1762, 1992.
- [227] K. Takanashi, H. Kurokawa, and H. Fujimori, “A novel hysteresis loop and indirect exchange coupling in Co/Pt/Gd/Pt multilayer films,” *Appl. Phys. Lett.*, vol. 63, pp. 1585 – 1587, 1993.
- [228] K. Geng, F. Zeng, Y. Gu, C. Song, X. Wei, and F. Pan, “Magnetic properties of Fe/Ho multilayers prepared by electron-beam evaporation,” *J. Phys. Soc. Jpn.*, vol. 75, no. 8, p. 084701, 2006.
- [229] D. Kim, C. Kim, C. Kim, S. Yoon, M. Naka, M. Tsunoda, and M. Takahashi, “Negative coercivity characteristics in antiferromagnetic coupled hard/soft multilayers,” *J. Mag. Magn. Mat.*, vol. 304, pp. e356 – 358, 2006.
- [230] Y. Zhao, S. Wang, K. Shono, X. Yui, M. Lui, and H. Zhai, “A new type hysteresis loop in SiN/GdFeCoSi/SiN sandwich structure,” *Modern Physics Letters B*, vol. 15, no. 26, pp. 1191 – 1196, 2001.
- [231] J. Long, Y. Zha, J. Chen, J. Du, M. Pan, M. Lu, A. Hu, and H. Zhai, “Magnetization property in Ta/NiFe/Ta sandwich structure,” *J. Mag. Magn. Mat.*, vol. 226-230, pp. 1823 – 1824, 2001.

- [232] X. Liu, T. Kanazawa, S. Li, and A. Morisako,
“Negative coercivity and spin configuration in Ni/TbFeCo/Ni trilayer,”
IEEE Transactions on Magnetics, vol. 45, no. 10, p. 4100, 2009.
- [233] S. Ohkoshi, T. Hozumi, and K. Hashimoto, “Design and preparation of a bulk magnet exhibiting an inverted hysteresis loop,”
Phys. Rev. B, vol. 64, p. 132404, 2001.
- [234] M. Chattopadhyay, S. Roy, and S. Chaudhary, “Magnetic properties of Fe_xCo_xSi alloys,” *Phys. Rev. B*, vol. 65, p. 132409, 2002. arXiv:cond-mat/0112346 v1.
- [235] J. Geshev, A. Viegas, and J. Schmidt, “Negative remanent magnetization of fine particles with competing cubic and uniaxial anisotropies,”
J. Appl. Phys., vol. 84, no. 3, pp. 1488 – 1492, 1998.
- [236] Y. Nam and S. Lim, “Negative remanent magnetization in a single domain particle with two uniaxial anisotropies,” *Appl. Phys. Lett.*, vol. 99, p. 092503, 2011.
- [237] E. Wohlfarth and D. Tonge, “The remanent magnetization of single domain ferromagnetic particles,” *Phil. Mag.*, vol. 2, pp. 1333 – 1344, 1957.
- [238] S. Byeon, P. Misra, A. Visscher, and W. Doyle, “Negative remanence in synthetic antiferromagnetically coupled FeCo/Ru/FeCo films,”
IEEE Transactions on Magnetics, vol. 40, no. 4, pp. 2359 – 2361, 2004.
- [239] H.-Y. Wang, K. Xun, and L. Xiao, “Individual monolayer analysis of anomalous hysteresis loops,” *Phys. Rev. B*, vol. 70, p. 214431, 2004.
- [240] T. Kobayashi, H. Tsuji, S. Tsunashima, and S. Uchiyama,
“Magnetisation process of exchange coupled ferrimagnetic double layered films,”
Jap. Journ. Appl. Phys., vol. 20, pp. 2089 – 2095, 1981.
- [241] A.-B. Guo and W. Jiang, “Susceptibility and inverted hysteresis loop of Prussian blue analogs with orthorhombic structure,”
Commun. Theor. Phys., vol. 8, no. 5, pp. 772 – 777, 2012.

- [242] H. Miyajima, K. Sato, and T. Mizoguchi,
“Simple analysis of torque measurement of magnetic thin films,”
J. Appl. Phys., vol. 47, no. 10, pp. 4669 – 4671, 1976.
- [243] R. Smith, *Smart Material System*. Philadelphia, PA: SIAM, 2006.
- [244] Quantum Design, *Magnetic Property Measurement System
SQUID VSM User Manual, Part Number 1500-100, C0*, 7 ed., 2011.
- [245] S. Demirtas, M. Hossu, M. Arikan, A. Koymen, and M. Salamon, “Tunable negative and positive coercivity for SmCo/CoGd exchange springs investigated with squid magnetometry,” *Phys. Rev. B*, vol. 76, p. 214430, 2007.
- [246] J. Beaujour, S. Gordeev, G. Bowden, P. de Groot, B. Rainford, R. Ward, and M. Wells, “Negative coercivity in epitaxially grown (110) DyFe₂ YFe₂ superlattices,” *Appl. Phys. Lett.*, vol. 78, no. 7, pp. 964 – 966, 2001.
- [247] M. Ziese, I. Vrejoiu, and D. Hesse, “Inverted hysteresis and giant exchange bias in La_{0.7}Sr_{0.3}MnO₃ /SrRuO₃ superlattices,”
Appl. Phys. Lett., vol. 97, p. 052504, 2010.
- [248] W. Schottky, “Halbleitertheorie der Sperrschicht,”
Naturwissenschaften, vol. 26, no. 52, p. 843, 1938.
- [249] S. Sze and K. Ng, *Physics of Semiconductor Devices*.
Hoboken, New Jersey: John Wiley + Sons, 2007.
- [250] W. Shockley, “The theory of p-n-junctions in semiconductors and p-n junction transistors,” *Bell System Technical Journal*, vol. 28, no. 3, pp. 155 – 178, 1949.
- [251] J. E. Lilienfeld, “Method and apparatus for controlling electric currents.”
Patent US1745175A, 1930.
- [252] O. Heil, “Improvement in or relating to electrical amplifiers and other control arrangements and devices.” Patent GB439457A, 1934.

- [253] D. Kahng and M. M. Atalla, "Silicon-Silicon Dioxide field induced surface devices," in *IRE-AIEE Solid-state Device Res. Conf.*, Carnegie Inst. of Technol., Pittsburgh, PA, 1960.
- [254] D. Kahng, "A historical perspective on the development of MOS transistors and related devices," *IEEE Transactions on Electron Devices*, vol. 23, p. 655, 1976.
- [255] H. Pao and C. Sah, "Effect of diffusion current on characteristic of metal-oxide (insulator)- semiconductor transistors," *Solid State Electronics*, vol. 9, pp. 927–937, 1966.
- [256] J. Brews, "The physics of the MOS transistor," in *Silicon Integrated Circuits Part A* (D. Kahng and R. Wolfe, eds.), Advances in Materials and Device Research Supplement 2, pp. 2 – 118, Academic Press, 1981.
- [257] S. Rogojevic, A. Jain, W. Gill, and J. Plawsky, "Interactions Between Nanoporous Silica and Copper," *J. Electrochem. Soc.*, vol. 147, pp. 2 – 118, 1981.
- [258] I. Tamm, "Über eine mögliche Art der Elektronenbindung an Kristalloberflächen," *Phys. Z. Sowjetunion*, vol. 1, p. 733, 1933.
- [259] W. Shockley, "On the surface states associated with a periodic potential," *Phys. Rev.*, vol. 56, pp. 317 – 323, 1939.
- [260] E. Snow, A. Grove, B. Deal, and C. Sah, "Ion transport phenomena in insulating films," *J. Appl. Phys.*, vol. 368, p. 1664, 1965.
- [261] M. Lannoo and J. Bourgoin, *Point Defects in Semiconductors I - Theoretical Aspects*, vol. 22 of *Springer Series in Solid-State Sciences*. Berlin: Springer, 1981.
- [262] W. Shockley and G. Pearson, "Modulation of conductance of thin films of semiconductors by surface charges," *Phys. Rev.*, vol. 74, pp. 232 – 233, 1948.
- [263] S. Miller, D. Fleetwood, and P. McWhorter, "Determining the energy distribution of traps in insulating thin films using the thermally stimulated current technique," *Phys. Rev. Lett.*, vol. 69, pp. 820 – 823, 1992.

- [264] J. Rosaye, N. Kurumado, M. Sakahita, H. Ikeda, A. Sakai, P. Mialhe, J. Charles, S. Zaima, Y. Yasuda, and Y. Watanabe, “Characterization of defect traps in SiO₂ thin films influence of temperature on defects,” *Microelectronics Journal*, vol. 33, pp. 429 – 436, 2002.
- [265] M. Lannoo and J. Bourgoin, *Point Defects in Semiconductors II - Experimental Aspects*, vol. 35 of *Springer Series in Solid-State Sciences*. Berlin: Springer, 1983.
- [266] P. Blood and J. Orton, *The Electrical Characterization of Semiconductors: Majority Carriers and Electron State*. London: Academic Press, 1992.
- [267] A. Marent, *Entwicklung einer neuartigen Quantenpunkt-Speicherzelle*. PhD thesis, TU-Berlin, 2011.
- [268] S. Wu, “A new ferroelectric memory device, metal-ferroelectric-semiconductor transistor,” *IEEE Transactions on Electron Devices*, vol. ED21, no. 8, pp. 499 – 504, 1974.
- [269] S. Samanta, S. Maikap, L. Bera, H. Banerjee, and C. Maiti, “Effect of post-oxidation annealing on the electrical properties of deposited oxide and oxynitride films on strained-Si 0.82 Ge 0.18 layers,” *Semicond. Sci. Technol.*, vol. 16, pp. 704 – 707, 2001.
- [270] T. Haneder, W. Hönlein, H. Bachhofer, H. vonPhilipsborn, and R. Waser, “Optimization of Pt/SBT/CeO₂/Si(100) gate stacks for low voltage ferroelectric field effect devices,” *Integrated Ferroelectrics*, vol. 34, p. 47, 2001.
- [271] M. Diestelhorst, K. Barz, H. Beige, M. Alexe, and D. Hesse, “Experimental observation of a torus doubling of a metal/ferroelectric film/semiconductor capacitor,” *Phil. Trans. R. Soc. A*, vol. 366, pp. 437 – 446, 2008.
- [272] M. Bozgeyik, J. Cross, H. Ishiwara, and K. Shinozaki, “Electrical and memory window properties of $Sr_{0.8-x}Ba_xBi_{2.2}Ta_{2-y}Zr_yO_9$ ferroelectric gate in metal-ferroelectric-insulator-semiconductor structure,” *J Electroceram.*, vol. 28, pp. 158–164, 2012.

- [273] Z. Hu, M. Li, Y. Zhu, S. Pu, X. Liu, B. Sebo, X. Zhao, and S. Dong, “Epitaxial growth and capacitance-voltage characteristics of BiFeO₃/CeO₂/Yttria-stabilized Zirconia/Si(001) heterostructure,” *Appl. Phys. Lett.*, vol. 100, p. 252908, 2012.
- [274] S. Miller and P. McWhorter, “Physics of the ferroelectric nonvolatile memory field effect transistor,” *J. Appl. Phys.*, vol. 72, no. 12, pp. 5999 – 6010, 1992.
- [275] H. Lue, C. Wu, and T. Tseng, “Device modeling of ferroelectric memory field-effect transistor (FEMFET),” *IEEE Transactions on Electron Devices*, vol. 49, no. 10, pp. 1790 – 1798, 2002.
- [276] S. Huang, X. Zhong, Y. Zhang, Q. Tan, J. Wang, and Y. Zhou, “A retention model for ferroelectric-gate field-effect transistor,” *IEEE Transactions on Electron Devices*, vol. 58, no. 10, pp. 3388 – 3394, 2011.
- [277] J. Sun and X. Zheng, “Modeling of MFIS-FETS for the application of ferroelectric random access memory,” *IEEE Transactions on Electron Devices*, vol. 58, no. 10, pp. 3559 – 3565, 2011.
- [278] J. Sun, X. Zheng, and W. Li, “A model for the electrical characteristics of metal-ferroelectric-insulator-semiconductor field-effect transistor,” *Current Applied Physics*, vol. 12, pp. 760 – 764, 1985.
- [279] J. Ran, J. Yang, and X. Cai, “Theoretical studies of the capacitance-voltage characteristics of metal-ferroelectric-GaN structures,” *Int. J. Numer. Model.*, vol. 25, p. 96, 2012.
- [280] C. Balocco, A. M. Song, and M. Missous, “Room-temperature operations of memory devices based on self-assembled InAs quantum dot structures,” *Appl. Phys. Lett.*, vol. 85, no. 24, pp. 5911–5913, 2004.
- [281] J.-H. Yoon, “Synthesis and charge storage properties of double-layered NiSi nanocrystals,” *J. Nanopart. Res.*, vol. 12, pp. 2387 – 2391, 2010.

- [282] S. Jung, S. Hwang, and J. Yi, “Memory properties of oxide-nitride-oxynitride stack structure using ultra-thin oxynitrided film as tunneling layer for nonvolatile memory device on glass,” *Thin Solid Films*, vol. 517, pp. 7362 – 7364, 2008.
- [283] W. Rodzaff, “Von der invertierten Hysterese zum Overunity-Oszillator,” *NET-Journal*, vol. 12, pp. 26–28, 2007.
- [284] W. Rodzaff, “From inverted hysteresis to the overunity oscillator.” http://www.borderlands.de/net_pdf/NET0107S26-28Det.pdf, 2007.
- [285] R. Unbehauen, *Grundlagen der Elektrotechnik*, vol. 1. Berlin: Springer, 1991.
- [286] H. Harradon, “The letter of Peter Peregrinus de Maricourt to Sygerus de Foucaucourt, soldier concerning the magnet,” *Terrestrial Magnetism and Atmospheric Electricity*, vol. 48, pp. 6–17, 1943.
- [287] W. Gary, “Wesley Gary’s magnetic motor,” *Harper’s New Monthly Magazine*, vol. 257, pp. 601 – 605, 1879.
- [288] W. Gary, “Magnetic motor.” <http://www.rexresearch.com/gary/gary1.htm>.
- [289] E. Vogels, “Perfect energy source - Minato wheel, experiments in Sweden,” *Energy Unlimited*, vol. 11, no. 2, pp. 2–183, 2003.
- [290] K. Minato, “Magnetic rotating apparatus.” Patent US5594289A, 1997.
- [291] K. Minato, “Magnetic rotating motor generator.” Patent EP1569322 A 1, 2005.
- [292] H. Johnson, “Permanent magnet motor.” Patent US4151431, 1979.
- [293] H. Johnson, “Magnetic force generating method and apparatus.” Patent US4877983, 1989.
- [294] H. Johnson, “Magnetic propulsion system.” Patent US5402021, 1995.
- [295] H. Johnson, “Magnet motor.” <http://www.rexresearch.com>, 2000.

- [296] S. Sandberg, “Der Searl-Effekt und der Searl-Generator,”
Raum & Zeit special -
Wunschtraum der Menschheit: Freie Energie, vol. 7, pp. 149 – 157, 1994.
- [297] H. Schneider and H. Watt, “Dem Searl-Effekt auf der Spur (I),”
Raum & Zeit special -
Wunschtraum der Menschheit: Freie Energie, vol. 7, pp. 174 – 180, 1994.
- [298] H. Schneider and H. Watt, “Dem Searl-Effekt auf der Spur (II),”
Raum & Zeit special -
Wunschtraum der Menschheit: Freie Energie, vol. 7, pp. 181 – 185, 1994.
- [299] <http://www.rexresearch.com>.
- [300] V. Roschin and S. Godin, “An experimental investigation of the physical effects in a dynamic magnetic system,”
Technical Physics Letters, vol. 26, pp. 1105 – 1107, 2000.
- [301] M. Yildiz, “Vorrichtung mit einer Anordnung von Magneten.”
Patent WO2009019001A2, 2009.
- [302] A. Schneider, “Der Magnetmotor des Erfinders Muammar Yildiz -
Öffentliche und private Vorführungen einer autonomen Energiemaschine,”
NET-Journal, vol. 15, pp. 21 – 26, 2010.
- [303] J. Naudin, “A free energy generator - the SMOT by Greg Watson.”
<http://jnaudin.free.fr/html/smotidx.htm>.
from jlnlabs.com - The Quest for Overunity, 1997
- [304] W.D. Bauer, “Permanent motor article -
do non-conservative potential perpetual running machines exist ?”
<http://www.overunity-theory.de/magmotor/magmotor.htm>, 1998.
- [305] B. Muvdi, A. Al-Khafaji, and J. McNabb, *Statics for Engineers*.
New York: Springer, 2007.
- [306] H. Herr, *Technische Mechanik Statik-Dynamik-Festigkeitslehre*.
Haan-Gruiten: Verlag Europa-Lehrmittel, 1996.

- [307] P. Campbell, *Permanent Magnet Material and their Application*.
Cambridge: Cambridge University Press, 1996.
- [308] A. Zangwill, *Modern Electrodynamics*.
Cambridge: Cambridge University Press, 2013.

Selected own Publications

- L. Jörgenson (pseudonym), Ein Überblick über die Grauzone in der Wissenschaft. WDB-Verlag Berlin 1990
- B. Schaeffer and W.D. Bauer, How to win energy with an adiabatic-isochoric-adiabatic cycle over labile states of the P-V-diagram. WDB-Verlag Berlin 1991.
- W.D. Bauer and W. Muschik, “Second law induced existence conditions for isothermal 2-phase region cyclic processes in binary mixtures,” *J. Non-Equilib. Thermodyn.*, vol. 23, no. 2, pp. 141–158, 1998.
- W.D. Bauer and W. Muschik, “Kink conditions for isobars in binary v-x- phase diagrams induced by second law,” *Archives of Thermodynamics*, vol. 12, no. 3-4, pp. 59–83, 1998.
- W.D. Bauer, “Magnetic monopoles in theory and experiment.” <http://arxiv.org/physics/0401151>, 2004.
- F. Wiepütz (pseudonym), “Actual candidates for second law violations,” *NET-Journal*, vol. 11, no. 3 pp. 18–21, 2006. http://www.borderlands.de/net_pdf/NET0306S18-21Det.pdf, 2006
- W. Rodzaff (pseudonym), “From inverted hysteresis to the overunity oscillator.” *NET-Journal*, vol. 12, no. 1, pp. 26–28, 2007. http://www.borderlands.de/net_pdf/NET0107S26-28Det.pdf, 2007.
- otherwise else see at <http://www.overunity-theory.de>

About the Author:

Wolf-Dietrich Bauer

born 1956

Diploma in Physics University of Ulm 1983

working as a technician in a research environment

hobbys: playing music in old style jazz bands (piano, clarinet, saxophone)

otherwise: interested in crazy physics

Index

Subject Index

- 2DEG, 115
- acceptor, 121
- acentric factor, 37
- AFM, 104
- Alnico, 132
- anisotropy energy, 110
- Argon-Methan, 43
- azeotropic line, 60
- azeotropic point, 68

- barometric pressure, 20
- Bender equation, 37
- benzene, 56
- benzene, 63, 67
- binary mixture, 78
- Boltzmann factor, 80
- Brownian motor, 102

- canonic probability function
- capacitance, 108
- capacitance spectroscopy, 117
- capacitance TU5822, 123 ff., 125
- Casimir forces, 104
- CCD, 115
- centrifugal field, 20
- centrifuge, 44 ff.
- charge jump, 108
- charge traps, 115 ff.
- chemical potential, 19
- conduction band, 117
- conduction edge, 121
- conservativeness, 9
- continuum regime, 73
- Coulomb shielding, 122
- critical point, 43
- critical radius, 72, 75, 77,
- critical temperature, 64
- crystal battery, 104
- Curie point, 107

- Dimethylacetonylose, 34
- distribution function, 24
- DNA, 104
- Doczekal cycle, 69
- donator, 121
- DRAM-cell, 105
- droplet spectrum, 86
- droplet class, 86, 87
- dual effect, 47
- Dufour effect, 97

economy, 7
 efficiency, 51, 71, 125
 electromagnetic symbols, 141
 energy conservation, 11
 enthalpies, 62, 66, 82ff.
 entropy, 18 ff., 91
 equation of state, 37 ff.
 equilibrium conditions, 20
 erasing time, 122
 Euler-Heun algorithm, 88
 Euler-Lagrange equation. 22 ff.

 FEMM 4.2, 130
 Fermi potential, 121
 FET, 114 ff.
 Fitz-Nagumo equation, 93
 fixpoint stabilization, 94
 fluctuation , 35, 72, 101 ff.
 Fowler emission, 119 ff.
 free enthalpy, 76 ff., 85
 fugacity coefficient, 38

 Gauss integral theorem, 100
 Gauss-Newton algorithm, 39
 Gauss-Raphson algorithm, 39
 Gibbs equilibrium, 38
 group theory, 10
 gravimolecular pressure, 33 ff.
 gravitational field, 20

 Hamilton energy, 17 ff.
 Hamilton function, 4
 heat conduction, 82

heat conductivity, 64
 Heisenberg formalism, 112
 Helmholtz decomposition, 107
 Hess heat theorem, 7
 heterogeneous condensation, 72
 homogeneous condensation, 72
 hydrostatic pressure, 30
 hysteresis curve, 121
 hysteresis, ferroelectric, 104

 inductivity, 108
 internal energy, 18
 inverted capacitance, 118f.
 inverted hysteresis, 5, 104 ff.
 inverted hysteresis system, 106
 inverted loops, 112 ff.
 inverted pendulum, 94
 Irinyi-Rankine cycle, 71
 isentrope, 67

 isothermal cycle, 44
 kinetic regime, 73
 kinetic rotation cycle, 44
 Lagrange function, 21
 Laplace equation, 20
 Laplace law, 74, 78
 Legendre transformation, 23
 linear stability analysis, 92
 loading time, 122
 London dispersion forces, 103
 loop analysis, 139
 Lorenz force, 107
 Lyapunov stability, 93

magnetic charge, 109
 magnetic inverted hysteresis, 111
 magnetostrictive energy, 110
 material data, 62
 maximum entropy principle, 92 ff.
 Maxwell demon, 5, 119
 Maxwell Equations, 106 ff.
 Maxwell stress tensor, 137
 mechanics, 1
 memory window, 127
 Mercury, 56
 MFIS-capacitance, 105
 MFIS-FET, 117
 minimum entropy production, 92
 MOKE, 109
 molar density, 65 ff.
 molar ratio, 65 ff.
 Mollier approximation, 60 ff.
 multiphysics, 15

 Neodymium magnets, 130 ff.
 Nickel, 130
 noise, 102 ff.
 Noise, 35
 non extensive thermodynamics, 27
 non-conservative coupling, 5
 non-conservative field, 5
 non-equilibrium thermodynamics, 72
 non-linear dynamics, 93
 nonlinear oscillation, 58

 Octane number, 56
 overunity, 15

 p-n - diode, 114
 parametric oscillation, 122 ff., 138
 partial pressure, 65
 Peltier element, 30
 permanent magnet motor, 128 ff., 132
 perpetuum mobile, 1
 phase diagram 43 ff., 60 ff.
 phase transition 1st order, 35
 Poisson equation, 20
 Poisson PDE, 124
 Pontryagin theorem, 21
 potential, 4
 Poynting relation, 136
 Poynting theorem, 104
 pressure, 18, 65
 Prussian blue, 112

 quantum dots (QD), 118 ff.
 quantum noise, 103
 Rankine cycle, 52
 ratchet, 101 ff.
 real gases, 89
 reduced temperature, 64
 reference pressure, 74
 reference temperature, 74
 reproducibility, 6
 Rowland effect, 107

 Schottky contact, 117, 121
 Schottky diode, 114
 Schottky gate, 117
 Second Law, 1, 88, 91
 Seebeck effect, 7

selfexcitation, 125 ff.
 semiconductor capacity, 113 ff.
 semiconductor, 114 ff.
 specific heat, 60, 62
 spontaneous condensation, 72, 80
 SQUID, 110
 stability criterion, 91
 steam engine, 50, 55 ff.
 steam, 50
 Stefan flow, 99
 Stiel factor, 37
 stochastic resonance, 103
 Stoner-Wohlfarth-model, 110 ff.
 stratification, 30
 supersaturation, 72
 Supraconductivity, 35 ff.
 susceptibility, 109
 symmetry, 6
 system theory, 3

 temperature, 28
 thermal noise 103
 thermodynamic fluxes, 97
 thermodynamics, 17
 thermodynamics,4
 torque magnetometry, 109
 torque, 102
 transition regime, 73
 transport field, 82
 traps, 115 ff.
 Tsallis distribution, 27
 tunnel emission, 121

 undersaturation, 75
 vander Waals forces, 103
 voltage jump, 108
 vortex system, 5
 VSM, 109

 Wagner equation, 66
 water, 62,67
 water-benzene, 47ff.,79
 water-gasoline, 56
 Weiss-demagnetisation, 110

 Yusa-Sakaki FET, 105, 117 ff.

 Zeeman-field, 110
 zero point energy, 103

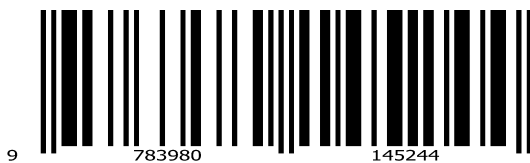
Name Index

- Aharoni, 105
al-Sharif, 110
Baranowski, 97 ff.
Becker, 73
Bedeaux, 73
Bender, 37
Bernoulli, 1
Bessler, 1
Boltzmann, 80
Boyle, 1
Brews, 114
Cahn, 73
Capek, 36
Carnot, 47
Casimir, 103
Clausius, 91 ff.
Collins, 99
Dallwitz-Wegner v.
Dircks, 1
Doczekal, 47ff. , 53 ff.m 88
Doering, 73
Dubonos, 35
Einstein, 12
Electrolux, 33
Faraday, 106
Farkas, 73
Farkas, 73
Feder, 81
Feynman, 101
FIAT, 55
Fred, P. ,30
Frenkel, 78
Frisch, 73
Frisch, 99
Geshev, 112
Gibbs, 29,77, 91
Gibbs, 73,74, 91
Godin, 128
Graeff, 30
Grosse, 52
Gurtovoi, 35
Gyarmathy, 84
Haenggi, 103
Hamilton, 1
Hedbäck, 77ff., 82 ff., 97ff.
Heil, 114
Heisenberg, 103
Helmholtz, H. v., 4, 13
Helmholtz, R.v. , 73, 75
Hielscher, 48
Hillard,73
Holm, 33
Horsch, 73
Irinnyi, 47 ff.
Jackson, 107
Johnson, 128
Kelvin, 73, 75, 91, 96
Ketterer, 51
Kimball, 99
Laplace, 73,74ff.,
Leipniz, 1
Lerche, 49
LESA-Gmbh, 49, 58
Lilienfeld, 114

Lim, 112	Searl, 128
Lorenz force, 107	Serogodsky, 48
Loschmidt, 29	Shaw, 30
Marent, 118 ff.	Sheehan, 34
Mason, 64, 73	Shockley, 114
Maxwell, 29, 106 ff.	Shyu, 38
Mayer, 12	Smoluchowski, 101
Mayer, 22	Sze, 116
Meyer, 50	Thodos, 64
Minato, 128	Thomson, J.J., 73, 77, 93, 96
Mollier, 60	Tsai, 38
Muschik, 93	Tsallis, 27
Nam, 112	Urach, 48
Nikulov, 36, 137	vander Waals, 29
O'Shea, 110	vanPlaten, 33
Ord-Hume, 1	Volmer, 73, 77, 80
Oswatisch, 73	Wassilewa, 64
Peregrinus, P., 128	Wittgenstein, 13
Platzer, 38	Wu, 117
Polder, 103	Yildiz, 128
Pontryagin, 22	Young, 73, 74
Poulopolos, 112	Zakhoransky, 81
Prigogine, 91 ff.	Zeldovich, 81
Rack, 118 ff.	
Rankine, 52	
Ray, 64	
Reiss, 73,76	
Reiter,30	
Risken, 132	
Roschin, 128	
Saxena, 64	
Schaeffer, 48 ff., 52, 58	
Schottky, 114	

This book investigates perpetual mobile and overunity claims from a theoretical point of view. The history, the motivation and the mathematical foundations of the first and second law are analyzed in order to find the field for alternative systems beyond the conventional energy science. So systems are discussed which go beyond the conservative beliefs. Among them there are energy cycles of non-conservative systems or electrical cycles implementing quantum mechanical processes. It is shown that physics can predict overunity features under certain conditions. ~~Similarly permanent running magnet motors are explained quite naturally.~~

Scientific research today has a very high level and many results need much effort of money and brain to be understood, to be evaluated and to be developed. This work goes back to the basics of physics. The book is written by a single person not by a system. It is simple and can be understood by engineers and by physics student at an undergraduate level. The results may become important if they are confirmed.



ISBN: 978-3-9801452-4-4